Universidade de Aveiro Departamento de Química
2017

Layla Mhemmed Mbrouk Alghanduri

Caracterização Reológica de Petróleos Parafínicos Líbios

Rheological Characterization of some Libyan Waxy Crude Oils

Universidade de Aveiro Departamento de Química
2017

Layla Mhemmed Mbrouk Alghanduri

Caracterização Reológica de Petróleos Parafínicos Líbiaos

Rheological Characterization of some Libyan Waxy Crude Oils

Tese apresentada à Universidade de Aveiro para cumprimento dos requisitos necessários à obtenção do grau de Doutor em Engenharia Química, realizada sob a orientação científica do Professor Doutor João Manuel da Costa Araújo Pereira Coutinho, Professor Catedrático do Departamento de Química da Universidade de Aveiro, do Professor Doutor José António Teixeira Lopes Da Silva, Professor Auxiliar do Departamento de Química da Universidade de Aveiro e do Professor Doutor Jean-Luc Daridon, Professor do Departamento de Física da Université de Pau et des Pays de l'Adour.

Esta tese foi desenvolvida com o suporte financeiro do Instituto Líbio do Petróleo

To my parents, my husband and my daughters

o júri

presidente

Prof. Doutor Luís António Ferreira Martins Dias Carlos
Professor Catedrático da Universidade de Aveiro

Prof. Doutor João Manuel da Costa e Araújo Pereira Coutinho
Professor Catedrático da Universidade de Aveiro

Prof. Doutora Catrina Marques Mendes Almeida da Rosa Leal
Professora Coordenadora, instituto Superior de Engenharia de Lisboa

Prof. Doutor Eduardo Jorge Morilla Filipe
professor Auxiliar, Instituto Superior Técnico, Universidade de Lisboa

Doutor Jerome Pauly
Meître de Conferences, Université de Pau et des Pays de l'Adour, França

Doutor António José do Nascimento Quimada
Consultor Sénior, KBC Process Technology (A Yokogawa Company), Reino Unido

Acknowledgments

This work could not have been possible without the help and support of many people. Completing this dissertation had turned out to be an endurance test and had required a lot of patience and consistency.

First and foremost, I would like to express my sincere gratitude to my advisor Professor Joao Coutinho for his guidance all the time, effort and encouragement he has put and none of this work would be have been possible without him throughout the course of my graduate study. I am very thankful to him for his exceptional research philosophy and high standard of excellence that he has instilled me. I consider myself blessed to have been his student, part of his research group and hopefully I have shown very good attitude.

Also I would like to express my sincere thanks to my second advisor Professor Lopes Da Silva for providing me an opportunity to work with him. I have obtained a lot of knowledge about rheology. He has provided great guidance and support in this thesis report. I am very thankful to him for his enlightening discussion and meaningful suggestions.

“The PhD work” was financially supported by Libyan Petroleum Institute, and I would like to take the opportunity to thank all the staff of the institute who helped me through all my studying period.

Thank you my parents, it is your great credit that I continued my graduate studies. Thank you my husband “Wajdi” for your love, support, encouragement, and patient with me all these years.

Thank you my friend Fathia for your never-ending support and encouragement throughout the process of completing this study.

Finally, I would like to thank all the group of the Path at the Chemistry department of University of Aveiro and everyone who assisted in some way to the completion of this work.

palavras-chave

Garantia de fluxo, petróleo bruto, cera, ponto de fluxão, características de fluxo, gel, tensão de inércia, propriedades viscoelásticas.

resumo

A precipitação de cera em petróleos brutos a temperaturas inferiores ao seu ponto de escoamento, conduz à formação de uma estrutura de cristais de cera e à gelificação do óleo. Assim, é muito importante ter uma boa compreensão do comportamento dos óleos brutos e da precipitação de cera durante o transporte a baixa temperatura, bem como do comportamento reológico do crude gelificado, já que esta seria uma informação útil para o projeto e operação de sistemas de oleodutos, e que permitiria diminuir os custos de produção e transporte.

Esta tese foi motivada pela falta de informação sobre as características de óleos brutos parafínicos da Líbia e do seu comportamento reológico a temperaturas inferiores ao ponto de fluxão. A caracterização do óleo e da sua cera pode fornecer informação útil necessária para a engenharia operacional e o desenvolvimento de processos, incluindo a modificação do processamento dos petróleos brutos. Este estudo utilizou DSC para medir a temperatura de formação da cera em cinco óleos brutos de petróleo Líbio; a distribuição dos alcanos presentes nestas ceras foi determinada por GC-FID; extensa informação sobre a composição estrutural destas ceras foi obtida usando C-RMN; e informações sobre a estrutura cristalina dessas ceras foi obtida usando difracção de raios-X.

Neste trabalho tentamos desenvolver um conhecimento mais aprofundado acerca do comportamento reológico de alguns petróleos brutos parafínicos da Líbia. A caracterização reológica de petróleos parafínicos é uma contribuição importante para a indústria petrolifera Líbia. Isto pode ser explicado pelo facto de o comportamento reológico de óleos parafínicos próximo do ponto de fluxão ser útil para caracterizar a estrutura do gel, a sua resistência e a estabilidade da rede resultante da deposição de cera, permitindo assim prever os perfis de escoamento do petróleo em dutos, a pressão de arranque e a capacidade da bomba, minimizando problemas de operação, reduzindo o uso de produtos químicos perigosos e impactos ambientais negativos, e em geral, os custos associados ao processo. Baseado nestes argumentos expostos acima, esta tese foca-se no estudo do comportamento reológico dos óleos selecionados abaixo das suas temperaturas de ponto de fluxão. O efeito da tensão aplicada sobre as propriedades de escoamento e de gelificação e a quebra de gel de amostras de petróleo em bruto, após um tempo de envelhecimento especificado foi investigada. Por último, a fim de explorar a elasticidade, a estabilidade e a resistência dos géis formados por petróleos parafínicos, estudamos experimentalmente as propriedades viscoelásticas dos óleos acima e abaixo do ponto de fluxão.

keywords

Flow assurance, waxy crude oil, pour point, flow characteristic, gelled oil, yield stress, viscoelastic properties.

abstract

The precipitation of wax in crude oils at temperatures below their pour point leads to the formation of a network structure of waxy crystals and the gelation of the oil. It is thus very important to have a good understanding of the behavior of waxy crude oils during transportation at low temperature, and the rheological behavior of the gelled crude, as this would be useful information for the design and operation of pipeline systems that would help decrease the costs of production and transportation.

This thesis was motivated by the lack of information on the characteristics of the wax phase of Libyan waxy crude oils and of their rheological behavior at temperatures below the pour point. The characterization of the oil and wax provides useful information required for operational engineering, and process development, including modifications to the processing of the crude oils. This study used DSC to measure the wax appearance temperature for five Libyan crude oils; the carbon number distribution of these waxes was determined by GC-FID; extensive information about the structural composition of these waxes was obtained using C-NMR; and information about the crystalline structure of these waxes was obtained using X-ray diffraction.

A better understanding and more detailed knowledge of the rheological behavior of some Libyan waxy crude oils was developed in this work. The characterization of the rheological characteristic of Libyan waxy oils is an important contribution to the Libyan oil industry. This can be illustrated by the fact that the rheological characterization of gelled waxy oils near their pour point is useful to extract information about the gel structure, the gel strength and to further explore the network stability due to wax deposition, i.e. the flowability of crude oils in pipelines by prediction of the successful start-up pressure and pump capacity required after shutdown. This will allow to avoid operational problems and reduce the cost of production by the use of hazardous chemicals, which are not only costly but also have negative environmental impacts, while minimizing losses by reduced production due to line blockage. Based on the considerations exposed above this thesis focus on the study of the flow behavior of the oils below their pour point temperatures. Furthermore the effect of stress applied on the gelling properties and the gel breakdown of crude oil samples after a specified aging time was investigated. Lastly, in order to explore the elasticity, stability and strength of the crude oils gels we have experimentally studied the viscoelastic properties of the oils above and below the pour point.

Table of Contents

List of Tables

List of Figures

Nomenclature

List of Abbreviations

T- Temperature

ASTM- American Society for Testing and Materials

UOP- Universal Oil Products

API- American Petroleum Institute

GC-FID- Gas chromatography (Flame Ionization Detector)

CS_2- Carbon disulfide

WAT- Wax Appearance Temperature

PP- Pour Point

SG- Specific Gravity

Mw- Molecular weight

K_f - Freezing point depression constant

T_f – Freezing temperature

m_{oil}- Weight of the crude oil

m_{xyl}- Weight of xylene

CCN- Critical Carbon Number

DSC- Differential Scanning Calorimetry

NMR- Nuclear Magnetic Resonance

CDCL3- Deuterated Chloroform

K- Consistency index

XRD- X-Ray Diffraction

DMA- Dynamic Mechanical Analysis

LVR- Linear Viscoelastic region

G'– Storage modulus

G''– Loss modulus

t- Time

Greek Symbols

ρ - Density

μ - Viscosity (Pa.s)

$\dot{\gamma}$ - Shear rate

γ - Shear strain

δ- Phase angle

τ- Shear stress

τ_e - Elastic yield stress

τ_s - Static yield stress

τ_f - Fracture yield stress

τ_F - Flow yield stress

ω -Frequency

1 General introduction

1.1 General context

Crude oils are complex hydrocarbon fluids for which a change in temperature and/or pressure may cause the precipitation of heavy organic compounds. These deposits formed in crude oils include wax and other heavy hydrocarbons such as asphalthenes or naphthenic acids and their naphthenates. It is essential to the producers of crude oils to be able to predict potential organic deposition problems so that the systems may be designed, and the production planned, to prevent or mitigate it [1]. The deposition of these compounds on the pipelines is a costly problem in oil production and processing as it is responsible for losses of billions of dollars yearly worldwide [2]. Consequently the correct prediction of wax deposition is essential to understand and describe the wax formation process in order to reduce operation costs [3]. The costs could be reduced significantly if approaches to predict the wax precipitation and the characteristics of the deposits were available. Therefore, it is crucial to develop reliable experimental techniques as predictive tools to study the wax formation in crude oils. The industry has focused great efforts on this goal over the past few years [4, 5].

The purpose of this study is to evaluate the characteristics of some Libyan crude oils, as well as their waxes. Libya is Africa's second-largest oil producer after Nigeria and one of Europe's biggest North African oil providers. It has been a producing country for four decades and is expected to continue the oil production for years to come. Only 25% of the area of the Libyan land is explored for oil and gas and Libyan crude oils are known for their good quality (low sulfur, high API gravity) with high yield of gasoline and middle distillates. However some Libyan crudes contain moderate to high contents of paraffinic waxes that may cause flow assurance problems. The oils selected to be studied in this thesis are Remal, Sarir, Sedra, Bouri, and Faregh, and they were supplied by three companies operating in Libya, Waha, ENI[1]-Oil, and Arabian Gulf Oil, through the National Oil Corporation.

[1] ENI stands for ENTE Nazionale Idrocarburi, the original Italian name of the company

The oils were chosen because of the wax problems that they present during transport. The location of these wells is presented in Figure 1.1, showing the sedimentary basins of Libya. The Bouri oilfield off Libya's western coast is the largest producing offshore oilfield, estimated to contain 2 billion barrels in proven recoverable crude oil. The Sirte basin contains around 80% of Libya's established oil reserves and production. Sedra provides the largest contribution to crude oils export, whereas Sarir is regarded as the second most important contribution for exportation [6]. These Libyan waxy crude oils present problems in transportation through pipelines because of thermal environmental changes. These crudes, mainly during wintry weather or at night, present a decreasing flow because of the deposition of a solid phase that obstructs the pipeline, and, as result of that, the flow handling becomes difficult. Because of the long distance that the oils travel through the pipelines from the field to the coast terminals (e.g., the distance from the Sarir field to the coast terminal is about 513.6 km)[7], thermal or mechanical treatment and flow improvers are always applied to these crude oils to avoid the transportation problem, which severely increases their production costs.

The solubility of heavy paraffins depends very strongly on temperature. With lowering temperature, their solubility quickly decreases and the temperature at which the first organic crystal appears is called the wax appearance temperature (WAT) [8]. As the temperature keeps decreasing below the WAT, the amount of solids increases forming a 3D network that eventually prevents the fluid of flowing, reaching what is known as pour point. This temperature is widely used as the industrial standard to define the gelling temperature of crude oils [9]**.** During shutdown the temperature may drop below the pour point and it may be difficult to restart the pipeline. Consequently this temperature is considered as an important physical property of crude oils, at which they begin to behave as semi-solid materials and their rheological properties change considerably. This behavior is related to an increase in the formation of wax-crystal structures during the cooling process [10, 11].

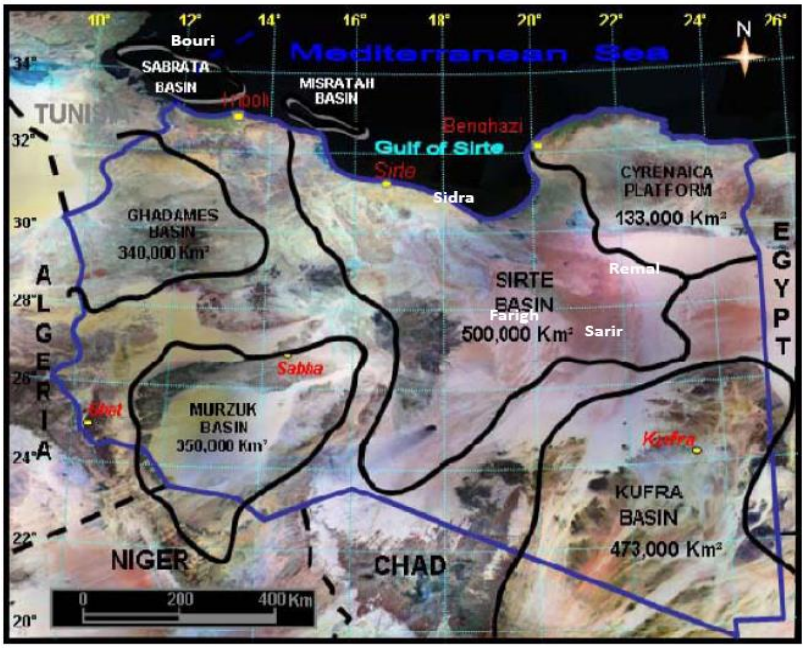

Figure 1.1 Map showing the location of the investigated oil wells [6].

The development of an improved understanding of the rheology of waxy crude oils has a considerable interest to the petroleum industry [12]**.** As expected from the solubility behavior of paraffins, the rheology of waxy crude oils is particularly sensitive to temperature, due to the wax precipitation and the formation of a gel-like structure [13]. As the gels formed by wax precipitation may result in the blocking of a flow-line that can cause a halt in production, it is necessary to understand the nature of these waxes, and the behavior of these gel-like structures at temperatures below the pour point. Being able to understand the properties of waxy crude oils and to have information that may help predict/understand their rheology can provide insights into the right (thermal-chemical-mechanical) solution to deal with the costly restart of the flow in the pipeline after shutdown, for operational or emergency reasons, in locations with low ambient temperature.

Although this thesis was initiated before the unrest that has taken hold of Libya in the last few years, its subject has only become more pressing since the political situation has led to several productions stops in various fields, leading to the need to contemplate the restart of oil transport in pipelines that sometimes were partly or totally blocked by the deposition of waxes. This thesis is thus aimed at the characterization of the nature of

some Libyan waxy crude oils and their rheological study from a flow assurance perspective. Studies were carried in order to attempt understanding the relationship between the nature of the oils and their waxes, and their rheological behavior. Moreover the adequate knowledge and characterization of these fluids is of relevance as it helps the refiners to optimize the conversion of raw materials into high value products.

1.2 Scope and objectives

As discussed above, experimental measurements can provide insights into the structural and rheological behavior of waxy-oils. The main aim of this research is a rheological study of waxy crude oils using Libyan oils as models. The study is essentially experimental but based on the sound theoretical principles of rheology. By rheological study, it is meant here gauging the spectrum of the behaviour of waxy crude oils, near and below pour point in order to investigate the characteristics of wax-oil gels by study their flow and viscoelastic behaviours. Thus the control of temperature is a key aspect of the measurements schedule. A set of measurements are typically used to envisage the probable flow-assurance issues that can be performed for waxy crudes, from laboratory studies.

The objectives that need to be fulfilled to achieve the aim of this work are divided into two main parts:

1. Sourcing suitable Libyan waxy crude oils and characterising their basic properties, particularly measuring their physical and chemical properties, as the key indicators of their nature using a combination of various analytical techniques.

As there is no single analytical method that can provide a complete picture of the chemical and physical nature of the crude oils, a number of techniques comprising, GC-FID, NMR, XRD, DSC, densimetry, and elemental analysis will be applied to characterize the following five Libyan crude oils and their waxes: Remal, Sarir, Sedra, Bouri, and Faregh.

2. The second contribution of this thesis is performing a comprehensive rheological measurements of three waxy oils, Faregh, Sarir and Sedra, at various temperatures using three different techniques, including controlled stress tests, creep- recovery tests and oscillations measurements. This is the principal aim of this research. To achieve this, a controlled-stress rheometer (AR1000, TA Instruments) fitted with a parallel plate measuring system (4 cm diameter, roughened surface, 0.5 mm gap) will be used. This part will be divided in three sections:

- Study of the flow behavior of the crude oils below their pour point temperatures. The basic rheological characteristics of waxy crude oils will be evaluated by studying the viscosity behavior as a function of shear rate and temperature, to characterize their non-Newtonian behavior and thermal dependence. Measurements imposing shear stress ramps at constant temperature will be used to evaluate yield stress before and after flow start and to assess time-dependent aspects as flow starts.
- Rheological characterization of time-dependent and stress applied to the crude oils.
- Study of the Viscoelastic properties of the crude oils near their pour point temperatures. Oscillatory rheological tests at low strain amplitudes will be also used to provide information about both the viscous-like and the solid-like properties.

One other objective not listed above and very important is the carrying out of a literature survey to assess prior knowledge in the research area. This will be part of chapter three.

The chapters of the thesis are written such that they can be read independently with the general knowledge of the related background presented in this introduction. Due to this format, there may be some repetition of introductory material from chapter to chapter. The experimental details are given as they pertain to each chapter. An overview of the main chapters is given below.

Chapter 2. This chapter addresses the overview of the analytical techniques used to characterize the Libyan waxy crude oils and their waxes. Subjects include the evaluation of some important characteristics used in the oil industry, such as the pour point

temperatures, wax appearance temperatures and paraffin content of these oils as well as the characteristics of their waxes, in order to further contribute to a more detailed knowledge, and thus a better understanding, of the behavior of the oils, mainly with the purpose to explain the causes of the deposition during their production, transportation and storage.

Chapter 3. This chapter provides the study of the flow behavior of the oils, including the effect of temperature on the yield stress and viscosity, near the pour point temperatures, and also the effect of the stress applied and time on the crude oils while they are studied. Furthermore, the viscoelastic properties of oil gels near pour point temperatures are also analyzed. The stability and strength at low temperatures (below the pour point) have been established to understand the behavior of the crude and its solid deposits at low temperatures. This approach allowed to achieve a deeper understanding of the deposited solid phase (gelled oil) and get further knowledge about the parameters that cause the plugging of pipelines during flow (transportation)

In the last part of the thesis (**Chapters 4)** final conclusions as well as proposals for upcoming research are established from the experimental results presented in the previous chapters. The experimental approaches used in this dissertation were found to be well suited to develop a better understanding of the flow and viscoelastic characteristics and low temperature behavior of the Libyan waxy oils and their solid deposits with a respectable predictive ability that will allow an easy evaluation and optimization of the operating variables and process configurations, what is clearly of interest for the oil companies. Recommendations for future developments of the work plan show that additional work in the field of the characterization of crude oils should still be performed. More specifically some other techniques may be used to get more information about the physical and chemical nature of the oils and their waxes and use the results from the thesis to develop a reliable deposition models for Libyan waxy crude oils as new contribution, are proposed.

1.3 References

1. Theyab, M.A. and Diaz, P., 2016, October. Experimental Study on the Effect of Spiral Flow on Wax Deposition Thickness. In *SPE Russian Petroleum Technology Conference and Exhibition*. Society of Petroleum Engineers.

2. Sansot, J.M., Pauly, J., Daridon, J.L. and Coutinho, J.A., 2005. Modeling high-pressure wax formation in petroleum fluids. *AIChE journal*, *51*(7), pp.2089-2097.

3. Espada, J.J., Coutinho, J.A. and Pena, J.L., 2010. Evaluation of methods for the extraction and characterization of waxes from crude oils. *Energy & Fuels*, *24*(3), pp.1837-1843.

4. Coto, B., Coutinho, J.A.P., Martos, C., Robustillo, M.D., Espada, J.J. and Pena, J.L., 2011. Assessment and improvement of n-paraffin distribution obtained by HTGC to predict accurately crude oil cold properties. *Energy & Fuels*, *25*(3), pp.1153-1160.

5. Ji, H.Y., Tohidi, B., Danesh, A. and Todd, A.C., 2004. Wax phase equilibria: developing a thermodynamic model using a systematic approach. *Fluid Phase Equilibria*, *216*(2), pp.201-217.

6. Najah, T., El-Moudir, W., Libyan crude oils, their characteristics and suitability for further processing. Presented at the OAPEC/IFP Seminar, Rueil-Malmaison, France, June 2006.

7. Etoumi, A., 2007. Microbial treatment of waxy crude oils for mitigation of wax precipitation. *Journal of Petroleum Science and Engineering*, *55*(1), pp.111-121.

8. Mirante, F.I. and Coutinho, J.A., 2001. Cloud point prediction of fuels and fuel blends. *Fluid Phase Equilibria*, *180*(1), pp.247-255.

9. da Silva, J.A.L. and Coutinho, J.A., 2004. Dynamic rheological analysis of the gelation behaviour of waxy crude oils. *Rheologica Acta*, *43*(5), pp.433-441.

10. Coutinho, J.A., Knudsen, K., Andersen, S.I. and Stenby, E.H., 1996. A local composition model for paraffinic solid solutions. *Chemical engineering science*, *51*(12), pp.3273-3282.

11. Jennings, D.W. and Weispfennig, K., 2006. Effect of shear on the performance of paraffin inhibitors: coldfinger investigation with Gulf of Mexico crude oils. *Energy & fuels*, *20*(6), pp.2457-2464.

12. Hoffmann, R., Amundsen, L., Huang, Z., Zheng, S. and Fogler, H.S., 2012. Wax deposition in stratified oil/water flow. *Energy & Fuels*, *26*(6), pp.3416-3423.

13. Venkatesan, R., Östlund, J.A., Chawla, H., Wattana, P., Nydén, M. and Fogler, H.S., 2003. The effect of asphaltenes on the gelation of waxy oils. *Energy & fuels*, *17*(6), pp.1630-1640.

2 Characterization of the crude oils and their waxes

2.1 Abstract

The prediction of wax formation and the understanding of the physicochemical characteristics of the wax phase are of major importance in flow assurance. The characterization of the oil and waxes can provide useful estimates of the parameters and processes required for operational engineering developments and/or physical modifications to the processing of crude oils, aiming at the reduction of costs of production and transportation.

Five Libyan crude oils and their waxes were characterized using various experimental techniques. Waxes were extracted using the Universal Oil Products (UOP) 46-64 method and purified by column chromatography. Differential scanning calorimetry was used to study the wax appearance temperature for these crude oils. Extensive information about the structural composition of these waxes was acquired using ^{13}C nuclear magnetic resonance spectroscopy (^{13}C-NMR), and information regarding the crystalline structure of these waxes was obtained using X-ray diffraction (XRD).

This study shows that the five Libyan crude oils studied have wax contents between 8 and 24 wt % with WAT in the range of 22.5-68.2 °C. The isolated waxes are shown to be paraffinic (macrocrystalline wax) with an orthorhombic structure.

2.2 Introduction

The heavy saturated fraction of crude oil, known as wax, tends to precipitate during the extraction and transport of crude oils as a result of the temperature (T) and pressure drop (P) of the fluid. As soon as the P-T conditions fall within the solid region of the phase envelope, i.e., the temperature of the oil falling below the wax appearance temperature (WAT), there will be formation of deposits on the reservoir or pipelines. The wax deposition causes the plugging of pipelines and clogging of transport equipment, being a well-known and expensive problem in the petroleum industries [1, 2]. A better understanding of the oil composition and the paraffinic hydrocarbons present in the crude oils can help face this problem both preventively and providing remediation whenever necessary. Several useful analytical techniques have been proposed in the

petroleum industry to study the petroleum fluid characteristics in general, and they can provide adequate information concerning the wax formation to facilitate production developments and thus avoid shutdowns and operational problems, which cost billions of dollars per year during oil production and transportation [3]. Although predictive models are available today for wax formation [4, 5] and deposition [6, 7] in crudes, they always require detailed compositional knowledge of the oils for an adequate performance.

As mentioned before the purpose of the study is to evaluate the characteristics of five different Libyan crude oils, as well as their waxes. These oils are named Remal, Sarir, Sedra, Bouri, and Faregh.

In practice, the characterization of the oils and their waxes can be achieved through various physicochemical and compositional analyses, such as American Petroleum Institute(API) gravity and viscosity, WAT, wax content, and pour point, and further characterization of the waxes by gas chromatography(GC), differential scanning calorimetry (DSC), nuclear magnetic resonance (NMR), and X-ray diffraction(XRD), among others [8,9]. The information obtained by these techniques can be of great importance to explain the causes of wax deposition and to be able to understand, predict, and prevent it during transportation, production, and storage of petroleum. In this work, a number of these techniques were used to characterize the five Libyan crudes under study. The WAT was measured by DSC; the wax content was measured by the Universal Oil Products (UOP) 46-64 method; and the waxes recovered were further purified by column chromatography. The purified waxes were then analyzed by GC, DSC, NMR spectroscopy, and XRD spectrometry for a full characterization of their nature, as discussed below.

2.2.1 Wax Structure

Crude oils are the largest single source of petroleum waxes. Figure 2.1 show examples of these hydrocarbons in the form of structural formulas [10].

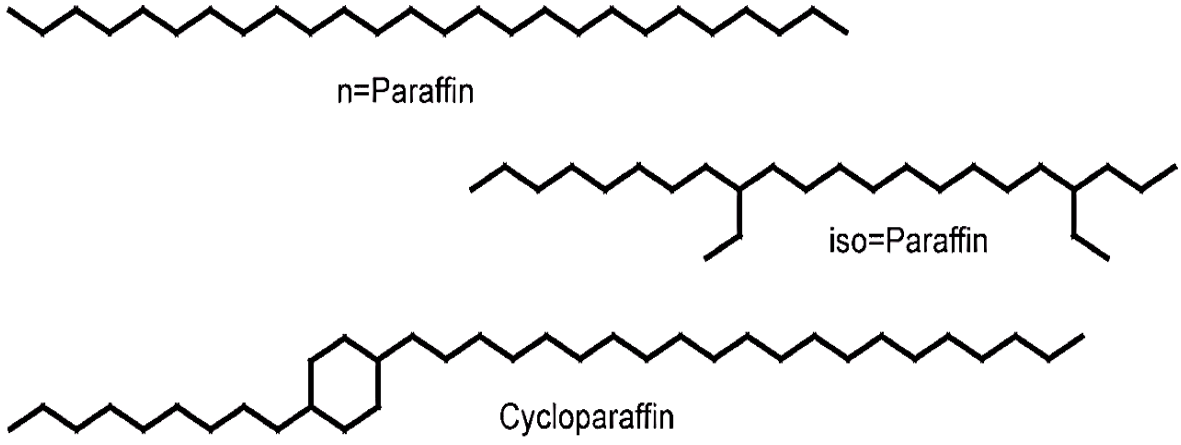

Figure 2.1 Typical structures of petroleum waxes

Petroleum waxes are generally classified as paraffin wax and microcrystalline wax. Paraffin wax is essentially a mixture of normal alkanes; whereas, microcrystalline wax is a mixture that contains, in addition to straight-chain paraffins, iso and cycloparaffins. Among these, paraffin wax is the major constituent of most solid deposits from crudes. **Table2.1** shows typical compositions and properties of paraffin and microcrystalline waxes [10].

Table 2.1. Typical composition and properties of paraffin and microcrystalline waxes.

	Paraffin Waxes	Microcrystalline Waxes
Normal paraffins, Wt.%	**80-95**	**0-15**
Branched paraffins, Wt.%	**2-15**	**15-30**
Cycloparaffins, Wt.%	**2-8**	**65-75**
Melting point range (°C)	**50-65**	**60-90**
Average molecular weight (gm/gmol)	**350-430**	**500-800**
Typical carbon number range	**18-36**	**30-60**

2.2.2 Paraffin wax chemistry

Paraffin wax are normal (straight – chain) or branched alkanes of relatively high molecular weight (C_{18} to C_{70}) represented by the general formula C_nH_{2n+2}. They have rather high melting points (C_{18}; 28°C to C_{60}; 102°C), and low solubilities in hydrocarbons. Pure paraffin deposits are mixtures of these alkanes and consist of very small crystals that usually agglomerate to form solid particles. (The term wax usually refers to solid paraffin). The wax varies in consistency from a soft mush to a hard, brittle material, increasing hardness as the amount of long chain alkanes also increases. Paraffin waxes are soluble in most liquid petroleum fractions, and their solubility generally decreases with an increase in molecular weight. They are soluble in both aliphatic and aromatic petroleum derivatives [11].

2.3 Experimental procedures and equipment

This section deals with the methods of preparing the samples and those analytical techniques used to evaluate the characteristics of the chosen five Libyan crude oils as well as their waxes.

2.3.1 Crude oil characterization

2.3.1.1 Viscosity and density

The viscosity and density measurements were carried out using an Anton Paar Viscometer (Figure 2.2), Model SVM3000, according to ASTM D 445-06 and ASTM D 5002-99 respectively[12], at the temperatures of 40 and 80 °C.

The SVM 3000 measures the dynamic viscosity [mPa.s] and the density of the sample and calculates the kinematic viscosity [mm^2/s] from these values. Kinematic viscosity (v) is defined as the ratio between the dynamic viscosity and the density of the fluid (ρ).

The standard S3 from Paragon scientific was used to calibrate the viscometer. The samples were heated above the Wax Appearance Temperature before the viscosity measurements to make sure that all wax particles were dissolved. Syringes were used to inject the samples into viscometer. A small sample volume, about 2.5 mL were injected slowly and continuously to the measuring cell until a drop emerges from the opposite end of the tube. After reaching the set temperature, the viscosity and density were read.

Figure 2.2 Anton Paar Viscometer, SVM 3000

2.3.1.2 API Gravity

The petroleum industry uses American Petroleum Institute gravity (API) as the preferred gravity scale to estimate the quality of a crude oil. It presents an approximate indication of the amount of low-boiling fractions contained in crude oil, i.e., crude oil with higher API gravities are expected to have a higher amount of low boiling components obtained on distillation of the crude oil, while crude oils with lower API gravity, will have higher quantities of residue.

The crude oils are sorted using the API gravity as **Table 2.2** displays. The highest commercial price is for the oils that have API gravity of 40-45 degrees. The values outside this range have a lower commercial price. The values of API Gravity for each crude oil were estimated based on the following equation using density values at 40 °C except for Remal that used values at 80 °C due to its high pour point:

$$\mathrm{API} = \frac{141.5}{\mathrm{SG}} - 131.5 \qquad \textbf{(2.1)}$$

Where SG is the oil specific gravity:

$$SG = \frac{\rho_{oil}}{\rho_{H_2O}} \qquad \textbf{(2.2)}$$

Where ρ_{oil} is the density of the oil and ρ_{H_2O} is the density of water.

Table 2.2 Crude oil sorting using API gravity

Crude oil	API gravity (°)
Light	>31.1
Medium	22.3-31.1
Heavy	<22.3
Extra- heavy	<10

2.3.1.3 Wax appearance temperature (WAT)

Thermal analysis techniques can be applied to measure the heat flow and temperatures associated with transition in materials as function of time and temperatures. DSC is one of the most popular and widely used thermal methods for predicting the wax appearance temperature of petroleum due to the high enthalpies of crystallization of the paraffins [8].

The WAT is the temperature at which some heavy paraffinic molecules start to precipitate from solution. It is considered as one of main guidelines for system design, production operations, and the planning of the exploration of a reservoir [8].

To measure the WAT, crude oil samples of about 10 mg, were heated to 30 K above their pour point temperatures and then cooled with a cooling rate of 1 or 3 K /min to evaluate the effect of the cooling rate on the WAT. Thermal characterization of the crude oils (WAT) was carried out on a Mettler DSC822e (Figure 2.3) calibrated with indium and flushed with dry nitrogen. The samples used weighed between 8.3 and 21.8 mg.

Figure 2.3 Differential scanning calorimetry, Mettler DSC822e

Three runs were carried for each oil, cooled at two different rates (1 and 3 °C/min), and average results are reported. The WAT was here taken as the onset temperature of the exothermal peak observed.

2.3.1.4 Pour Point

The pour point of a crude oil is the temperature at which the oil gels due to the crystallization of waxes and loses its flow characteristics. The pour point measurements of waxy crude oils are vital to address pipeline gelling and restart issues.

Pour point temperatures of the crude oils were measured using the standard test method for pour point ASTM D97– 06 [12] where the oils are first heated up and cooled down at a specified rate and examined for flow characteristics at intervals of 3°C. The observed temperature was recorded when no motion is detected while the jar is tilted horizontally for 5s and 3°C is added to the observed temperature (Figure 2.4) and the result is the pour point temperature.

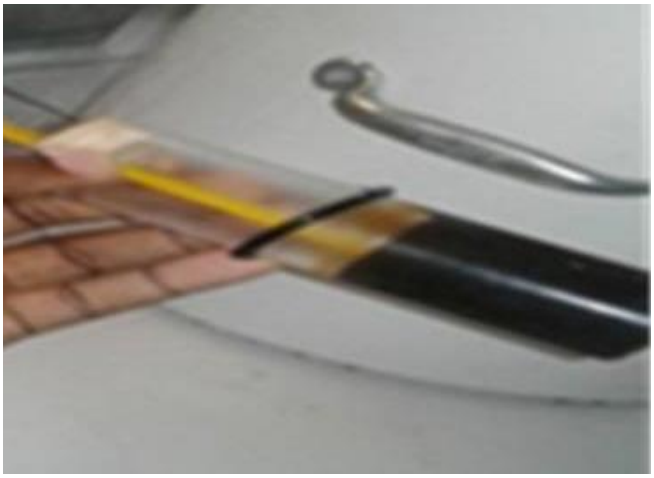

Figure 2.4 Crude oil sample at pour point

2.3.1.5 Water content

The water content of the oils was evaluated in the oil samples as received using a Metrohm 831 Karl Fischer (KF) coulometer [13].

2.3.1.6 Wax content

As the composition, type and properties of the waxes precipitating from a crude oil differ with the crude oil source, it is important to extract them out of its hydrocarbon matrix in order to evaluate their chemical composition and structural characteristics. The UOP 46-64 method [14] was used to extract the wax from the crude oil. Circa 2 g of crude oil was dissolved in 500 ml of petroleum naphtha and 15 g of fuller's earth were added to the solution. The mixture was then filtered and evaporated. Finally 200 ml of a mixture 1:3 of petroleum naphtha and acetone were added to the solution and the liquid was chilled to about -17 °C and filtered by cold filter funnel, after which the sample was washed with hot naphtha and the petroleum naphtha evaporated to recover the wax. This was weighed and the wax content evaluated.

2.3.1.7 Molecular weight

The average molecular weight of the crude oils was determined by cryoscopic depression of xylene by the relation

$$M_w = \frac{1000 k_f m_{oil}}{\Delta T_f m_{xyl}} \qquad \textbf{(2.3)}$$

Where:

k_f is the freezing point depression constant of xylene (4.3 Kg. °C/mole), m_{oil} is the weight of the crude oil (gm), m_{xyl} is the weight of xylene (gm) and

$\triangle T_f$ = freezing point of xylene(°C) – freezing point of the mixture [crude oil& xylene] (°C)

2.3.2 Wax characterization

After a preliminary characterization of the crude oils under study, their waxes were extracted as mentioned above and were further purified by cleaning the waxes using a silica gel column to remove the polar material that remains after precipitation. The wax samples were dissolved in n-hexane and passed through a 50 cm silica chromatographic column. The procedure was based on the method described by Musser and Kilpatrick [9].

2.3.2.1 Gas chromatography

Gas chromatography is one of the analytical methods used to provide quick qualitative identification of the composition of crude oils and the quantification of the distribution of n-alkanes and non-n-alkanes within each single carbon number group present in waxes [15]. In this study a Varian gas chromatograph (CP3800) with a flame ionization detector (FID) was used for the characterization of the wax composition [Figure 2.5]. A capillary column CP-5, 30 m long and with 0.32 mm internal diameter and 0.25 µm film thickness, was used. The wax was dissolved in CS_2, and the samples were injected into the column using an auto-sampler, with the injector at a temperature of 250 °C, with a split/splitless ratio of 1:50. The detector temperature was 300 °C. Analysis were performed under a helium flow rate of 1.2 mL/min and a temperature program of 40-280 °C at 12°C/min and held for 5 min at the highest temperature.

Figure 2.5 Varian gas chromatograph (CP3800)

2.3.2.2 Elemental Analysis

Elemental analysis (C, H, N, and S) for the purified waxes were carried out using a CHNS analyzer (Leco TruSpec 630-200-200) as this technique uses a combustion process to break down substances into simple compounds which are then quantified.

2.3.2.3 Thermal characterization by DSC

Mettler DSC822e was used in this study to measure the melting temperature and enthalpies for the waxes. The heat of fusion and melting point temperature were determined from the melting point curve. The area under a melting endotherm is proportional to the latent heat of fusion of the sample. The heating rate was 3 K/min for all wax samples.

2.3.2.4 ^{13}C-NMR Spectroscopy

Nuclear magnetic resonance spectroscopy (NMR) has become the preeminent technique to identify functional groups of organic compounds. It is documented as a powerful technique for chemical analysis [16] and can be employed as a successful analytical analysis for the characterization of petroleum waxes [17].

In this study Carbon NMR was used to provide a value for the relative proportions of aliphatic and aromatic carbons in the wax. Quantitative ^{13}C NMR spectra were collected on a Bruker Avance 300 spectrometer operating at 75.47 MHz.

Wax samples were diluted at 50% in CDCl3, and the spectra were recorded at 295 K with tetra methylsilane (TMS) as the internal reference. The inverse gate decoupling sequence, which allows for quantitative analysis and a comparison of signal intensities, was used with the following parameters: pulse angle, 30; acquisition time, 3.48 s; relaxation delay, 60 s; data points, 32000; and scans, 5000.

Information concerning the different types of carbon present is based on the works by Carman et al. [17] and Sperber et al., [18] and the aromatic content is quantified according to ASTM D5292-99[12] .

2.3.2.5 X-ray diffraction Spectra.

In order to gain insight into the wax crystalline structure X-ray diffraction was here used. Diffractograms of the waxes at room temperature were acquired on Philips X'Pert equipment, which operates in the reflection mode with Cu KR radiation (λ=1.5406 A °).

Diffraction data were collected in a 2θ range from 2 to 60, with a step of 0.02 and a time per step of 2 s, with incident and diffracted beam anti-scatter slits of 1, divergence slit of 1, and receiving slit of 0.1 mm, on curved graphite diffracted beam monochromator.

2.4 Results and discussion

2.4.1 Crude Oil Properties.

Analyses were carried out to characterize the five crude oils studied in this work. Specific gravity (SG), API gravity, viscosity, pour-point temperature, wax content, average molecular weight, and water content of each crude oil were measured as described above, and the results are reported in **Table 2.3**.

Table 2.3. Physical Properties for the Studied Libyan Crude Oils

Oil samples	Wax content (wt%)	Pour point (°C)	Kinematic Viscosity /mm^2 s^{-1}		Density/g cm^{-3}		Mw/	API gravity,	Water content
			@40°C	@80°C	@40°C	@80°C	gm/gmol	(°API)	(ppm)
Remal	18.7	51	------	18.68	----	0.886	331	25.1	-----
Bouri	15	12	20.47	7.22	0.883	0.860	249	25.7	820
Sarir	13.6	24	13.56	5.27	0.829	0.810	244	35.6	1327
Sedra	8	0	5.25	-----	0.827	------	200	36	206
Faregh	24	21	4.44	2.55	0.79	0.772	217	43.4	576

The high pour point of Remal precluded the measurement of the viscosities and densities at 40 °C and also the water content.

The oil characterization shows that the crudes studied here are medium or light crude oils with high wax content. As expected, the wax content correlates well with the API gravity and the viscosity of the crudes at 40°C. The crudes (with exception of Faregh) with a larger wax content present lower API gravities and higher viscosities.

The WATs for the five oils were measured using DSC as the onset temperature of the exothermal peak observed upon cooling. Figure 2.6 shows an example of a thermogram generated by a DSC for Bouri oil at cooling rate of 3°C.min^{-1}. WAT is seen as a deviation from the base line of the thermogram.

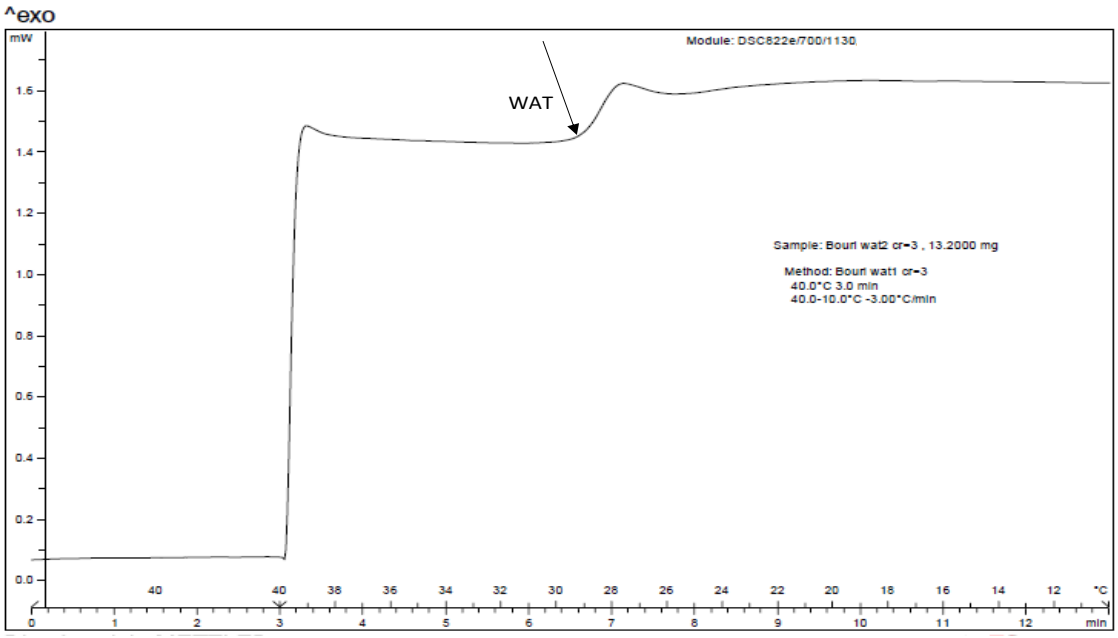

Figure 2.6 DSC thermogram of Bouri oil [Cooling rate= 3°C.min^{-1}]

Results for the WAT measured at two cooling rates are reported in **Table 2.4**.

Although the WATs measured at 1 K/min are consistently higher than at 3 K/min, the difference between the values obtained at the two cooling rates are in general within the uncertainty of the measurements, estimated as 2 times the standard deviation. It is also quite remarkable that, although the WAT would be expected to increase with the wax content of the oil, there seems to be no direct relation between the two, with Faregh presenting one of the highest wax contents, while it is WAT is inferior to those of Remal and Sarir. This is a clear indication that the WAT is dependent upon not only the wax content but also on wax composition, as previously suggested [8]. The pour point, however, displays a very good linear dependency upon the WAT for all fluids of 23±3 K below the measured WAT. The WAT is thus, for these crudes, a good indicator of their pour point.

Table 2.4. Wax appearance temperature at two cooling rates for the studied oils. Uncertainty assigned is two times standard deviation of the measurements

Crude oil samples	WAT/°C @ 3 K/min	WAT/°C @ 1 K/min
Remal	67.3±1.92	68.2±0.38
Bouri	29.2±0.54	29.7±0.28
Sarir	48.7±0.36	49.6±0.10
Sedra	22.5±0.04	23.2±0.88
Faregh	42.1±0.22	43.1±0.14

2.4.2 Wax Characterization

2.4.2.1 Wax Composition

The wax composition was determined by GC-FID analysis according to the procedure described above. The n-alkane distributions and the content of non-n-alkanes of each oil are reported in **Table 2.5**.

The results indicate that all waxes extracted are highly paraffinic macrocrystalline waxes. They vary from being essentially made up of n-alkanes, as is the case for Sedra and Faregh, to oils, such as Bouri, that, although highly paraffinic, present a non-n-alkane content slightly above 20 wt%. The two other oils, Remal and Sarir, present waxes very rich in n-alkanes, with the n-alkane content above 90 wt %.

To obtain more detailed information on the composition of the waxes, in particular, to evaluate the amount of tertiary and aromatic carbons present in the wax, elemental analysis and ^{13}C NMR were used. The peaks on the NMR spectra were assigned to carbon types according to the suggestion of Carman et al. [17] and Sperber et al. [18].

The elemental analysis, reported in **Table 2.6**, presents H/C ratios higher than 2 for all waxes, except Sedra, with an H/C ratio of 1.95. These values are typical of macrocrystalline paraffinic waxes with a high degree of saturation.

Table 2.5. Composition (wt %) of the waxes studied.

	Remal	Bouri	Sarir	Sedra	Faregh
C11		0.213			
C12		0.176			
C13		0.316			
C14		0.735			0.189
C15	0.405	1.763	0.46	0.394	0.480
C16	0.65	2.183	0.92	0.574	0.860
C17	1.03	2.865	2.065	1.148	1.233
C18	1.915	4.063	4.182	2.226	3.498
C19	3.598	5.083	7.054	4.831	4.543
C20	5.453	5.983	9.14	8.159	7.921
C21	7.679	6.207	10.443	10.489	11.267
C22	8.371	6.195	9.979	10.961	11.474
C23	8.804	5.392	9.577	10.3	9.834
C24	8.395	5.16	7.754	9.034	9.356
C25	8.331	4.203	7.04	7.67	6.949
C26	7.71	3.839	5.674	6.043	6.338
C27	7.378	3.297	4.662	5.503	5.058
C28	6.12	3.8	3.797	4.753	4.561
C29	5.477	2.816	3.236	4.07	3.427
C30	4.163	2.504	2.44	3.364	2.873
C31	3.126	2.259	1.713	2.646	1.928
C32	2.158	1.848	1.242	1.927	1.648
C33	1.595	1.554	0.989	1.535	1.127
C34	0.319	1.374		1.156	1.113
C35		1.228		1.006	0.896
C36		0.736			0.485
C37		0.653			
C38		0.546			
C39		0.354			
C40		0.351			
Total n-alkanes	*92.68*	*77.7*	*92.37*	*97.79*	*97.06*
Iso & cyclo alkanes	*7.32*	*22.3*	*7.63*	*2.21*	*2.94*

Table 2.6. Elemental analysis and H/C ratio of the waxes extracted from the oils.

	C (wt%)	H (wt%)	H/C (mol/mol)
Remal	85.28	14.72	2.07
Bouri	85.52	14.48	2.03
Sarir	85.66	14.34	2.01
Sedra	86.02	13.98	1.95
Faregh	85.09	14.91	2.10

The aromatic carbon content was estimated according to the ASTM D5292-99[12] using the following equation:

$$\% C (Ar) = [A/ (A + B)]* 100 \quad \textbf{(2.4)}$$

Where A is the peak area of the aromatic portion of the spectra (100-170 ppm), while B is the peak area of the aliphatic portion of the spectrum (10-70 ppm).

The results are reported in **Table 2.7**, where it can be seen that Sedra has the highest content of aromatic carbon, with the other waxes presenting an aromatic carbon content equal or inferior to 1%. A good correlation was observed between the H/C ratio and the aromatic carbon content obtained from ^{13}C NMR Spectra, allowing for an explanation for the lower H/C ratio observed for Sedra in the elemental analysis.

Using the peak identification mentioned above, an identification of the different carbon types was carried out and is reported in **Table 2.8** using the nomenclature suggested by Sperber et al. [18].

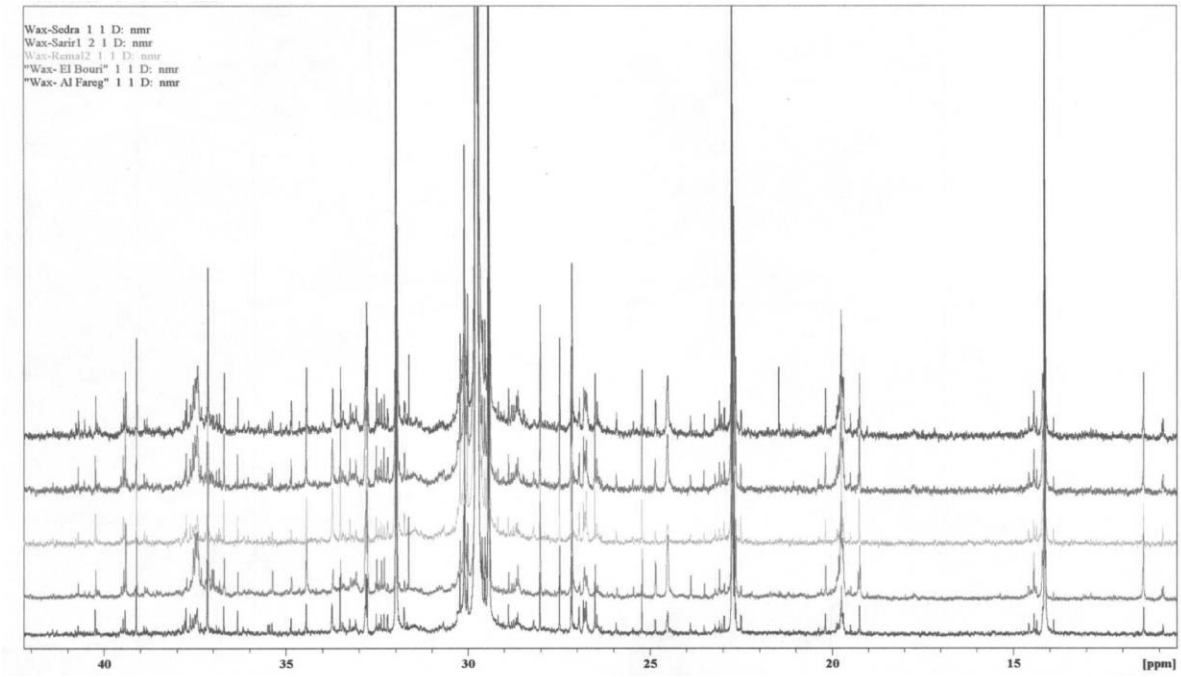

Figure 2.7 ^{13}CNMR spectra for the waxes studied in the aliphatic region. The spectra correspond, from top to bottom, to Sedra, Sarir, Remal Bouri and Faregh

Table 2.7. Total aromatic carbon content of the waxes under study measured by ^{13}C-NMR

	Remal	Bouri	Sarir	Sedra	Faregh
% C(Ar)	0.7	1.1	0.9	1.8	0.6

The ^{13}C NMR spectra show that the waxes are formed essentially by alkyl chains with very limited amount of carbons in cyclic structures (CN<0.5%) or tertiary carbons (CH), with the exception of Bouri, with a content of tertiary carbons close to 1.5%. The tertiary carbon content also seems to be related to the higher content of non-identified structures in Bouri wax. This indicates that the content of isoparaffins in Bouri must be higher than in the other waxes, as also suggested by the GC-FID analysis, and it must have some impact on the crystalline structure of the wax.

Table 2.8. Characterization of the aliphatic portion of the waxes by ^{13}C-NMR

Structure		ppm	Remal	Bouri	Sarir	Sedra	Faregh
α-CH_3	CH3	14.14	5.073	4.134	5.329	4.474	5.861
$1B_1$		20.06	0.048	0.23	0.116	0.144	0.152
$1B_2$		11.46	0.07	0.36	0.123	0.142	0.076
$1B_{3-6}$		14.54	0.053	0.111	0.077	0.068	0.06
β-CH_2	CH2	22.85	5.381	4.46	5.497	4.72	5.96
γ-CH_2		32.16	5.691	4.301	5.695	4.839	6.301
δ-CH_2		29.9	53.966	39.409	52.189	49.896	56.693
αδ^+-B_1		37.48	0.193	0.557	0.402	0.319	0.249
αδ^+-B_2		34	0	0.071	0	0	0
αδ^+-B_{3-6}		34.48	0.083	0.519	0.17	0.199	0.119
βδ^+-B_1		27.26	0	0	0	0	0
βδ^+-B_{2-6}		27.21	0.112	0.32	0.496	0.465	0.12
γδ^+-B_1		30.28	0.445	0.557	0.517	0.505	0.384
γδ+-B_{2-6}		30.39	0	0.024	0	0	0
$2B_2$		27.59	0.148	0.296	0.185	0.255	0.16
CHB_1	CH	33.16	0.094	0.298	0.148	0.133	0.075
CHB_2		34.61	0.036	0.154	0.092	0.114	0.045
CHB_{3-6}		37.01	0.41	0.964	0.435	0.496	0.32
CN1	CN	26.84	0.093	0.145	0.094	0.102	0.113
CN2		33.85	0.271	0.286	0.285	0.261	0.212
% Identified			*72.167*	*57.196*	*71.851*	*67.131*	*76.901*
% Not identified			*27.833*	*42.804*	*28.149*	*32.869*	*23.099*
% Terciary carbon			*0.54*	*1.416*	*0.675*	*0.743*	*0.44*

2.4.2.2 Melting characteristic of the waxes

DSC was used to further characterize the structure of the waxes through the determination of their melting temperatures and heats of fusion. Panels a-e of Figure 2.8

show the thermograms for the various wax samples studied, while **Table 2.9** presents the measured melting point temperatures, as well as the heats of fusion.

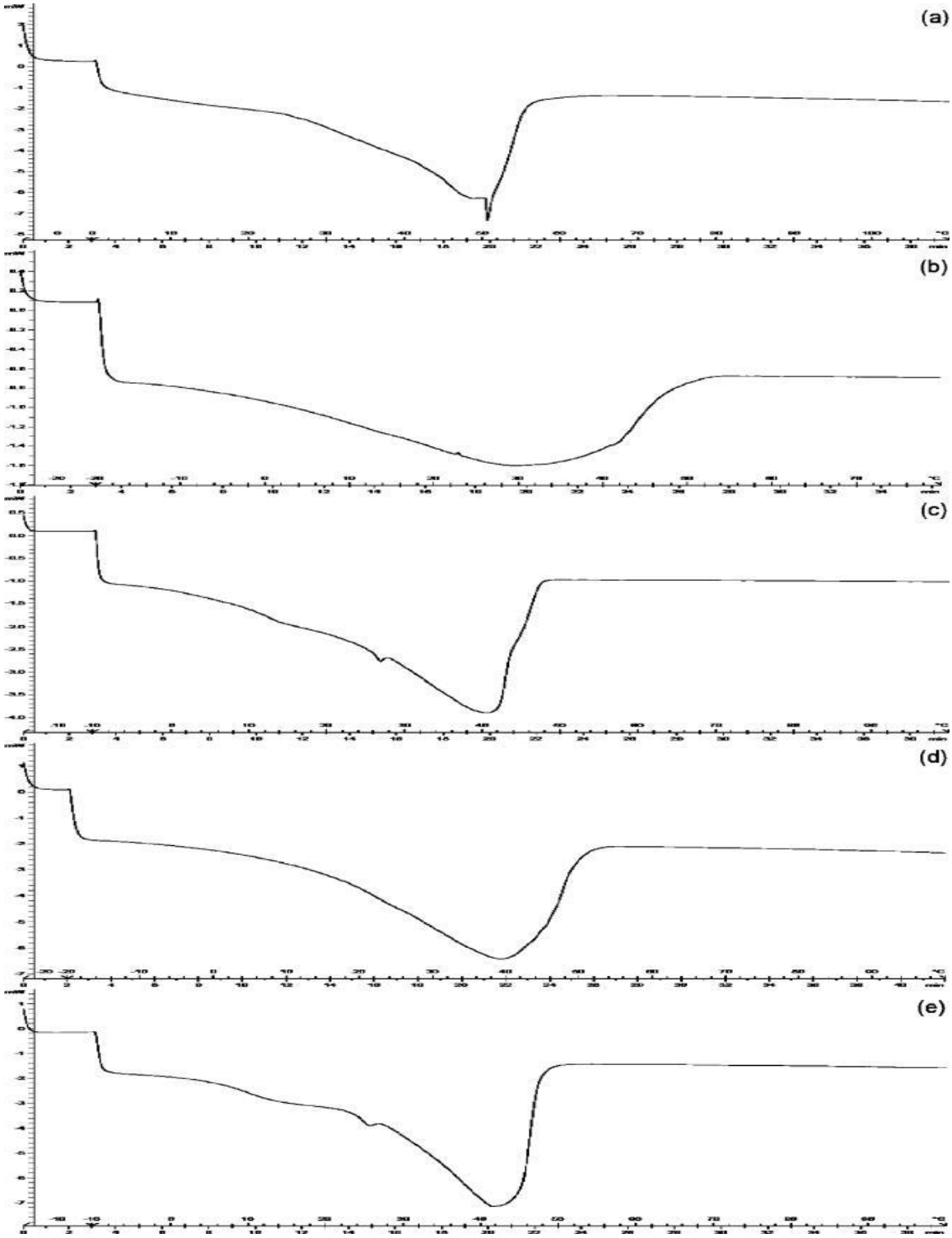

Figure 2.8 Thermograms for (a) Remal, (b) Bouri, (c) Sarir, (d) Sedra, (e) Faregh

Table 2.9. Melting point temperatures and heats of melting for the waxes studied

	Melting Temperatures / °C	Heat of melting / J g^{-1}
Remal	50.5	159.1
Bouri	30.2	83.0
Sarir	40.6	121.8
Sedra	39.2	119.7
Faregh	41.1	142.9

These values show how the thermograms are affected by the wax composition. Remal, which presents the higher concentration of heavy n-alkanes, displays a sharp peak with a narrow melting range and high heat of fusion. As the non-n-alkane content increases, the melting range becomes broader and the heats of fusion decrease. Bouri, with its relatively high content of branched paraffins, presents a very broad melting peak and the lowest heat of melting (83.0 J/g), indicating that this wax has a much lower crystallinity than the other waxes. A small secondary peak is observed for Faregh and Sarir at temperatures close to 25°C, which may be due to a solid-solid phase transition of n-alkanes. The large heats of melting observed are typical of macrocrystalline waxes.

A good correlation between the measured melting points and heats of fusion is observed for these waxes, with higher melting points corresponding to the higher heats of fusion. A good correlation is also observed between the heats of fusion/melting temperatures and the content of tertiary carbon reported in Table 2.6. The lower the tertiary carbon content, the higher the crystallinity of the wax and, thus, its melting temperature and heat of fusion.

2.4.2.3 XRD of the Waxes

To obtain information on the crystalline structure of the waxes extracted from the oils under investigation, XRD was performed here on the purified wax samples. The diffractograms of the five waxes are presented in Figure 2.9. The crystallinity of the samples can be associated with the 2θ=35-45º region. Remal and Faregh are the most crystalline samples, while Bouri is the less crystalline sample. This is in good agreement with the observed heats of fusion. The low crystallinity of Bouri seems to be related with the large content in tertiary carbon of the Bouri waxes, as observed from the NMR spectra. Waxes with a higher iso-paraffin content present poor crystalline structures, and their mechanical properties are also modified [19]. These waxes are favorable from a flow assurance point of view because they are softer and easier to melt and, thus, remove from the pipelines by pigging.

To evaluate if a thermal treatment would have any effect on the crystalline habit of the waxes, diffractograms were collected for the purified wax samples and samples undergoing different thermal treatments. No differences in the crystalline habit were observed with the thermal treatments.

Given the high n-alkane content of all of these waxes, it is not surprising that they all exhibit very similar XRD patterns. Their crystalline habit can be identified with an orthorhombic structure common in normal paraffins [19, 20].

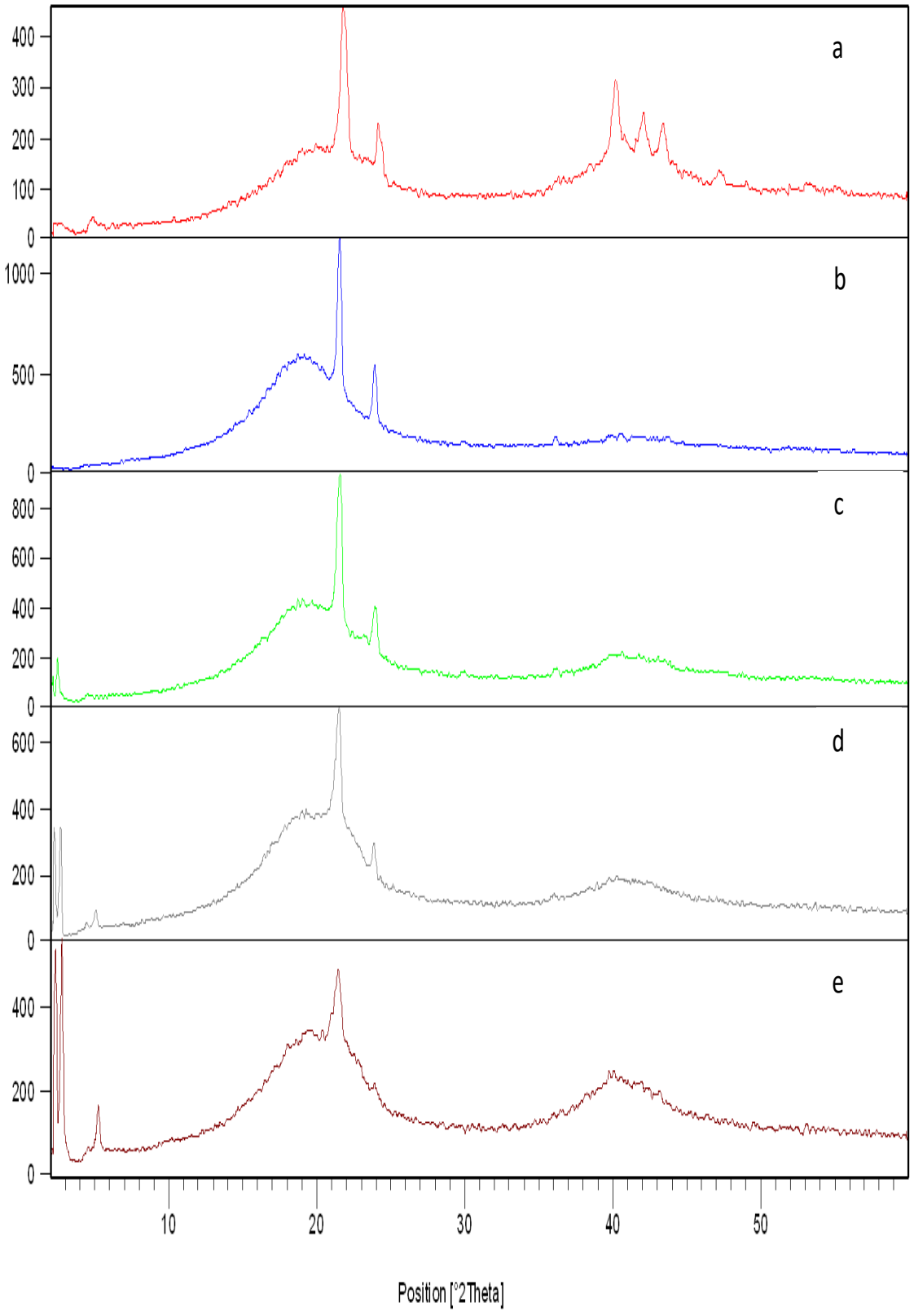

Figure 2.9 X-ray diffractograms of the studied waxes: (a) Remal, (b) Bouri, (c) Sedra, (d) Sarir, and (e) Faregh.

2.5 Conclusions

The characterization of waxy crude oils and their waxes is necessary to understand and predict their behavior and to avoid various problems during production, transport, and processing, such as plugging and clogging of pipelines. It is thus very important to obtain reliable information concerning the nature of waxes using a combination of various analytical techniques, because there is no single analytical method that can provide a complete picture of the chemical and physical nature of the wax. In this section, the characteristics of five Libyan waxy crudes, namely, Remal, Sarir, Sedra, Bouri, and Faregh, and their waxes were investigated.

Although the major characteristics of the oils seem to be in good agreement, displaying a good relationship between the average molecular weight, API gravity, viscosity, and wax content, it is shown here that the WAT is not just directly related with the wax content of the oil but also with its paraffin distribution. A correlation between the measured WAT and the pour points was also observed.

The results of ^{13}CNMR, elemental analysis, and GC-FID indicate, with a good agreement, that all of the studied Libyan crudes present macrocrystalline waxes composed of essentially straight-chain saturated paraffinic hydrocarbons as n-alkanes. The aromatic content in the waxes was marginal, with the largest value of 2% being presented by Sedra. The waxes from Bouri have a higher quantity of isoparaffins than the other samples, with an important impact on their crystalline structure and, consequently, their melting characteristics. The coherence between the results obtained from different analytical techniques helps to identify the most adequate, to provide the necessary information with lower effort and cost.

2.6 References

1. Sanjay, M., Simanta, B. and Kulwant, S., 1995. Paraffin problems in crude oil production and transportation: a review. *SPE Production & Facilities*, *10*(01), pp.50-54.

2. Merino-Garcia, D. and Correra, S., 2008. Cold flow: A review of a technology to avoid wax deposition. *Petroleum Science and Technology*, *26*(4), pp.446-459.

3. DOE, University of Tulsa Embark on Wax Deposition Study, *Oil & Gas J*. 2001, *99,:56*.

4. Daridon, J.L., Pauly, J., Coutinho, J.A. and Montel, F., 2001. Solid-liquid-vapor phase boundary of a North Sea waxy crude: measurement and modeling. *Energy & fuels*, *15*(3), pp.730-735.

5. Coutinho, J.A. and Daridon, J.L., 2001. Low-pressure modeling of wax formation in crude oils. *Energy & fuels*, *15*(6), pp.1454-1460.

6. Coutinho, J.A., Edmonds, B., Moorwood, T., Szczepanski, R. and Zhang, X., 2006. Reliable wax predictions for flow assurance. *Energy & fuels*, *20*(3), pp.1081-1088.

7. Edmonds, B., Moorwood, T., Szczepanski, R. and Zhang, X., 2007. Simulating wax deposition in pipelines for flow assurance†. *Energy & Fuels*, *22*(2), pp.729-741.

8. Coutinho, J.A. and Daridon, J.L., 2005. The limitations of the cloud point measurement techniques and the influence of the oil composition on its detection. *Petroleum Science and Technology*, *23*(9-10), pp.1113-1128.

9. Musser, B.J. and Kilpatrick, P.K., 1998. Molecular characterization of wax isolated from a variety of crude oils. *Energy & Fuels*, *12*(4), pp.715-725.

10. Pedersen, K. S., Aa Fredenslund, and P. Thomassen. "Properties of Oils and Natural Gases-Gulf Publ." *Company, Houston* (1989).

11. Nelson, W.L., 1958. Petroleum Refinery Engineering McGraw Hill Book Company. *Inc. New York*.

12. American Society for Testing and Materials (ASTM). *Annual Book of ASTM Standards;* ASTM: West Conshohocken, PA, 2008; Vol. 05.01.

13. Freire, M.G., Gomes, L., Santos, L.M., Marrucho, I.M. and Coutinho, J.A., 2006. Water solubility in linear fluoroalkanes used in blood substitute formulations. *The Journal of Physical Chemistry B*, *110*(45), pp.22923-22929.

14. Universal Oil Products (UOP). UOP Method 46-64, Paraffin Wax Content of Petroleum Oils and Asphalts, UOP Co., Des Plaines,IL, 1964.

15. Roehner, R.M., Fletcher, J.V., Hanson, F.V. and Dahdah, N.F., 2002. Comparative compositional study of crude oil solids from the Trans Alaska Pipeline System using high-temperature gas chromatography. *Energy & fuels*, *16*(1), pp.211-217.

16. Batsberg Pedersen, W., Baltzer Hansen, A., Larsen, E., Nielsen, A.B. and Roenningsen, H.P., 1991. Wax precipitation from North Sea crude oils. 2. Solid-phase content as function of temperature determined by pulsed NMR. *Energy & fuels*, *5*(6), pp.908-913.

17. Carman, C.J., Harrington, R.A. and Wilkes, C.E., 1977. Monomer sequence distribution in ethylene-propylene rubber measured by 13C NMR. 3. Use of reaction probability model. *Macromolecules*, *10*(3), pp.536-544.

18. Sperber, O., Kaminsky, W. and Geissler, A., 2005. Structure analysis of paraffin waxes by 13C-NMR spectroscopy. *Petroleum science and technology*, *23*(1), pp.47-54.

19. Petitjean, D., Schmitt, J.F., Laine, V., Bouroukba, M., Cunat, C. and Dirand, M., 2007. Presence of Isoalkanes in Waxes and Their Influence on Their Physical Properties†. *Energy & Fuels*, *22*(2), pp.697-701.

20. Heyding, R.D., Russell, K.E., Varty, T.L. and St-Cyr, D., 1990. The normal paraffins revisited. *Powder Diffraction*, *5*(02), pp.93-100

3 Rheological characterization of the three waxy oils, Faregh, Sarir and Sedra

3.1 Abstract

A better understanding of waxy crude oil rheology is critical for developing flow assurance strategies based on thermal management, pressure management, chemical treatments, and mechanical remediation, to guarantee optimum productivity of crude oils from an oilfield. The goal of flow assurance is to ensure continuous flow of production under adverse conditions, such as the presence of precipitates or non-Newtonian behavior. Regarding flow assurance problems, faced in the petroleum industry incurred by the precipitation of wax molecules during the production and transportation in the field pipelines, it is required to understand the deposition of wax under flow conditions and wax gelation, to solve restart problem after shut-in period in order to overcome the challenges in production and transportation. This wax precipitation occurs at ambient temperature, typically 20-30 °C in Libya, and can occur during the transport from the well to the terminal through hundreds of miles of pipelines. This part of the work is thus aimed at providing elucidation concerning the rheological behavior of three waxy Libyan oils analytically characterized in the previous chapter.

As mentioned above in chapter 2, the Libyan crude oils under study are composed of straight-chain saturated paraffinic hydrocarbons as n-alkanes. These hydrocarbons create difficulties in the transportation through pipelines because of the deposition of a solid phase that causes their plugging. As a result of all these issues, this study was focused on understanding the flow behavior of the oils below their pour point temperatures. The flow characterization tests were done by applying ramped shear stresses within defined intervals and also by studying the effect of temperature on the yield stress and viscosity of the crude oils.

In order to develop further knowledge and understanding about the parameters that can influence the oils' flow behavior, the effect of stress applied to the crude oils during a specified time was also studied. In addition, the viscoelastic properties of the oils were also analyzed to understand the oils' structural properties and to explore the stability and strength of the crude oils gels before and after the flow was discontinued (near pour point temperatures).

3.2 Introduction

Crude oil is an important material, the life blood of modern civilization. However as mentioned in the previous chapters, highly waxy crude oils can cause significant problems during the production and transportation such as choked of a pipeline because of the precipitation and deposition of select wax components. If wax precipitates during cooling of pipeline the apparent viscosity of the waxy crude oil will be increased, and increases the energy requirements associated with transportation of the oil [1-3]. Often Newtonian viscous flow is still observed [4], however most waxy oils when processed at low temperatures will be affected by this problem. Some waxy oils have a pour point higher than 35 °C, such as the Remal waxy crude[2] studied in this work (51 °C) [5]. Clearly upon cooling, this creates a serious problem with the wax oil gelling and blocking the pipeline.

This chapter discusses important rheological characteristics of three selected Libyan waxy crude oils, with significant importance to the research problem under study. The huge economic importance of oil entire world industry has led to much work, over the years, on the wax deposition problem, as the main cause of pipeline chocking. The problem, which is an important scientific issue in oil industry, is here put in the context of the Libyan oil industry which is used as a case study for this research.

As stressed in the introduction of the first chapter, rheology is the key for understanding the flow of waxy crude oils and predicting the pressure required to start-up gelled pipelines. Thus, in this chapter, the principles of rheology and research works specifically related to the start-up pressure of waxy crude oils are presented and discussed.

Many works have been carried out by the oil industry on the different aspects of wax flow assurance problems. In order to address the significant investigation issues, a literature survey will be presented in the third section of this chapter: 'Overview and background of the wax deposition' related to the research problem which is the Rheology

[2] Work published in *Energy & Fuels* (2010), pp. 3101-3107 (full paper in Appendix B)

of waxy crude oils, and restart flow phenomena. The various phases of waxy crude transformation during cooling, and the rheological techniques and test procedures used in this study are discussed in details in the subsequent sections.

Following the Introduction and literature review aspects, the "Materials and methods" (section 3.9) describes the pre-treatment of the selected samples and the various experimental tests carried out for their rheological characterisation. Worth to note that the general physical characteristics of the oils such as pour point, wax content, API and wax appearance temperature, and related methods, were described in chapter two.

The next part (section 3.10) "Results and discussion" will be devoted to the obtained results and their discussion: important data obtained about the rheological properties of the crude oils, including the measurements of flow behavior, yield stress, mechanical behaviour and viscoelastic properties, are presented and discussed in this section. Finally (section 3.11) will present the Conclusions for this part of the research.

3.3 Rheology of waxy crude oil

Under particular conditions (high temperature, high pressures) the waxy crude oil acts as a Newtonian fluid with a low viscosity since the solubility of heavy paraffins is sufficiently high to keep them totally dissolved. Once the waxy oil flows through the pipelines, the paraffins begin to deposit on the pipe wall when the temperature decreases and falls below wax appearance temperature due to the cooler surroundings [1, 6]. Consequently, if the oil is further cooled below its pour point temperature, this leads to the formation of a network structure of gelled oil during transportation through long distance pipelines.

Gelled waxy oils often show rheological behavior characterized by the existence of yield stress. Specially, there exists a range of stresses beyond which the viscosity of the gelled system decreases by several orders of magnitude, but below which no flow arises [7, 8]. Therefore, in order to restart flow in the pipeline, much larger pressure drops are essential to guarantee the constant flow rate. This issue is often so challenging that field

workers will insulate and/or heat pipelines to prevent this cooling from occurring [9, 10]. However, the precipitation of wax in pipelines at ambient temperatures, below the oil's WAT, is a well-known phenomenon in petroleum industry. The wax build-up causes the choking of flow lines, equipment failure, plugged tubing flow lines and increasing man power attention, decreasing the production. The production and transportation of these waxy oils become a challenge because they exhibit a complex non-Newtonian flow behavior. With lowering temperature the wax gel layer grows rapidly in thickness originating a solid-like (gel) layer that grows into a plug that impedes the flow [1, 11]. (Figure 3.1). Although the wax deposition phenomenon has been known for over a century, the remediation costs continue to escalate with the expansion of exploration and production.

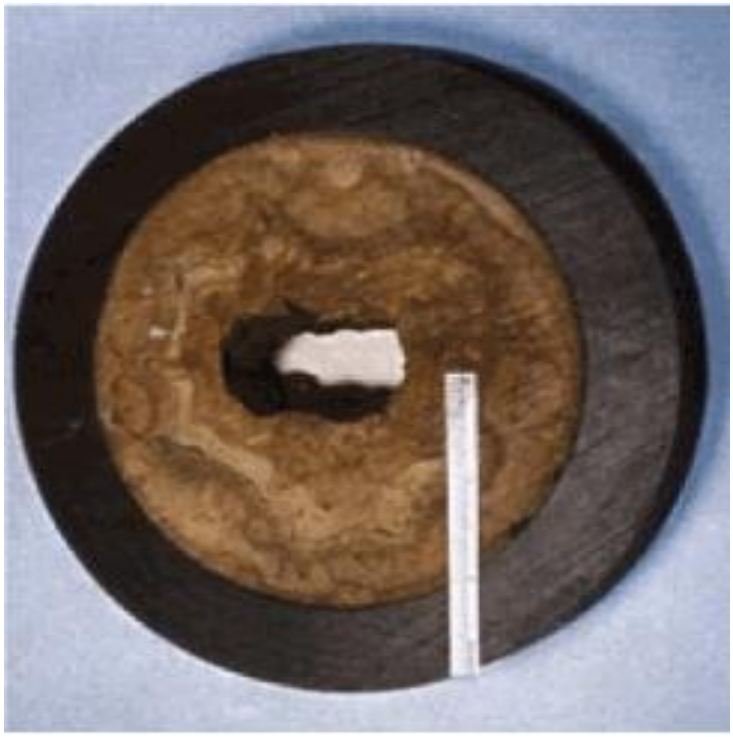

Figure 3.1 - Deposited wax in cross section area of a pipeline [1]

The preventive methods to minimize wax deposition (insulation of pipeline, injection of wax inhibitor, or combination of both) are costly and not always successful [1, 12]. In fact, it has been recognized that the available methods to solve wax deposition problems are still unsatisfactory for successful prevention and serious treatment of the problem, and new suitable methods are still needed. One of the most commonly corrective methods used in the fields is the use of a scraping device called a "pig". The pig is a solid

object which is launched into the pipeline and carried along by flow to scrape off the wax deposit. However, the pigging method cannot be utilized efficiently without a proper wax deposition prediction method, since sometimes it gets stuck inside the line (lodged) due to the existence of hard deposits making the situation even worse, as the production must be stopped in order to replace the plugged portion of the line, which is a severe costly problem. Another method is to use a fused chemical reaction with controlled heat emission [12-15] to remove the formed wax plug. Yet, it is critical to know the thickness profile and the wax fraction of the deposit as a function of axial location and time in order to use this technique successfully, since there could be unwanted local high temperature in the pipeline due to the failure of re-dissolving wax deposit. All these methods increase operating costs and the prediction of the characteristics of the paraffin deposits is of paramount importance to oilfield operators in their search for selecting and designing suitable economic remediation or deposit removal techniques. Consequently many works have been published in literature with considerable amount of work focused on the rheological behavior of waxy crude oils [16-28]. Within the oil industry, better understanding of the rheological behavior of waxy crude oils would facilitate the improvement of flow assurance, in order to achieve an economical and successful flow for crude oils in pipelines.

3.4 The yield stress of waxy crude oil

As stated earlier, once the temperature of the crude oil falls below the wax appearance temperature (WAT), wax crystals start to precipitate out of solution and a very rapid increase in viscosity indicates the onset of non-Newtonian shear thinning flow behavior [29-32]. The viscosity increase results in reduction of the effective capacity of the pipeline. Precipitated waxes produce severe problems such as deposition of wax crystallites on surfaces, high viscosity leading to pressure losses and very high yield stresses (that are time-dependent on the shear and temperature history of the crude), what demands the application of high stresses in order to defeat the gel strength of the waxy oil. [33-34]. Waxy crude oils cooled to a gelled solid-like state under static conditions (during a shut-down) typically exhibit a time-dependent Bingham plastic flow behavior during a restart situation where a constant shear stress (pumping pressure) is imposed on

the crude oil breaking down the gelled structure leading to decrease of the oil viscosity and an increase in the oil flow rate [35].

Many studies have been carried out to estimate the yield strength of the wax-oil gel and, ultimately, the pressure required to restart the plugged pipelines [17-20, 36-39]. However the yielding behavior of a wax-oil gel is a complicated process and various researchers have proposed different models to explain this phenomenon as it will be discussed in the next sections. Studies on this subject have demonstrated that the yield stress of waxy oils is influenced by thermal history, shear history, and fluid composition [40-50].

3.4.1 The effect of shear history

The effect of shear history on gel strength of waxy crude oils has been observed and studied by various researchers. Shear history includes both the shearing prior to cooling and shearing during the gelation of these crudes. After gelation of waxy crude oil, the viscosity will become infinite and the shear rate inside the gel phase becomes zero [51].

Some researchers [33] examined the gel strength of waxy crude oils under static and dynamic conditions. They showed that, the gels display a strong dependence of the yield stress on the shear history as they reported that static yield stress will be smaller if pre-shear duration (stress application time) is longer. The yield strength for a crude oil with a pour point of 21°C was found to be lower by a factor of 2-4 when wax crystallization occurred while the crude was in movement. Some researchers studied the strength of paraffin gels formed under flowing conditions showing that small amounts of shear during gelation results in an increase in crystal sizes, which correlates to an increase in the yield stress of the incipient gel, whereas larger amounts of shear had the effect of degrading the incipient crystal network, resulting in smaller average crystal sizes [48].

3.4.2 The effect of thermal history

Chang et al. [40] studied in detail the influence of thermal history on the structure of statically cooled waxy crude oil. They showed that temperature is the most important factor influencing the rheological properties of waxy crude oils: the slower the cooling rate, the larger the wax crystals and their consequent agglomeration and the higher their

yield stresses. The effect of isothermal holding time before measurements was found to be less important than the effect of temperature and cooling rate. Chang's observation was in agreement with the results obtained by Ronningsen [35] on different samples of waxy North Sea crude oils in a model pipeline as well as the results by Visintin [33] using oscillatory measurements in a controlled-stress rheometer.

3.4.3 The effect of composition

Oh et al. [47] determined the gel strength at temperatures below pour point by the measurement of yield stress with and without subjecting the samples to creep stress, and they reported that the paraffinic components contribute to the evolving gel strength of the oil when cooled below pour point temperature. Similar results were obtained for model oils supporting that the yield stress values are dependent on the wax amount and wax composition [52]. The n-paraffins present in the crude oils were shown to be the main responsible for its aging: the more these components diffuse into the gel deposit, the stronger the gel becomes [53]. Venkatesan et al. [48] observed that the properties of the gel deposit, such as the gelation temperature and the solid wax content, were strongly dependent not only of the waxy oil composition but also of the shear and thermal histories under which the deposit is formed. Therefore, in order to achieve effective remediation of the problem, it is significant to investigate the wax precipitation process and the nature of the wax precipitates.

The asphaltene content can also have an important effect on the strength of gelled waxy crude oils formed at cold shut-in circumstances [47]. Venkatesan et al. [54] observed a depression of gelation temperature and yield stress with increase in asphaltene content in a model waxy crude mixture, supporting the effect of asphaltenes on the gelation of waxy crude oils. Kriz et al. [55] demonstrated that the crystallization and the wax network strength is strongly dependent on the degree of asphaltene dispersion and defined a critical asphaltene concentration in the wax network below which the yield stress increased with asphaltene concentration. This critical value was 0.01 %wt., above which the yield stress reduced with increasing asphaltene concentrations.

Crude oils are always produced with some water cut and the presence of water in the composition of oils is also a significant factor affecting their rheological properties. Recently, Visintin et al [21] studied oil emulsion gels with various water cut volume percentages. They observed an increase in viscosity and yield stress when the water content exceeded 30% vol, in accordance with the observations achieved by Oliveira et al. [56] using three Brazilian waxy crude oils. Their measurements showed that the presence of water produce very stable and viscous emulsions with increased gel strength. These characteristics are ascribed to the network developed by the aggregation of the waxy crystals and water, especially when the volume of dispersed water is above 50%. Above this value, there is a sharp increase in the shear viscosity. The recent work of Sun et al. [39] investigated the yield stress of the gel formed by a water-in-oil emulsion and stated that the yield stress increases by one order of magnitude when water cut increases from 0 to 60%.

3.4.4 The effect of stress loading rate

Some studies also reported the effect of stress loading rate on the gel strength of waxy crude oils (the rate at which the stress is increased with time) [35, 57].

Chang et al [57] examined the effect of the stress loading rate on the yield stress while studying two different crude oils at four different rates. The results obtained showed a similar dependence on the stress loading rate for the two oils, with lower stress loading rates, corresponding to a longer time scale for the yielding creep process, causing lower static yield stresses. They explained that the dependence of static yield stress on the stress loading rate, which followed a power law relation, may be due to the yielding in the viscoelastic creep process. Similar effects were reported by Ronningsen [35]. This has an important practical consequence, meaning that the pump pressure required to start flow in a pipeline is dependent on how quickly the pipeline is started. Therefore, based on these results, when initiating or restarting a pipeline transporting waxy crude oil the pump pressure should be increased as slowly as possible, since a slower operation will require a lower pump pressure [57].

3.4.5 The effect of Aging

Aging, defined as the isothermal holding time after the gel is formed, is another factor that has been considered in the literature as affecting the yield stress of crude oils. Different aging effects on gel strength have been reported. Visintin et al. [33] measured a higher yield stress for longer holding time at temperatures 6 and 10 °C below pour point, with the maximum strength obtained after 4 h. Series of laboratory flow loop experiments using a model system of wax and oil were carried out for various lengths of time to elucidate the physics of the aging process of the gel deposit by Singh et al. [58]. These authors explained that the gel behaves as a porous medium into which wax molecules continue to diffuse resulting in an increase in the wax content of the deposited gel with time. The deposited gels were analyzed and the wax content of the gel was found to be a strong function of the aging time. Also Paso et al. [53] explained the aging phenomenon as a counter diffusion process where paraffin components having a number of carbon atoms greater than a critical carbon number (CCN, the highest carbon number of the n-paraffin components diffusing out of the gel deposit is defined to be the critical carbon number) diffuse from the bulk oil into the gel deposit and precipitate, while paraffin components containing a number of carbon atoms less than the CCN diffuse out of the deposit with time. Hence, the aging process causes an increase in the solid phase fraction of the deposit, resulting in a more rigid gel.

Coutinho et al. [59] proposed a mechanism for ageing based on Ostwald ripening, responsible for the hardening of paraffin deposits. They have demonstrated that this phenomenon whereby smaller paraffin crystals recrystallize, leads to an increase in the average crystal size and rheological strength of a wax-oil gel.

Some disagreements are also observed among previous reported results. Wardhaugh et al. [31] did not find any significant difference in gel strength after 65 hours of aging. Pedersen et al. [60] found that the same amount of wax was precipitated at a given temperature regardless of whether the sample was cooled at a rate of 10 °C/hr or was equilibrated for 24 hrs. Also Ronningsen [35] and Chang et al. [40] observed the absence of ageing effects or on their very low, often insignificant effect on gel structure. These

disagreements were attributed to poor temperature control during the experiments or to the compositional differences of the oils [40]. However Lopes da Silva and Coutinho [61] tested three different oils under careful control of the shear and thermal history, reporting that the ageing and solidification of the wax-oil gels do occur at temperatures close to the gelation temperature. They stated that 'the apparent disagreement can be attributed to the different degrees of supercoiling used in different studies'.

3.5 Wax deposition and gelation of waxy crude oil.

Here we discuss the available information on wax precipitation process and the nature of the wax precipitates i.e. the various phases of waxy crude transformation during cooling. As explained earlier, at high temperatures, well above the pour point, a waxy crude oil is in a liquid state with all the particulates fully dissolved in the solvent base of the oil. When the oil experiences cold ambient temperatures and the temperature falls below the wax precipitation temperature, the wax will precipitate out of oil solution [62, 63]. Precipitation of wax during cooling is described to consist of three stages: nucleation, growth and agglomeration. These processes describe the crystallization phenomenon of waxy crudes [64]. Wax nucleation and crystal growth occur along the pipe surface and within the bulk fluid and depend crucially on cooling rate [2].

When the oil is cooled below WAT, the wax molecules form crystal nuclei, which enhances further crystallization and growth in a clear solution. Then other wax molecules join increasing the size up to a certain critical volume after which nuclei become stable. This process is called nucleation [65, 66]. Nucleation can be homogeneous or heterogeneous; homogeneous nucleation usually occurs for a pure fluid and the nucleation sites are time dependent, whereas heterogeneous nucleation is the most common type in crude oils, since impurities such as asphaltenes, formation fines, clay and corrosion products play an important role acting as nucleating materials for wax crystals [67]. When the temperature is slightly below WAT the fraction of crystallized wax is quite small and the presence of crystals does not affect the rheology of the fluid.

With lowering temperature, typically 10–20 °C below the WAT, more molecules link the sites on an existing crystal faces forming ordered structures in mono or multi

molecular layers, giving rise to crystal growth. Crystallization continues via molecular diffusion of paraffin components from the liquid solution to the nuclei interface. Crystal growth continues till steady state is reached where the fluid is entrapped within a network of wax crystals with diverse and complex morphologies and structures, turning the oil into a gel-like, highly viscous material [65, 66, 68]. Using Differential Scanning Calorimetry [69, 70] and other analytical techniques [71] it has been established that gelation of crude oils takes place when as little as 1 – 6 wt.% of wax solids have separated from solution [4, 18, 19, 69, 72]. This process can cause the complete obstruction of the pipelines that can last several months before being removed with serious economic costs [73], supporting the importance of considering the precise value of the WAT and maintaining operation conditions well above this temperature.

3.5.1 Wax deposition in flow conditions

Wax deposition doesn't necessarily occur at the WAT value, but can occur on surfaces cooler than this temperature, such as pipe walls and production equipment [74]. Wax precipitation does not necessarily lead to solid deposition, complete blockage of pipeline is uncommon, but wax deposits do undesirably affect production due to increased flow resistance, as the effective area available for flow of reservoir fluids gradually decreases resulting in huge pressure drops across these flow lines and reducing the total throughput [75]. To develop an accurate prediction of the deposition rates along the pipeline and adequate remediation methods that would help in the design stages of the field, as well as in the scheduling of interventions in the pipeline, a sound understanding of the basic mechanisms responsible for the wax deposits is helpful and needed in order to assure the flow of oil at the desired rates [76].

3.5.2 Wax deposition mechanisms

In recent years wax deposition prediction has always been a hot and important research focus for scholars [77-91]. The available studies suggest different possible mechanisms for wax deposition, namely molecular diffusion, Brownian motion, shear dispersion and gravity settling.

3.5.2.1 Molecular diffusion mechanism

The initial wax deposited at the pipe wall is a 3-D network structure of wax crystals containing a significant amount of oil trapped in it [92]. These crystals grow as time progresses while there are radial gradients of thermal and mass transfer as a result of heat losses to the surroundings, i.e., the temperature and wax concentration at the pipe center being higher than at the pipe wall lead to a radial transport of wax molecules from the bulk of the fluid towards the wall, by molecular diffusion. Forming the soft solid deposits. This wax flux causes the wax deposit to become thicker as time progresses.

Molecular diffusion mechanism has been branded as the governing paraffin deposition mechanism [93]. Singh et al. [1] confirmed that shear dispersion, Brownian diffusion and gravity settling had little influence on wax deposition, suggesting that molecular diffusion was the dominant mechanism of wax deposition.

In fact, most available deposition models make use of molecular diffusion as the sole mechanism for predicting three-dimensional and time-based distributions of paraffin [75].

3.5.2.2 Shear dispersion mechanism

Wax deposition by shear dispersion is a mechanism of cross-stream transport of suspended solid particles in flowing fluid driving them towards the wall. The rate of deposition is expected to be governed by the shear rate and by the content of crystallized paraffins. This mechanism suggests that flow of oil is essential for deposition and theoretically no heat flux between the pipe and the environment sustains the deposition process. Suspended particles of crystallized paraffins within a fluid tend to travel with the mean speed of the fluid surrounding them. Particles have higher velocities at greater distances from the pipe wall, and the particles also rotate as they flow. These rotating particles will exert drag forces, causing displacement of the flow paths of any neighboring particles. Near the pipe wall the particle concentration will be high, the velocity gradient induces a lateral movement and the particles eventually settle on the pipe wall [89, 96].

Some studies [81, 94] kept the pipe wall at the same temperature as the oil, to guarantee that there would be no heat flux from the wall to the oil. Under these conditions, it was expected that suspended wax particles would be present throughout the flow and available for deposition. However, no deposition occurs under conditions of zero heat flux. Weingarten et al. [78] also did not observe any deposition without a wall colder than the bulk oil temperature. Although Hamouda et al. [93] considered that shear dispersion had an influence on wax deposition, they ignored the influence of shear dispersion when establishing the prediction model of wax deposition. Therefore, from the available results we may conclude that shear dispersion is a force which limits the growth of the deposit on the pipe wall [80, 83], but it is not relevant to the deposition process itself [75].

3.5.2.3 Brownian diffusion mechanism

In the mechanism of Brownian diffusion wax particles suspended in the oil animated with a random movement collide with thermally agitated oil molecules. These collisions originate an irregular wiggling motion of the suspended particles, which in the presence of a concentration gradient, leads to a net transport of the particles along the path of declining concentration, producing a net transport similar to diffusion, i.e., from high to low particles concentrations.

This mechanism has not been considered as a relevant deposition mechanism in literature [51, 81, 84, 89, 95]. Creek et al. [83] claimed that the contribution of Brownian diffusion is small, since it is compensated by the drag of the oil. Majeed et al. [95] neglected this effect on the basis that the concentration of wax crystals is highest at the pipe wall, hence Brownian diffusion flux would be away from the wall in the direction of the pipe centerline and not the opposite. However, Azevedo et al. [75] considered that there is no sufficient experimental evidence to support this conclusion. For instance the argument of Majeed et al. [95] fail to recognize their assumption; if the wax crystals are trapped at the immobile deposit solid layer at the wall, the concentration of solid crystals in the liquid at the wall is zero, or nearly zero.

3.5.2.4 Gravity settling mechanism

Gravity settling can occur because precipitated wax crystals are denser than the solvent oil. Burger et al. [89] determined typical size distributions of crystals and terminal settling velocities, and concluded that these velocities did not significantly contribute to the formation of wax deposits. Similar observation were obtained by Leiroz and Azevedo et al. [75, 94]. Gravity settling does not seem to be an important mechanism for wax deposition as various researchers have concluded that this effect is negligible and then usually neglected in flow models [96].

3.6 Structure of gelled Waxy Crude Oil

The characteristics of wax-oil gels depend on the crystal amount and morphology. Also, the structure of the crystal networks strongly depends on both thermal and shear histories [1, 97]. The crystallization of wax molecules below the WAT incurs formation of gels with a complex morphology. Wax crystals are considered to consist of straight chain, branched, and cyclic hydrocarbons in the range of C_{15} up to C_{80} [76].

The wax crystals will form macrocrystalline waxes at slow rate of cooling. The molecular weight of the components in macrocrystalline waxes varies between 250 and 450 and their melting point between 40 °C and 60 °C. Their crystals are plate-shaped or needle-shaped [2, 98]. When the cooling rates are higher, smaller crystal structures form. These microcrystalline waxes contain, in addition to normal hydrocarbons, large amounts of iso-alkanes and naphthenes with long alkyl side-chain and their melting point varies between 60 °C and 90 °C [98]. However, if the cooling rate is low, wax molecules will have appropriate time and flexibility to form large crystals and as a consequence the number density of crystals decreases. This morphology affects both the strength of the gel and the failure mechanism of the gel in the pipeline [99, 100]. The restart of the gelled oil may result from the breakdown of the gel structure itself (cohesive failure) or it may occur because of the breakage at the pipe-gel interface (adhesive failure) depending on the cooling rate and wax content [48, 99]. The cohesive yielding of the gel occurs when the applied stress exceeds the mechanical strength of the wax-oil gel structure maintained by the

mechanical interlocking of wax crystals formed by London dispersion or van der Waals forces between n-alkanes [33, 48, 99, 101].

3.7 Some rheological mathematical models

There are several mathematical models that can be fitted to flow curves in order to extract from them information on fluid rheological behaviour. For non-Newtonian fluids the three models presented below are the mostly widely applied [113].

3.7.1 Herschel-Bulkley model

The Herschel-Bulkley model is applied to fluids with a nonlinear behaviour and yield stress. It is considered as a precise model since its equation has three adjustable parameters.[114]

The Herschel-Bulkley equation describes the flow behaviour of shear thinning fluids that require some stress to initiate flow (dynamic yield stress):

$$\tau = \tau_{\circ} + K\dot{\gamma}^{n} \qquad \textbf{(3.1)}$$

Where τ, is the shear stress (Pa), $\dot{\gamma}$ is the shear rate (s^{-1}), τ_0 is the yield stress, *K* is the consistency index and *n* the flow behavior index. The Herschel-Bulkley model reduces to the power-law (Ostwald-de Waele) when $\tau_o = 0$, i.e., fluids with shear thinning flow without a yield stress.

The consistency index (*K*) gives an idea of the viscosity of the fluid. However, to be able to compare values for different fluids they should have similar flow behaviour index (n). The power-law exponent (*n*), or the flow-behavior index, has a value of $n < 1$ for shear-thinning fluids. The higher the *n* the more viscous the fluid, while the greater the departure of *n* from unity, the more pronounced are the non-Newtonian properties of the fluid. However, to be able to compare values for different fluids they should have similar flow behaviour index (n). When the flow behaviour index is close to 1 the fluid´s behaviour tends to pass from a shear thinning to a shear thickening fluid. When n is above 1, the fluid acts as a shear thickening fluid.

3.7.2 Ostwald model

The Ostwald model (Equation 3.2), also known as the Power Law model, is applied to shear thinning fluids which do not present a yield stress [114]. The power-law Model expressed as:

$$\tau = K\dot{\gamma}^{n} \quad \textbf{(3.2)}$$

The n-value in the above equation gives fluid behaviour information according to:

$$\tau = K\dot{\gamma}^{n} \quad \textbf{(3.2)}$$

$n < 1 \Rightarrow$ shear thinning behaviour

$n = 1 \Rightarrow$ Newtonian behaviour

$n > 1 \Rightarrow$ shear thickening behaviour

3.7.3 Bingham model

The Bingham model describes the flow curve of fluids with a yield stress and a constant viscosity and exhibits a decreasing viscosity with increasing shear rate (i.e. shear-thinning). This fluid will not flow until the applied shear stress exceeds a certain minimum value known as the yield point. The Bingham fluids are similar to Newtonian fluids in the sense that there is a linear relationship between shear stress and shear rate.

The Bingham model expressed as:

$$\tau = \tau_{\circ} + \eta \times \dot{\gamma} \quad \textbf{(3.3)}$$

The yield stress (τ_o) is the shear stress at shear rate ($\dot{\gamma}$) zero and the viscosity (η) is the slope of the curve.

3.8 Rheological techniques, instrument and test procedures used in this study

This section describes some rheological concepts and the various techniques used in this study to perform the characterization of the waxy oils. In this section no data on the waxy crude oils studied are presented.

3.8.1 Overview of Some rheological concepts & Approaches to Yield Stress phenomena

As mentioned earlier, waxy oils are not a simple suspension, but a suspension in which the particles have a potential to crystallize, combining together to form a structure. This is a structural feature that marks waxy oil complex materials rheologically. It is thus helpful to give a brief overview of some rheological behaviours that may be exhibited by crude oils and the principles of the rheological techniques considered in this research in order to investigate the gelled waxy crude oils that lead to the consideration of the difficult task of tracking the yielding process of the waxy crude oils and measuring the corresponding yield stresses before undertaking the rheological measurements.

3.8.1.1 Some rheological concepts

Newtonian fluids are named after Sir Isaac Newton (1642 - 1726) who described the flow behavior of fluids with a relation between shear stress and shear rate which implies that the applied shear stress τ is proportional to the rate of shear strain γ, also called shear rate. The constant of proportionality η, is the material's resistance to flow i.e. VISCOSITY.

Viscosity = Shear Stress / Shear Rate $\quad (\eta = \tau / \dot{\gamma})$ **(3.4)**

For a Hookean solid, Hooke's law states that the stress is proportional to the strain γ:

Stress = G* x Strain $\quad (\tau = G^* \times \gamma)$ **(3.5)**

Where G* is defined as the complex modulus or modulus of elasticity.

Newton's law and Hook's law have constant proportionality. Thus doubling the stress would double the strain i.e. the material behaves with a linear response.

Non-Newtonian fluids do not show a linear relationship between shear stress and shear rate. This is due to the complex structure and deformation effects exhibited by the materials involved in such fluids. There are different types of non-Newtonian behavior such as, shear thinning, shear thickening, viscoplasticity, thixotropy, linear and non-linear viscoelasticity. These are briefly defined below.

Shear thinning: the apparent viscosity of this fluid type decreases with increasing shear rate (Figure 3.2). Shear thinning fluids are also called pseudoplastic fluids.

Shear thickening: called dilatant fluids, exhibit increasing apparent viscosity with increasing the value of shear rate (Figure 3.2). However this type of non-Newtonian behavior is not characteristic of waxy oil gels. Examples of such fluids include honey, cement and peanut butter, etc.

Viscoplasticity: This type of non-Newtonian fluid needs a predetermined shear stress in order to start flowing which characterized by a yield stress, τ_0, below which the materials will not deform, and above which they will deform and flow according to different constitutive relations. The Bingham plastic and the Herschel Bulkley models [111] are examples for correlating this kind of behavior (Figure 3.3).

Viscoelasticity: Viscoelastic materials are the property of materials that exhibit both viscous and elastic characteristics when undergoing deformation. Such complex behaviour cannot be characterized purely in terms of simple parameters, such as the material viscosity or elastic modulus.

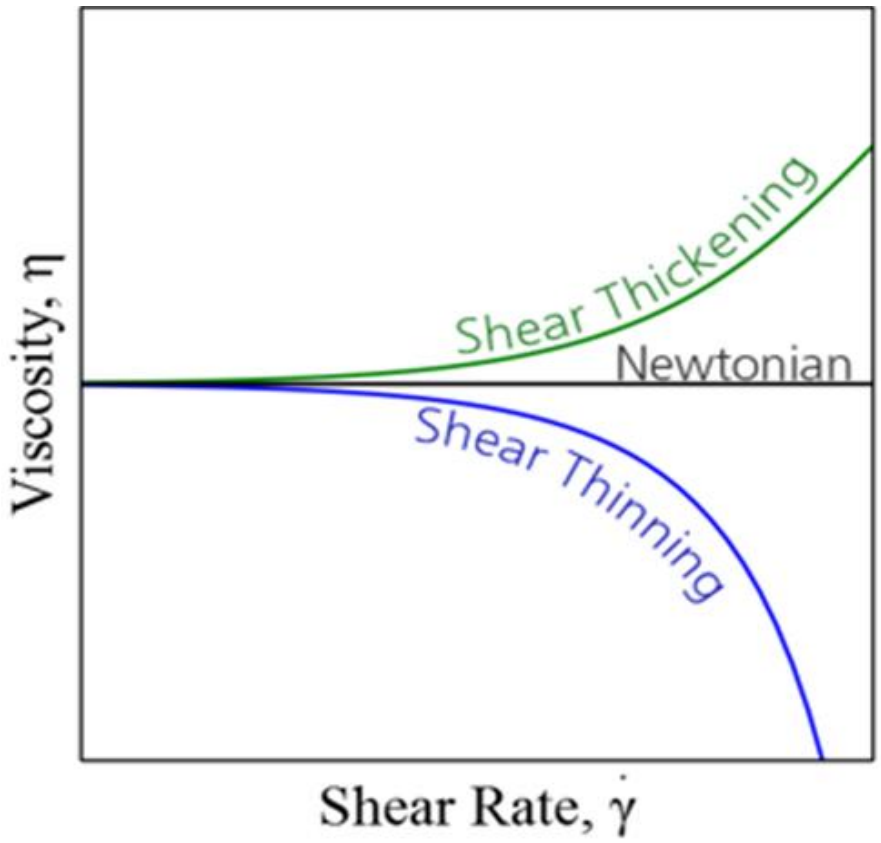

Figure 3.2 Viscosity of Newtonian, Shear thining and shear thickening fluids as function of shear rate

Thixtropy: This type of fluid has a time-dependent shear thinning property. Certain gels or fluids that are thick (viscous) under static conditions will flow (become thin, less viscous) over time when shaken, agitated, or otherwise stressed (time dependent viscosity). These time-dependent changes in viscosity are due to a gradual change in the microstructure of the fluid resulting from the application of shear. This mechanism is referred to as shear rejuvenation [102]. They then take time to return to a more viscous state, exhibit what is known as aging, which describes the ability of the fluids or gels to rebuild its initial structure under the absence of shear. The aging phenomenon is typically supposed to result from a slow internal, thermally driven rearrangement of the material's microconstituents [103]. Reference to this study, thixotropy is considered as an important feature of waxy crude oils as reported by several authors [29, 33, 104, 105, 110].

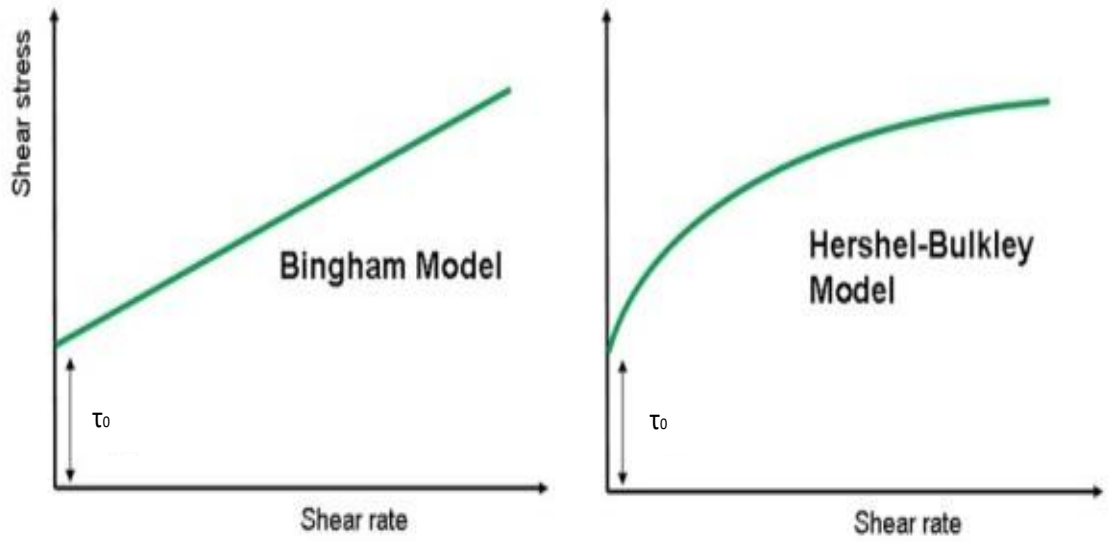

Figure 3.3 Bingham and Herschel-Bulkley model fits

Clearly, the range of behaviour mentioned above can be very complex and, most significantly, cannot be predicted, they have to be measured. In general, over a sufficiently wide range of shear, materials might exhibit some different characteristic made up of several of the above flow features. Particularly, the rheological behaviour which is relevant to waxy crude oil lies somewhere between that of a pure viscous liquid and an elastic solid which referred as mentioned above as viscoelastic behavior and the gelled crude oil may not flow until a certain level of stress is applied to it.

3.8.1.2 Yield stress Phenomenon

In the previous section, yield stress was defined as the minimum stress required by the material to flow. In fact, this is a very simple definition for a system that may exhibit complex solid-liquid transition when sheared beyond a critical deformation. That critical deformation corresponds to a critical stress, which also marks the transition from solid, viscoelastic to the liquid regime. Such transition between solid like behavior and flow introduces significant complications into the changing features, which, as a result, created more fundamental problems with the concept of yield stress.

For waxy crude oils, the yield stress is an important fluid property to be taken into account to pipeline designers and operators. The yielding process and yield stress of

gelled waxy crude oils has turned to be a difficult task to determine experimentally since its deformation depends on different factors as discussed previously.

Various researchers have proposed models to explain the yielding behaviour of waxy crude oils that have general acceptance of its practical usefulness in engineering design and operation of processes. Wardhaugh et al. [77] show that the yielding behaviour of waxy crude oils is accompanied by three distinct characteristics, an elastic (Hookean) response followed by slow deformation (creep); and finally fracture-like behaviour resembling the fracture of solids and defined the yield stress as the "shear stress at which the gelled oil ceases to behave as a Hookean solid". Barens [106] also defined the yield stress as the stress corresponding to the transition from elastic to plastic deformation.

Chang et al. [40, 57] proposed three distinct yield stress values that can be investigated for waxy crude oils at low temperatures. These yielding stresses can be summarized as an initial elastic response when the stress is lower than the elastic yield stress, the shear stress below which only recoverable deformation occurs, followed by a viscoelastic creep region, above elastic yield stress since the structure of the sample is partially damaged (static yield stress), and finally a fracture when the flow begins since the shear stress is larger than static yield stress (the broken down structure after yielding). The dynamic yield stress describes the broken down structure after yielding. Figure 3.4 shows the curve recorded for the studied waxy crude oil. It illustrates the differences between static and dynamic yield stresses.

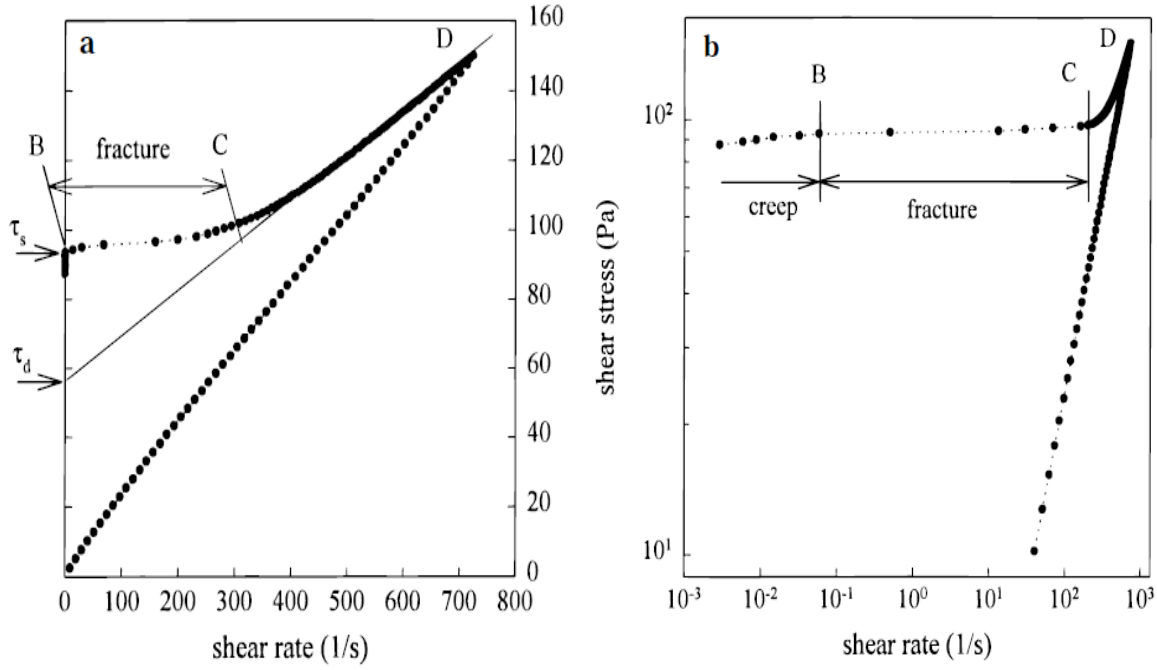

Figure 3.4 Difference between static and dynamic yield stress for waxy crude oil, (a) linear scale; (b) logarithmic scale [57]

It is important to note the need to use both linear and log scale to enlarge the scale and enable the identification of the yielding regions. In this illustration, point B is identified as the starting of the fracture and defined as static yield stress and point C is the end of the fracture region. The dynamic yield stress is determined from the up curve by extrapolating tangentially from D as shown in the illustration (Figure 3.4 a).

Complete yielding process can be clearly shown by an oscillatory test as proposed by the same authors [57]. Figure 3.5 shows a typical curve recorded for the same waxy crude oil in which the shear strain is measured in the test rather than shear rate. As can be seen in this figure, before point A which is the initial linear regime represents an elastic behaviour where the strain increases linearly with shear stress, after that Creep occurs with the stress-strain relationship slowly deviating from linear. Fracture starts at point B, showing the breakage of the oil microstructure where there is a significant increase of the strain.

The entire process is differentiated with two yield stresses which are the elastic limit yield stress, the stress transition between elastic and creep and the static yield stress, the stress at the start of the fracture.

Nevertheless the static stress value effectively determines the pump capacity required to initiate the gelled oil flow and ensure pipeline restart.

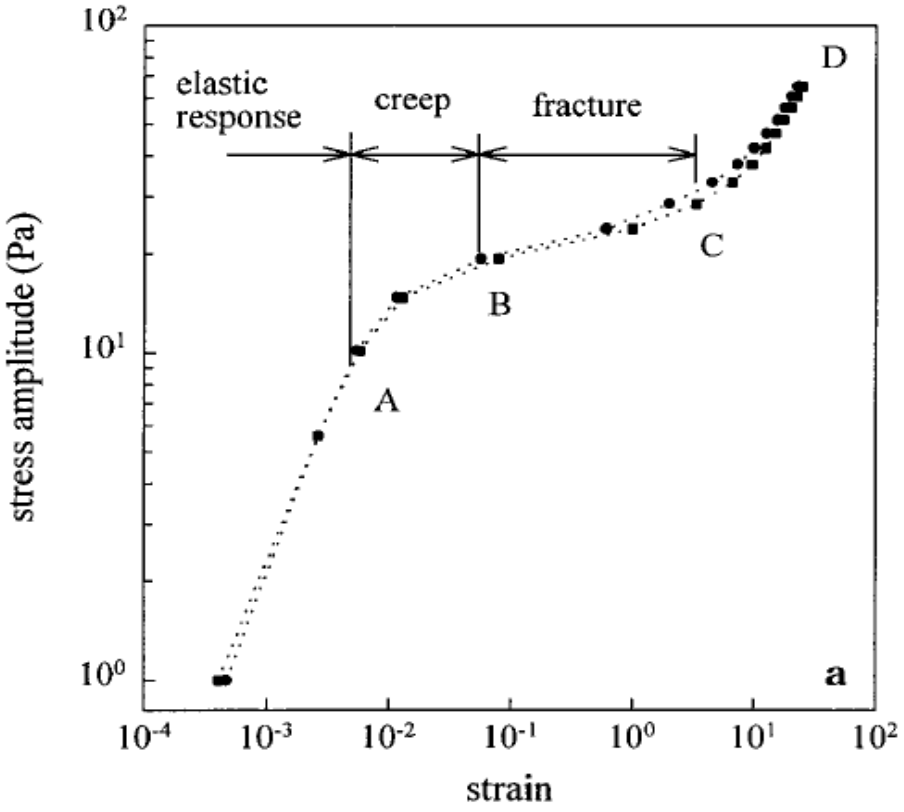

Figure 3.5 the yielding process by oscillatory test [57]

Venkatesan et al. [48] conducted tests to determine the yield stress by using samples prepared with various amounts of wax. (Figure 3.6) shows the typical rheometric responses of viscosity shear stress data. Initially, at low values of the applied shear stress, the rheometer cannot determine the viscosity in as much as no sample movement can be recorded. When the shear stress reaches close to the yield value, a creep response is observed and, at about 190 Pa for one sample and 850 Pa for another, the point of fracture is reached and is displayed in the form of a sudden decrease in the viscosity. Thus, the yield stress is taken for the two cases as 190 and 850 Pa.

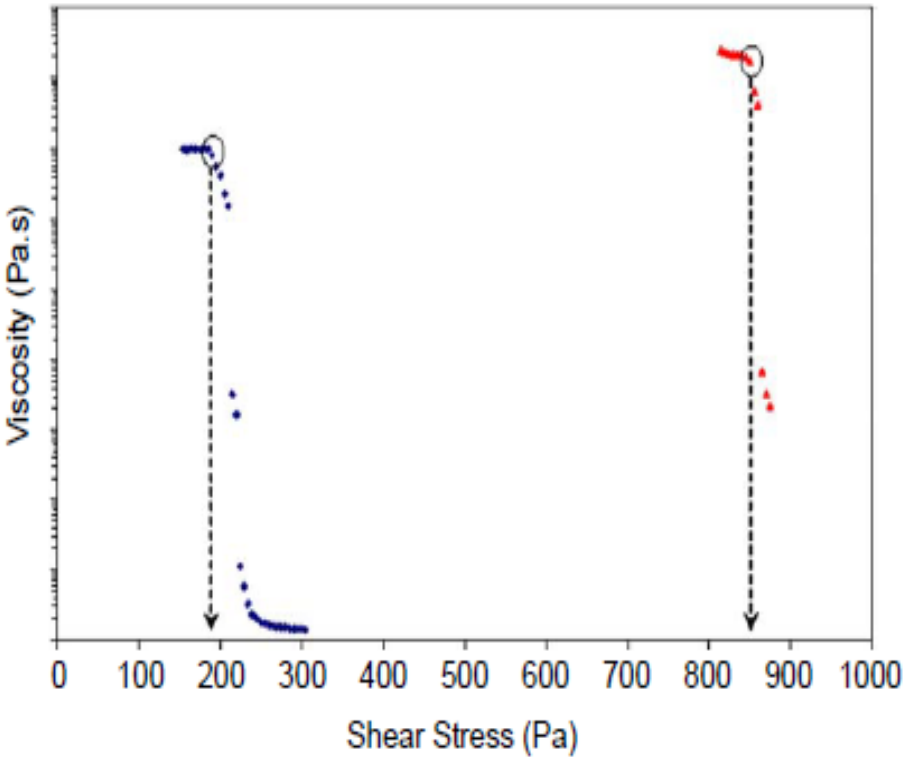

Figure 3.6 yield stress measurment of typical rheological experiments [48]

However, waxy crude oils can be characterized using a number of techniques in the rheologist's toolbox. For instance, investigating the effect of shear rate or shear stress on the apparent viscosity and the yielding of a heavy crude oil in order to develop reliable and accountable sets of experimental data bases of the rheological features can lead to a better understanding of the flow behaviour and the type response of the structures present within the crude oils. The viscoelastic behavior of the oil may be also measured by imposing constant stress and observing the resulting deformation or strain rate. This technique is called creep test. Oscillatory measurements is another technique that allows to explore the viscoelastic properties in order to understand the microstructures of non-Newtonian behaviour that waxy crude oils exhibit.

The above mentioned techniques require rheological equipment that can be operated in controlled stress, oscillatory and creep modes, the three techniques most appropriate to analyze the structure of the material at rest and give information about storage stability, elasticity over long time scales and measure the yielding process of gels and materials that contain solidifying particles such as waxy crude oils. The laboratory at

Aveiro University is equipped with a TA (AR 1000) instrument that answers these requirements. This instrument has been used in this study to characterize the three waxy oils under investigation. The principles of using each technique used to perform the characterisation of the waxy oils, measure their rheological properties are considered below.

3.8.2 Principles in the flow measurements

Since the relationship of shear stress to shear rate are strictly related to flow, then the flow characteristics of a material can be displayed by plotting shear stress (τ) vs shear rate ($\dot{\gamma}$). A graph of this type is called a Flow Curve or Rheogram.

Flow rheological measurements at constant temperature starting from a strong gel state can provide information on the presence of yield stress before and after flow start and assess time-dependent aspects as flow start. The reliable technique for defining this dynamic behavior, by evaluating those aspects and getting an overview on how the waxy oils behave in a flow restart, would be from direct measurements using a controlled stress rheometer, in which a shear stress is applied and shear response is measured.

Controlled stress tests or steady shear flow tests can be performed by ramped shear stress with defined intervals along this shear gradient (linearly). To detect the stress at which the oil flows, i.e. yielding occurs, the rheometer must be operated by ramping the stress up, increasing the applied stress linearly in specific time, from a very low value or zero to a value higher than the yield stress. Already, we can suspect that in order to measure the yield stress we will need an instrument that is capable of applying very small stresses and measuring the smallest movement (shear rate). However no data can be recorded in the stress curve before the shear rate reaches the resolution limit of the rheometer. This is the most serious limitation of this technique which by definition cannot give the elastic limit yield stress unless the rheometer is designed to measure very small shear rates.

3.8.3 The principles of creep-compliance tests

Creep is the steady deformation of a material that is placed under a constant load. Creep tests allow evaluating the yielding characteristics of the fluid. If the stress is below a minimum yield stress limit, after an initial deformation, no flow will be observed. If the applied shear stress is higher than yield stress, the fluid sample will start flowing within some time, depending on the applied stress magnitude, material properties, exposure time and exposure temperature.

The extent of the sample recovery can be measured, after a sample imposed to creep, by abruptly relieving the imposed stress and measuring the resultant strain. The yielding process of the crude oil under constant stress applied (creep) can be occurring in three distinct stages: elastic deformation which is a rapid elastic increase in strain (primary creep) followed by viscoelastic creep as a slower linear rise in strain (secondary creep or steady state creep), and finally fracture creep range with the deformation of the gel structure (tertiary creep) (Figure 3.7).

Creep tests may start from the same state of the material and detect its response to different imposed shear stresses. If the oil exhibits some kind of internal arrangement or structure, below its elastic limit yield stress value, then the gel only exhibits elastic response and after an initial deformation, no flow would be observed. If the stress value in between elastic yield stress and static yield stress value, the waxy gel is expected to exhibit slow “creep”. However, if the applied shear stress on the gel exceed its static yield stress value, then within some time the gel breaks down and shows viscous flow, depending on the applied stress magnitude.

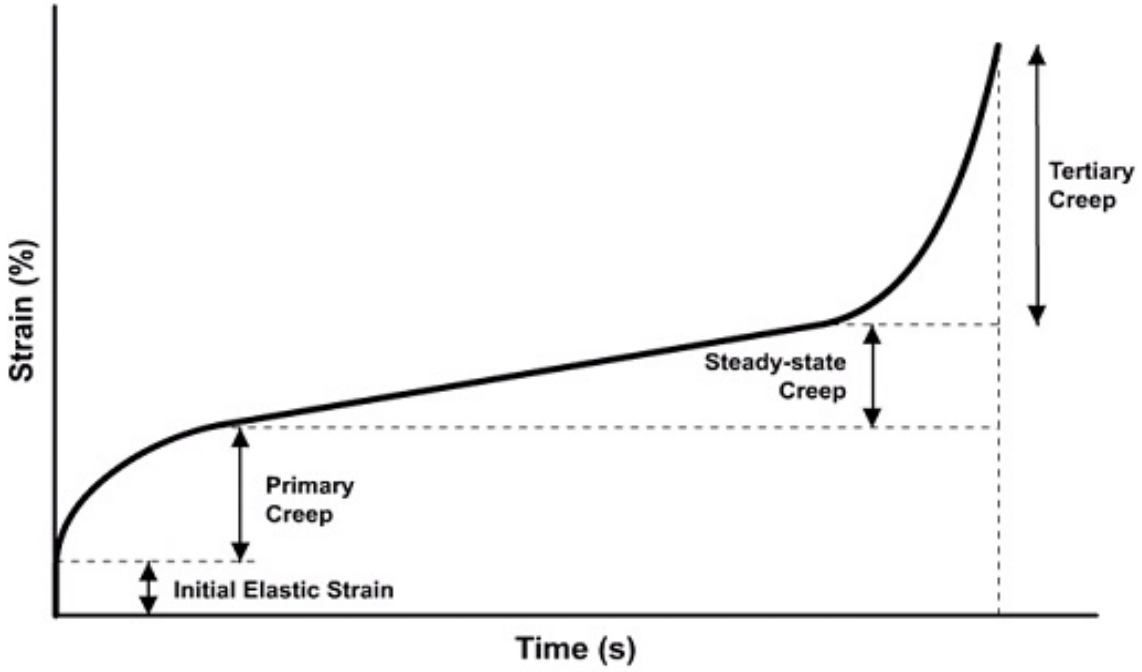

Figure 3.7 Schematic Diagram of Creep-test showing the three stages of creep [115]

A sequence of creep tests using a varied range of shear stresses can specify the yielding characteristics of the oil if the steady state flow is reached. However this mode allows not only to evaluate the yielding process and related yield stresses but also enables to analyze the structure of the material at rest.

3.8.4 Principles of oscillatory tests

Oscillatory tests also referred to as dynamic mechanical analysis (DMA). Studying the mechanical behavior of waxy crude oils are complicated by the fact that their response is viscoelastic, intermediate between that of solids and liquids (viscoelastic). Oscillatory techniques are commonly used to analyze such complex rheological behavior; it provides information on the viscous-like and the solid-like properties, and the relation of this strength with the gel composition and its stability. In this method, both stress and strain vary cyclically with time, with sinusoidal variation being the most commonly used. This is the most popular method to characterize viscoelasticity, since relative contributions of viscous and elastic response of materials can be measured.

The basic principle of an oscillatory test is to induce a sinusoidal shear deformation in the sample and measure the resultant stress response; the time scale probed is determined by the frequency of oscillation, ω, of the shear deformation.

Figure 3-8 shows oscillatory motion induced mechanically in a plate and plate system. The sample is placed between the two plates. While the bottom plate remains stationary, a motor rotates the top plate, thereby imposing a time dependent strain on the sample.

Shear strain will be in the form [116]:

$$\gamma(t) = \gamma_o * \sin(\omega t), \quad \textbf{(3.6)}$$

Where γ_o is the strain- amplitude (the maximum applied deformation) and ω is the angular frequency of the oscillation. The time dependent stress (t) is quantified by measuring the torque that the sample imposes on the bottom plate. Measuring this time dependent stress response at a single frequency immediately reveals key differences between materials.

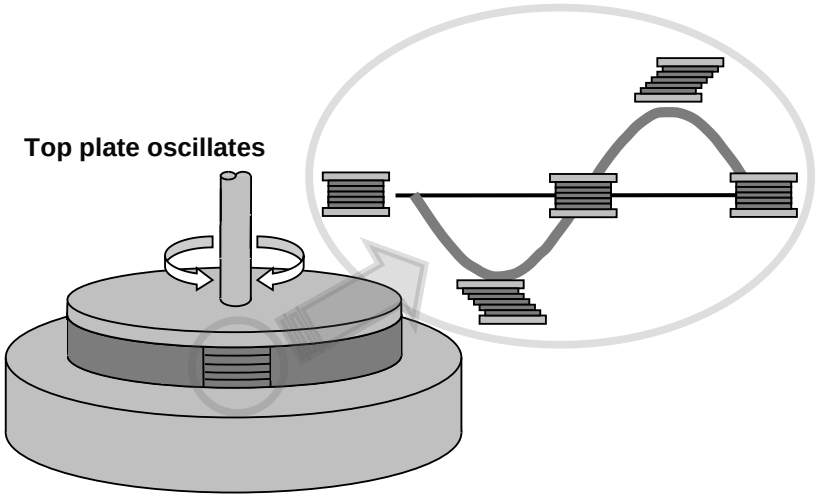

Figure 3.8 Schematic representation of a typical rheometry setup, with the sample placed between two plates.

If the material is an ideal elastic solid, then the sample stress is proportional to the strain deformation, and the proportionality constant is the shear modulus of the material

(Figure 3.9 a). The stress is always exactly in phase with the applied sinusoidal strain deformation.

In contrast, if the material is a purely viscous fluid, the stress in the sample is proportional to the rate of strain deformation, where the proportionality constant is the viscosity of the fluid (Figure 3.9 b). The applied strain and the measured stress are out of phase, with a phase angle $\delta=\pi/2$.

Viscoelastic materials show a response that contains both in-phase and out-of-phase contributions (Figure 3.9 c); these contributions reveal the extents of solid-like (red line) and liquid-like (blue line) behavior.

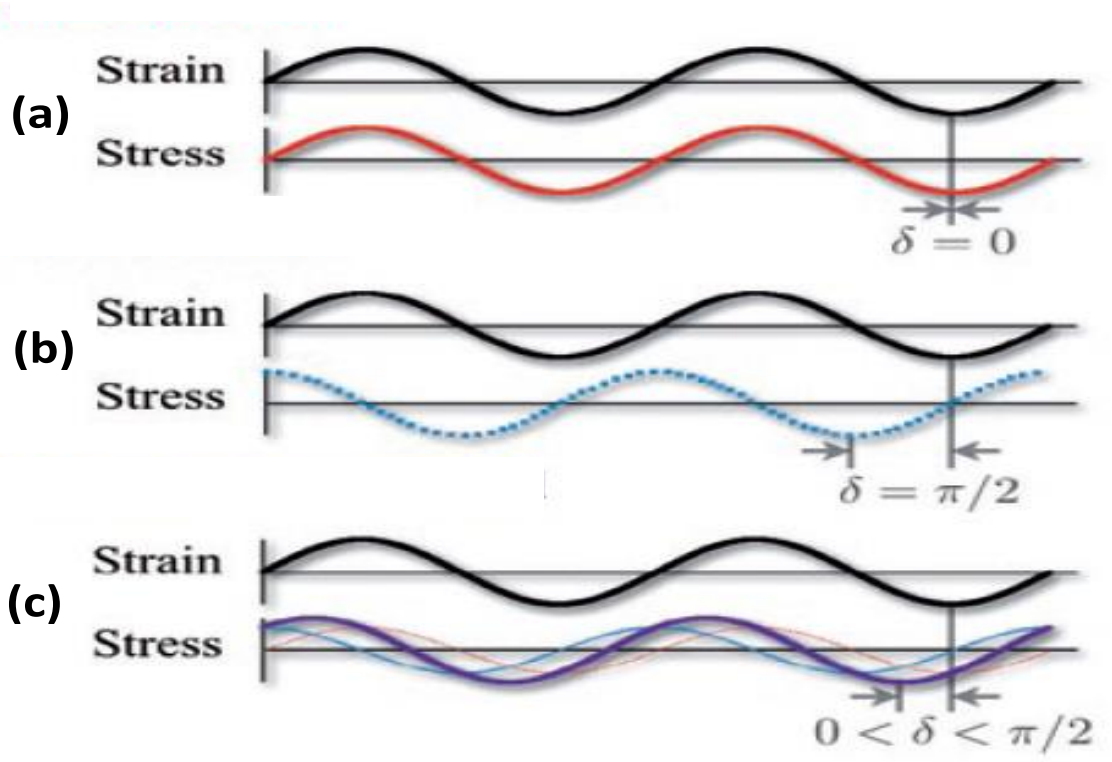

Figure 3.9 Schematic stress response to oscillatory strain deformation for an elastic solid, a viscous fluid and a viscoelastic material.

As a consequence, the total stress response (purple line) shows a phase shift δ with respect to the applied strain deformation that lies between that of solids and liquids, $0<\delta<\pi/2$.

The response of material in terms of stress and strain will show a phase shift angle δ between 0° and 90° and can be written as [116]:

$$\gamma = \gamma_o * \sin(\omega t+\delta), \qquad \tau = \tau_0 \sin(\omega t+\delta) \qquad \textbf{(3.7)}$$

Using trigonometric identities, the stress wave can be decomposed into two components, one in-phase with the strain and the other out-of-phase by 90 degrees:

$$\tau = \tau_0 \sin(\omega t)\cos(\delta) + \tau_0 \sin(\delta)\cos(\omega t) \qquad \textbf{(3.8)}$$

Using equations 3.7 and 3.5 it is clear that the complex modulus G* is defined as:

$$G^* = \tau_o/\gamma_o \qquad \textbf{(3.9)}$$

This complex modulus is made up of two components, the elastic and viscous moduli, G' and G'' defined from vectorial decomposition as:

$$G' = G^* \cos(\delta) \quad \& \quad G'' = G^* \sin(\delta) \qquad \textbf{(3.10)}$$

We can rewrite the above expression (equation 3.8) in terms of two material functions (G' and G''):

$$\tau = \gamma_o [G' \sin(\omega t) + G'' \cos(\omega t)] \qquad \textbf{(3.11)}$$

Elastic modulus, $G' = (\tau_o/\gamma_o)\cos(\delta)$ **(3.12)**

Viscous modulus, $G'' = (\tau_o/\gamma_o)\sin(\delta)$ **(3.13)**

The elastic modulus, G', which is related to the stress in phase with the imposed strain, provide information about the elastic nature of the material. Because elastic behaviour implies the storage informational energy in the system, this parameter is also called the storage modulus. The viscous modulus, G'', on the other hand, is related to the stress component, which is completely out of phase with the displacement. This parameter characterize the viscous nature of the material. Because viscous deformation results in the dissipation of energy, the parameter is called the loss modulus.

Also tan δ can be defined, from the vector decomposition linking the phase angle to these moduli:

$$\tan \delta = G''/ G' \quad \textbf{(3.14)}$$

If G'= 0, the sample is a purely viscous fluid. If G''= 0, the sample is a Hookean solid. A viscoelastic material exhibits non-zero values for both G' and G''.

The analysis above assumes that the measurements are made in the "linear viscoelastic regime (LVR) of the sample. The conditions for linear viscoelasticity are that the stress be linearly proportional to the imposed strain. This condition requires that the modulus, G' and G'', in the LVR, should be independent of the strain amplitude.

Consequently, as we are seeking to determine the yielding of the waxy crude oils at temperatures below pour point, it is important to operate in the region where the oil sample remains solid, i.e. deforms elastically and "push" it just until it breaks and begins to show viscous flow. As mentioned above, this translated in rheometric terms means to operate the oscillatory test in the Linear Viscoelastic Region, LVR, then following this in the nonlinear region, as it can be seen in (Figure 3.10), at the beginning of the test, the elastic modulus is higher than the viscous modulus. As the amplitude of the oscillations increases, the elastic modulus decreases, eventually to a value lower than the viscous modulus. At that point the material is said to exhibit a more viscous than elastic behavior, characterizing a predominant liquid behavior. Thus in this study, the measurements were done at a fixed low frequency whilst increasing slowly the amplitude of the oscillation and measuring the strain response in both linear and nonlinear regions, from which the storage modulus (G') and the loss modulus (G'') during the entire yielding process can be determined.

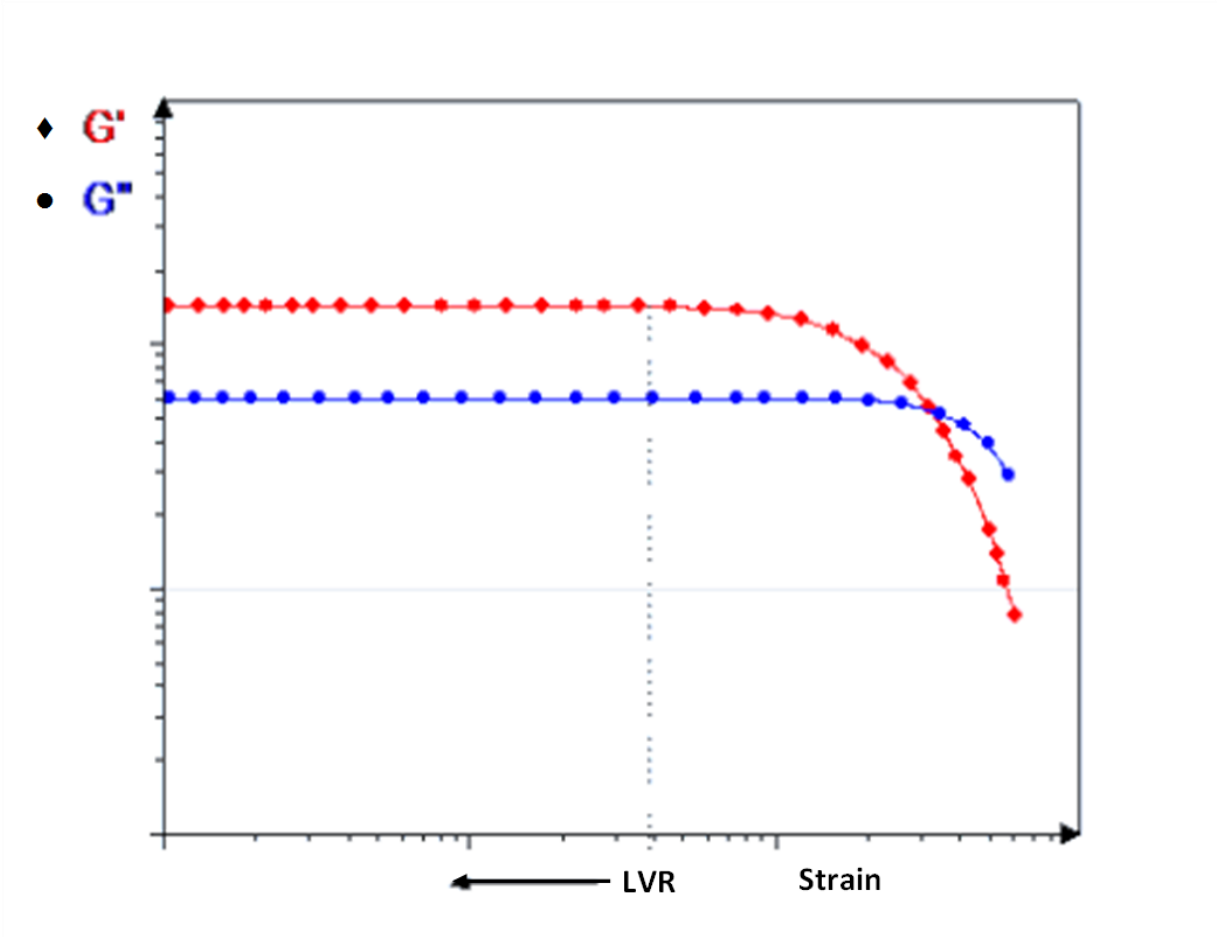

Figure 3.10 Typical graph, the process of yielding in oscillatory measurements

As the advantage of dynamic shear is that it allows to characterize the sample without disturbing the microstructure in the process, the linear viscoelastic modulus reflect the microstructure at rest. This is to be contrasted with steady shear, where the material functions are always obtained under flow conditions that correspond to relatively drastic deformations. Consequently, the microstructure under steady flow will be very different from microstructure under static conditions. It can therefore, correlate dynamic rheology to static microstructures and steady rheology to change in microstructure caused by flow. This is called in rheometric terms frequency sweep measurements. During the frequency sweep the frequency is varied while the amplitude of the deformation or alternatively the amplitude of the shear stress is kept constant. Figure 3.11 shows some types of response seen in dynamic frequency spectra [107].

Figure 3.11, (a) is typical of a non-associated particulate dispersion, and consists of dominant viscous modulus, G", over the elastic modulus, G', over the complete range of experimental frequencies and both of these are highly dependent on the frequency. In this situation, sedimentation is likely to occur. The viscosity is almost independent of the frequency.

The viscous modulus will still dominate over the elastic modulus in Figure 3.7 (b) as it shows a weakly- structured system. However, the difference between these is smaller than in the non-associated system. The viscosity is dependent on the frequency.

Figure 3.11 (c) shows what could be classified as a well-structured (gelled) system and called a gel. The dynamic mechanical spectrum of a gel shows a frequency-independent elastic modulus, G' that greatly exceeds the viscous modulus, G". Thus, a gel behaves principally as an elastic material because of the presence of a continues network

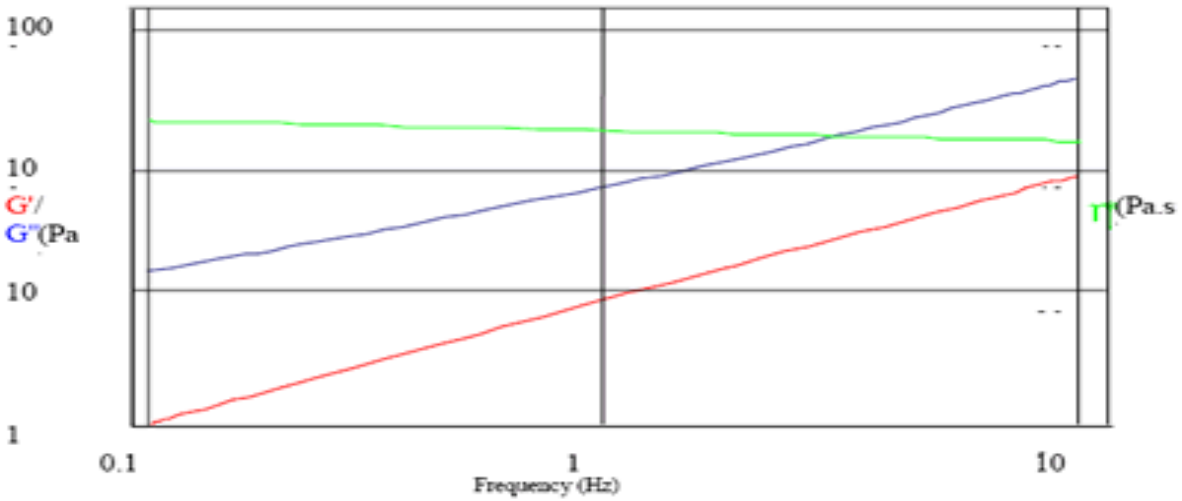

(a)

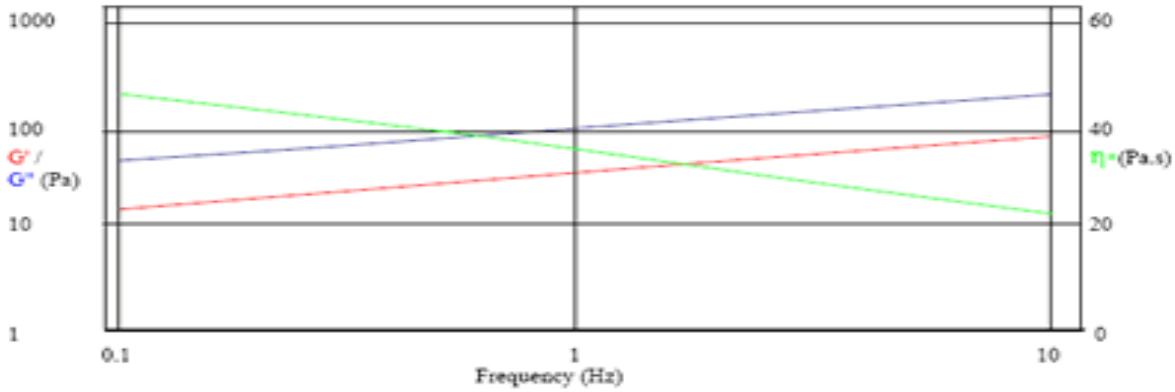

(b)

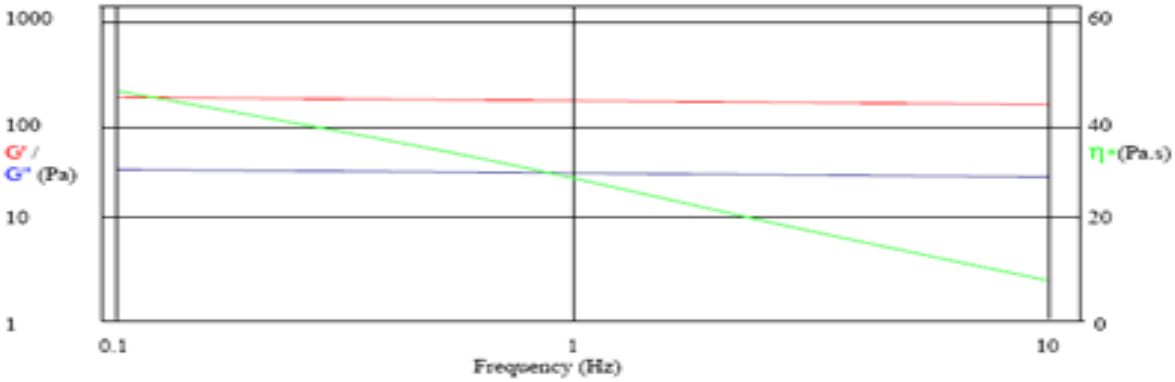

(c)

Figure 3.11 Dynamic rheology. G' and G'' and viscosity as functions of frequency, ω, are shown with their corresponding microstructure. (a) Non-associated particulate dispersion. (b) Weakly- structured system with viscous modulus dominant over the elastic modulus. (c) A well-structured (gelled) system [107]

3.8.5 Rheometer and measuring systems

Figure 3.12 shows the controlled stress rheometer, AR1000, TA instruments, which was used in this study. In this rheometer design, an air bearing is provided with technology for digitally controlling the shear stress in a range 0.0008 to 508,000 Pa and the shear rate in a range 10^{-6} to 11,000 s^{-1}. The range is thus very large, enabling to detect very small yield stress values. Also important with this instrument which is fitted with a Peltier device, is the ability to accurately control heating and cooling. The Peltier system uses a thermo-electric effect. This function as a heat pump system with no moving parts, and this is ideally suited to rheological measurements.

Figure 3.12 Controlled stress rheometer, AR1000-TA instruments

The AR 1000 Rheometer can accommodate three types of measuring systems, the cone and plate, the plate and plate and concentric cylinders systems and operates in both rotational and oscillatory modes. These systems are described below.

Cone-and-Plate System: Figure 3.13 shows the geometry of the system which consists of a circular cone and a plate. The sample is held between cone and plate to be tested. The dimensions of the conical area of the flow filed are defined by the cone radius

R and the cone angle α. The standard diameters available are 20mm, 40 mm and 60 mm with cone angles of 0.5° to 4° in 0.5° increments.

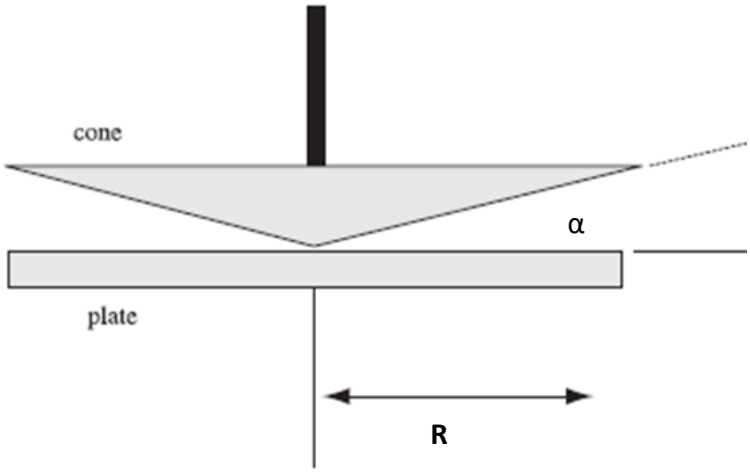

Figure 3.13 A schematic diagram of cone-and-plate measuring system

Cone and palate geometries are commonly used for single phase homogenous samples or samples with sub-micron particles. Samples containing particulate substances are usually unsuitable for cone and plate geometries as the particles will tend to transfer to the apex of the cone and will get jammed in the truncation area, resulting in incorrect measurements.

Parallel-plate System: Figure 3.14 shows the geometry of the system which consists of two parallel plates separated by a gap where the sample is held. The parallel plate system allows samples containing particles to be efficiently measured. The gap size can be controlled to accommodate a variety of particle sizes. The main disadvantage of using the parallel plate system is that the stress is not uniform across the entire diameter.

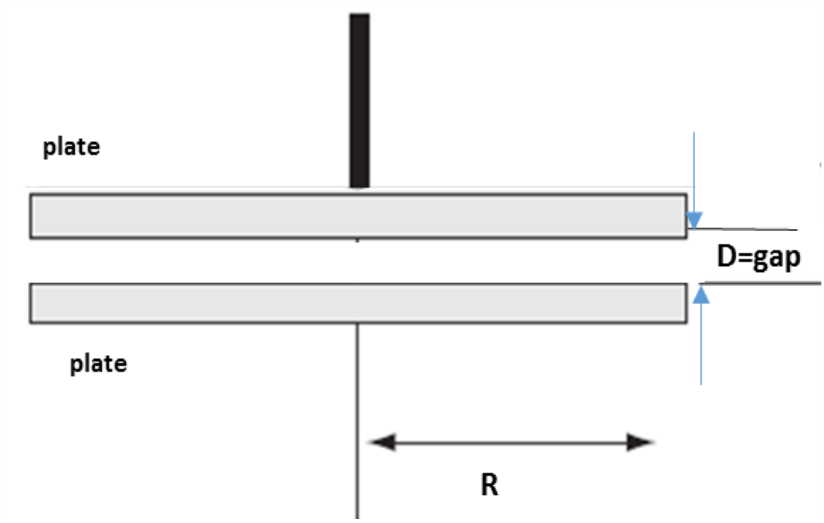

Figure 3.14 A schematic diagram of parallel plate measuring system

Concentric cylinders system: also called (cup and pop). Concentric cylinders are generally used for lower viscosity samples that would otherwise not be constrained within the gaps of cone and plate or parallel plate systems. There are several different types of concentric cylinders systems. Figure 3.15 shows three concentric cylinders systems that can be used in TA instruments, ddouble concentric, conical end and recessed end.

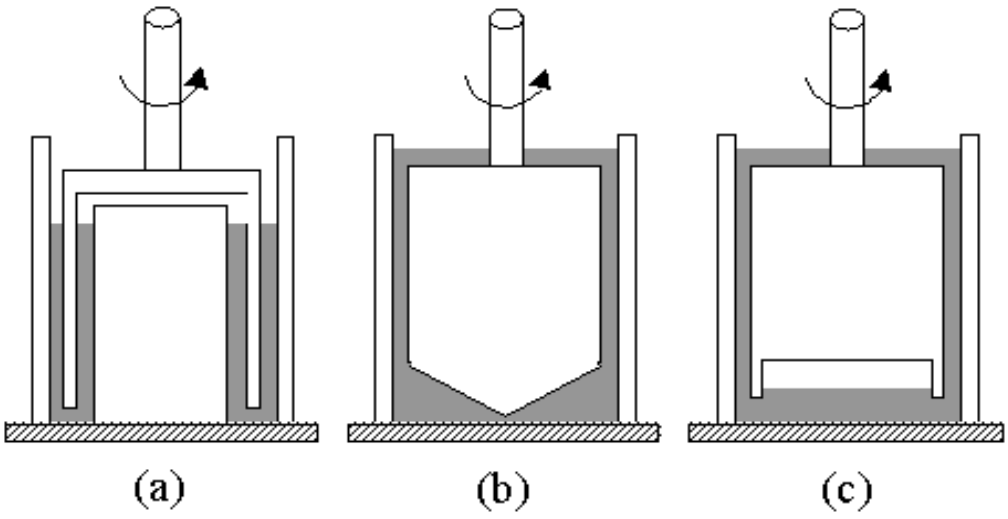

Figure 3.15. Schematic diagram of different concentric cylinders system: (a) Double concentric, (b) conical end, (c) Recessed end.

3.9 Materials and methods

This section describes the experimental procedures used to perform the characterization of the waxy oils, namely to measure their rheological properties. Data obtained will be discussed in the next section.

3.9.1 Crude oil samples

The three oils as well as their waxes (Faregh, Sarir and Bouri) considered in this chapter were characterized using various physicochemical and compositional analyses described in the previous chapter. The main characteristics of these oils are reported in **Table 2.1.** (Chapter 2).

3.9.2 Pre-treatment the crude oil samples

As the rheological properties are the key to this research, it was necessary to prepare the samples in a systematic manner so that no previous rheological history could affect the planned measurements. So previous to any rheological measurement, a pre-treatment was considered for the preparation of the crude oils samples.

The first step of the sample preparation was heating the samples to 10 °C above wax appearance temperature (WAT) in opened bottles whilst stirring using agitator for 3 hrs, to evaporate the light ends and to achieve a more stable chemical composition. Then, to provide samples from the same bottle throughout the whole experimental investigation each bottle was divided into small volumes flasks of 10 cm^3, and stored at room temperature until further analysis.

Before each experimental measurement each flask was heated to 10 °C above WAT for 20 minutes to erase any previous thermal history or any possible waxy structure of the oil. Such a method of preparation is widely used for rheological testing of waxy crude oil [68].

3.9.3 Rheological measurements

After the pretreatment process, each pre-treated sample was loaded onto the rheometer plate, pre-set at the same preheated temperature, and then cooled to the

desired test temperature at 0.5 °C/min. After cooling the sample to the desired temperature on the rheometer plate, under a small applied shear rate (2 sec^{-1}), each sample was left for 10 minutes before starting any rheological measurements. Each test was performed under isothermal conditions. A plastic cover was placed over the measuring cell to minimize evaporation.

Rheometer

As mentioned above, the rheometer used in this study is a controlled stress rotational rheometer (AR 1000, from TA Instruments). This equipment is appropriated to the direct measurements of yield stress and the yielding process of gels and materials that contain solidifying particles such as waxy crude oils, the measurements of viscosity, creep-compliance tests and oscillatory measurements

This rheometer was fitted with a parallel plate measuring system (4 cm diameter, steel roughened surface, 500 µm gap). This gap size is thought to be in the appropriate range according to recommendations of Marchesini et al. [42], allowing to minimize shrinkage effects and optimize temperature control.

Three direct measurements were performed: 1) controlled stress test measurements were carried out in order to obtain flow curves and viscosity data; 2) Creep-recovery tests; and 3) Oscillatory linear tests at low strain amplitude.

3.9.3.1 Controlled stress test

The flow behavior of the gelled crude oils was investigated by shear stress ramps (from 0 to 180 Pa) for 5, 10 and 20 minutes to achieve the rate of 36, 18 and 9 Pa min^{-1} respectively. Apparent viscosity and yield stress values were measured. For the three oils, all measurements were carried out at equivalent temperatures (3, 5 and 9 °C below pour point). Four characteristic yield stresses, namely a primary yield stress, a static yield stress, fracture yield stress and a dynamic yield stress were described.

3.9.3.2 Creep-recovery test

The creep-recovery tests were performed on the gelled crude oils at shear stresses 8, 16, 25 and 32 Pa for one minute and the shear stress was reduced to zero for 20 minutes to investigate the effect of shear stress on the creep behavior. Also the effect of the magnitude of the applied constant stress of 16 Pa within different time periods 1, 5 and 20 minutes were studied for two oils (Faregh and Bouri). The measurements were performed at a constant temperature, 3 °C below pour points of each crude oil.

3.9.3.3 Oscillatory test

Dynamic test measurements were carried out to measure the viscoelastic parameters as a function of time and oscillatory frequency, with particular focus on the effect of test temperature. The isothermal time sweep tests at different temperatures above and below pour points were performed for each oil at a constant frequency of 2 rad/s and 60 minutes holding time. The mechanical spectra of the cured waxy gels (frequency sweep experiments) were obtained in the frequency range 0.1-100 rad/s (0.0159 - 15.94 Hz). For both types of tests, the viscoelastic moduli, the storage modulus (G'), the loss modulus (G'') and loss angle (δ), were determined. All measurements were performed at a low strain of 0.1 %.

Also, in this study, shear stress amplitude tests were performed, In order to investigate the yielding process and examine the stability and strength of the structure of gelled oils. Oscillatory tests were conducted at fixed low frequency of (1 rad/sec), while the shear stress is varied during the amplitude sweep from 0 to 100 Pa. The measurements were performed at 3 °C and 5 °C below pour point temperatures for each oil. Three yield stresses were described, namely elastic yield stress, a static yield stress and flow yield stress.

3.10 Results and Discussion

Data on rheological properties, steady-shear flow, time-dependent creep and dynamic behaviour, of three waxy crude oils used in this study are presented in this section. These were Faregh from Waha, Bouri from ENI-Oil and Sarir [3] from Arabian Gulf Oil Company of Libya. Recall that these oils have different wax contents, 24, 15 and 13.6 % respectively, so we may consider that they cover a representative range of waxy oils available throughout the world, as well as their pour points of 21, 24 and 12°C, respectively. It is interesting at the outset to remark that these pour points are relatively high but not abnormal and stress the observation that gelling of waxy crude oils occurs commonly at ambient temperatures. In Libya, the temperature changes from about 40 °C during the day in summer and autumn to 10 °C during the night. During the winter, the temperature can reach around 0 °C in the day time and may drop to values marginally below zero during the night.

From the review of literature, on the yielding process of the waxy crude oils, it can be established that the key element is a proper evaluation of the rheology of the waxy crude oils below or near their gel point [31, 40, 57, 77]. Near pour point, the oil starts to lose its flowability, i.e. wax deposition and interactions between wax crystals lead to gel formation. Thus, the results from the various rheological tests were obtained at temperatures near and below the oils pour points and are presented and analyzed in detail to define the characteristic flow and mechanical behaviour of three Libyan waxy crude oils, aiming to contribute for a suitable solution to reduce the costly problems of operation and transportation due to wax precipitation and blockage of the pipelines. The results are thus organised in three sub-sections, firstly the characterization of the flow behavior of the crude oils, followed by the characterization of the time-dependent behaviour and finally the results regarding the viscoelastic behaviour of the three gelled waxy crude oils.

[3] Technical information about Faregh and Sarir oil fields are available in Appendix A

3.10.1 Flow behavior of the crude oils below their pour point temperatures

From a basic rheological point of view, to achieve steady state operating conditions, and to manage the subsequent stresses required once the start-up after shutdown has been successful, it is necessary to know the oil apparent viscosity, how it depends on the applied stresses and how it changes with time, so that the operating stresses/pressures can be reduced and consequently the cost kept to a minimum. In order to assess the oil-gel structure state and predict the yield stress, the flow behavior of the three Libyan waxy oils mentioned above was studied at temperatures below pour point. All tests were performed with the same temperature history and by applying the same controlled cooling profile.

In all cases, the oils were cooled from the high temperature imposed (samples heated 10 °C above WAT as described in section 3.9.2, to avoid memory effects). These temperatures were 53 °C for Faregh oil, 59 °C for Sarir oil and 39 °C for Bouri oil. After loading the samples onto the rheometer plate, heated to the above temperature depending on the sample, each sample was cooled *in-situ* at a pre-specified cooling rate (0.5 °C/min) down to the test temperatures of 18, 16 and 12 °C for Faregh oil (pour point 21°C), 21, 19 and 15 °C for Sarir oil (pour point 24°C) and 9, 7, and 3 °C for Bouri oil (pour point 12°C), hence corresponding to temperatures 3, 5 and 9 °C below the pour point of each oil. A subsequent holding time (10 min) was then applied at the desired test temperature before each experiment to allow the gel network to mature [35]. After that, the measurements were conducted under controlled shear stress mode, by applying a stress ramp from 0 to 180 Pa, during 10 minutes (ramping rate of 18 Pa/min), and recording the resulting shear rate, and consequently, the apparent viscosity. The measurements were carried out three times for repeatability.

3.10.1.1 Shear data to measure the variation of apparent viscosity at different temperatures

Under the applied stress, the structure will gradually break in time until flow begins. Estimation of the effect of the same stress loading rate (time scale) on apparent viscosity

was carried out at equivalent temperatures below the pour points for the three oils (3, 5 and 9 °C below pour point) as mentioned above.

Figures 3.16 to 3.18 present the data of viscosity as a function of applied stress for Bouri, Sarir and Faregh oils, respectively, at the three tested temperatures. The crude oils show non-Newtonian shear thinning (viscosity reduction with increasing shear rate) behavior over the range of shear stresses studied. The results mimic the gradual development of viscosity before and at the beginning of re-start flow. As it can be seen, Two different regimes, a rapid decline regime (*b*-*c*), corresponding to an infinite viscosity as the shear rate approaches zero supporting the existence of true and significant yield stress, and a lower gradual decrease in viscosity as the shear stress increases, regime (*c*-*d*), i.e. viscosity changes are larger at low shear stresses (regime *b*-*c*) than at higher shear stresses (regime *c*-*d*).

For example, as shown in Figure 3.16 for Bouri oil at 9°C, during the first regime the increasing applied stress causes the viscosity to drop drastically, falling from approximately 4551 Pa.s (point b) to a low value of 229.2 Pa.s (point *c*) within stress range of (55 to 75) Pa. Lower gradual decrease of viscosity was observed during the second regime, decreasing to a lower value of 9.88 Pa.s (point c) at the end of the measurement. The pronounced decrease in viscosity with applied stress (or shear rate) is likely associated to the breaking of the existing structure within the oils, decreasing the aggregation among the wax crystals and/or allowing for an effective dispersion of wax agglomerates in the continuous phase originally immobilized within the agglomerate. As the shear rate increases, the chain type molecules disentangled, stretched, and reoriented parallel to the driving force, and hence reduced the heavy crude oil viscosity and the flow encounters less resistance at higher shear rates [112]. A similar qualitative behavior can be observed at temperatures of 7 and 5 °C for Bouri oil, and also for the other oils.

Bouri oil shows more stable aggregates of the waxy structure forming the first regime than Sarir and Faregh oils. for example at 3°C below pour point for each oil, the viscosity reduction was about 94%, while the reduction is more than 99% for Sarir and

Faregh oils respectively. The high yield stress value (higher than 180 Pa) of Faregh oil at 12 °C precluded the rheological measurement.

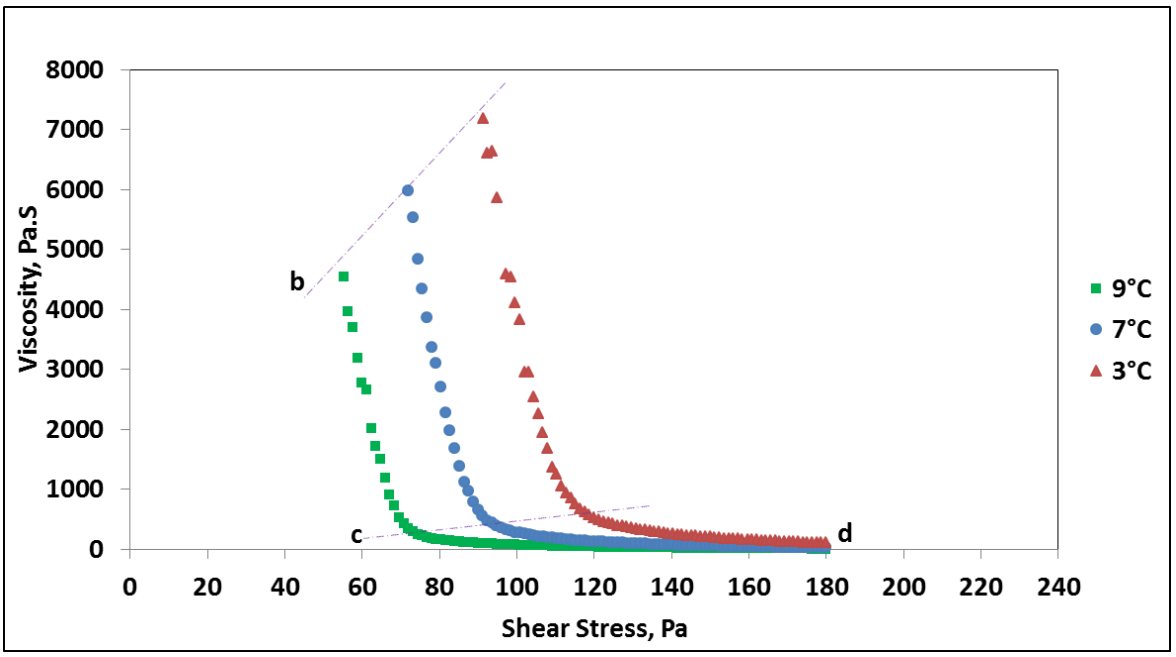

Figure 3.16 Apparent viscosity variation with applied shear stress for Bouri crude oil at different temperatures [stress loading rate=18 Pa/min].

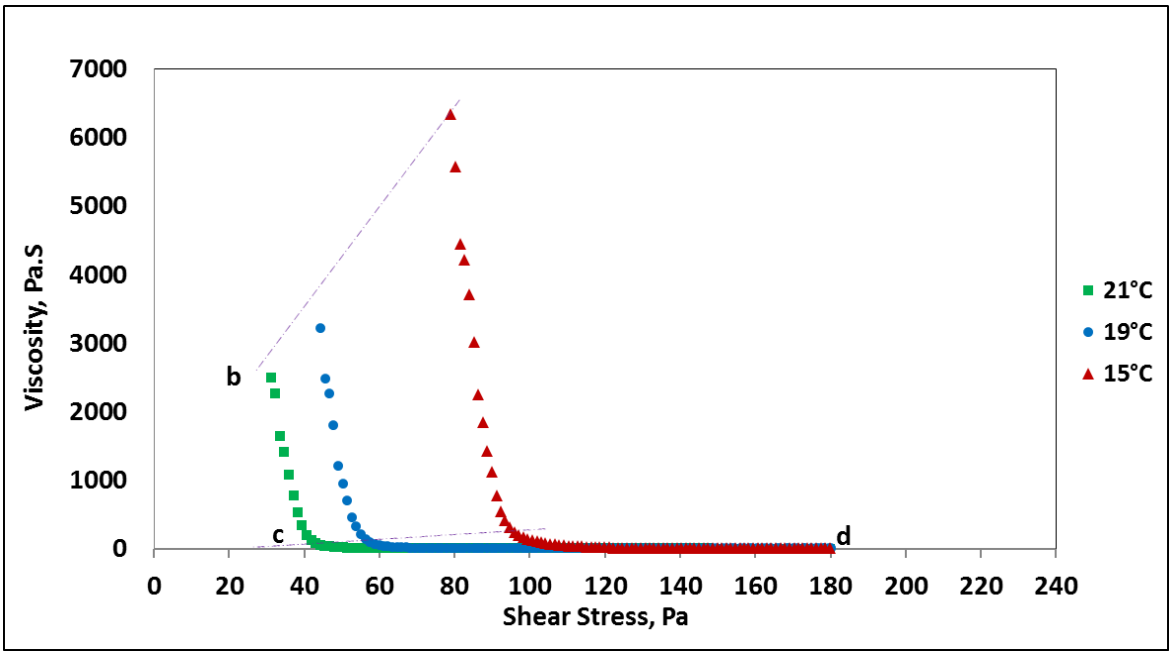

Figure 3.17 Apparent viscosity variation with applied shear stress for Sarir crude oil at different temperatures [stress loading rate=18 Pa/min].

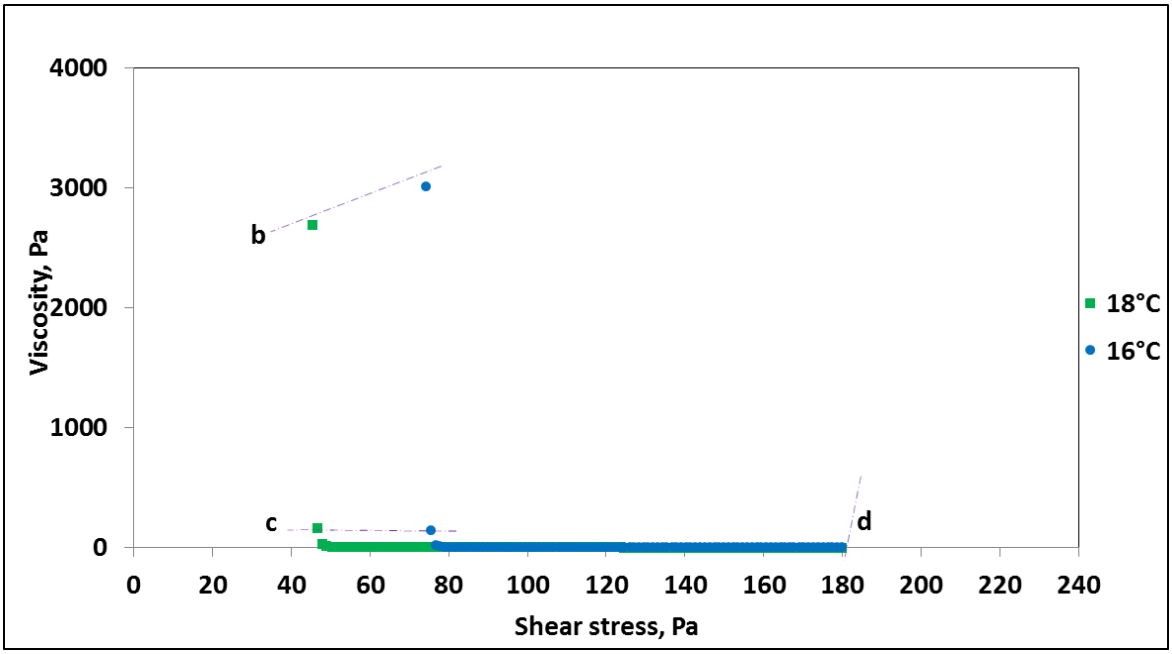

Figure 3.18 Apparent viscosity variation with applied shear stress for Faregh crude oil at two different temperatures [stress loading rate=18 Pa/min].

Figure 3.19 displays the effect of temperature on viscosity at shear stress of 100 Pa at the studied temperatures. As it can be seen the temperature has a strong effect on the oil's viscosity. The apparent viscosity decreases with increasing temperature. For example the viscosity of Faregh oil decreased from 5.07 Pa.s to 1.442 Pa.s (about 72%) with decreasing temperature from 18°C to 16°C. The observed variation with temperature is attributable to crystallization of wax components and possible aggregation at lower temperatures, hence increasing the oil viscosity. With increasing temperature, the ordered structure of the aggregates of these chemical components decreases, thus reducing the oil viscosity [108]. Comparing the apparent viscosity of the three oils, and for the same decrease of temperature below PP, we can observe that Bouri has higher viscosity values than Sarir and Faregh oils.

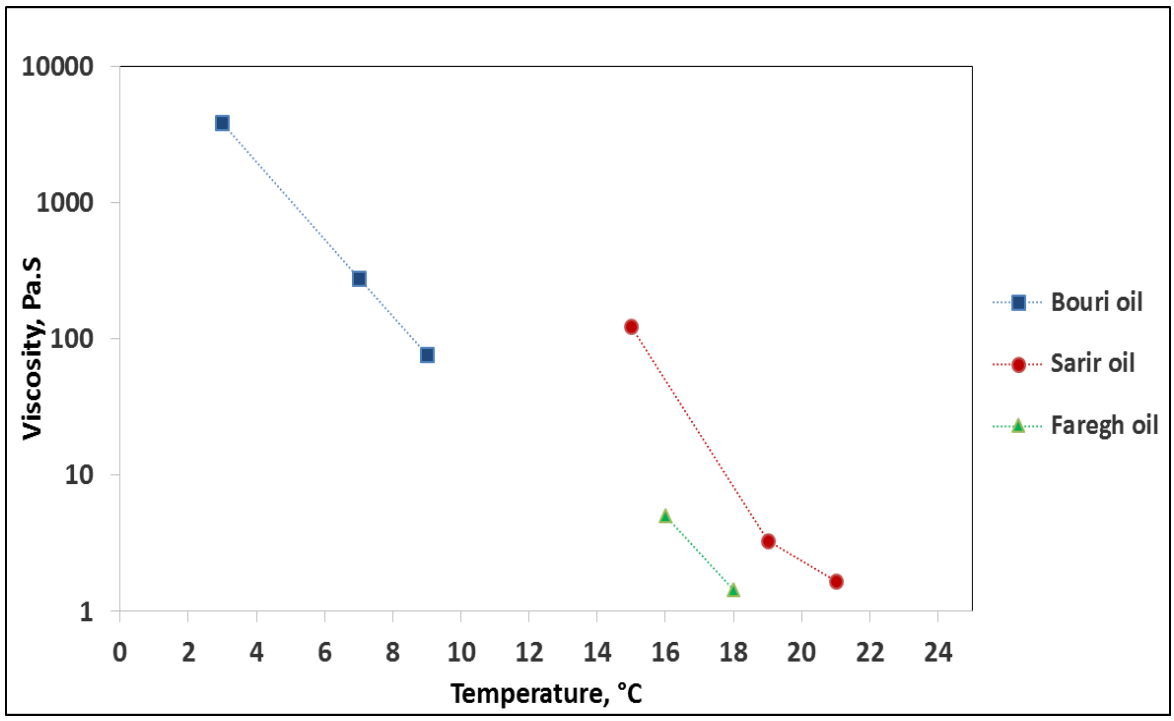

Figure 3.19 Apparent viscosity at the different studied temperatures for the three oils at shear stress=100 Pa.

In order to understand the behavior of theses oils more clearly, the characteristic of each oil will be described in details in terms of its yielding during the shearing process in the next subsection.

3.10.1.2 The yielding process of the three waxy crude oils

As discussed before (section 3.8.1) the yield stress of crude oils is an important technological parameter and its knowledge is of great importance to define the more appropriated protocol to restart plugged pipelines. Here we have calculated the yield stress values following the criterium of Chang et al. [57], who defined three yield stresses to characterize the initial yielding of a waxy crude oil: τ_e, the elastic-limit yield stress, below which the fluid exhibits a linear elastic response; τ_s, the static yield stress, the stress at the starting point of immediate fracture or flow; and τ_d, the dynamic stress, an extrapolated shear stress at zero shear rate obtained from the flow curve or from an instantaneous flow curve corresponding to a given sheared state.

Figures 3.20 to Figure 3.27 display representative flow curves for Bouri, Sarir and Faregh oils obtained for the temperatures under consideration.

The stress was gradually increasing with no shear flow reported till the first yield stress is reached. The shear rate of the samples was monitored to find the breaking point of the gel. The breakage is considered to have occurred when the shear rate starts to increase rapidly (point *C*).

Figures 3.20 -3.22 show the yielding process of Bouri oil and the location of the shear stress values that characterize that process accordingly to the criteria mentioned above. The elastic limit yield stress is independent of the time scale of the measurements and can be evaluated by creep-recovery or oscillatory tests [57]. It cannot be accurately determined from these measurements because of the resolution of the rheometer, as the shear rate in those region is very small. Here we tentatively determined a primary yield stress (τ_p) corresponding to the beginning of flow (shear rate ≠0), an approximation to the beginning of the creep region, the the static (τ_s) and the dynamic yield stress (τ_d).

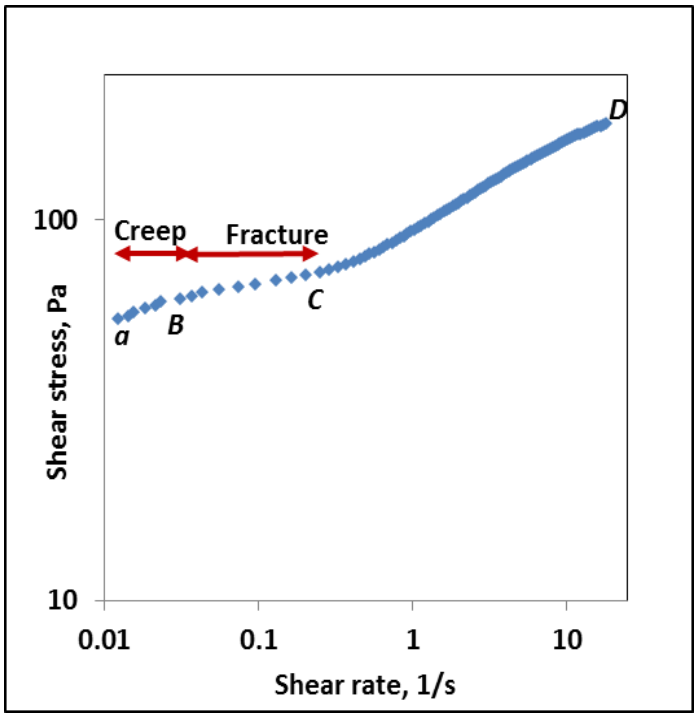

Figure 3.20 - Flow curve for Bouri oil: Shear stress vs shear rate during the yielding process at 9 °C [stress loading rate=18 Pa/min] .

The data recorded before point *B* show that the shear rate increases gradually with the increasing shear stress during creep process, therefore in this discussion, the first value recorded by the rheometer, point *a*, is defined as the primary yield stress. For instance, as it can be seen from Figure 3.20, for Bouri oil at 9 °C, no data were recorded before the shear rate reaches 0.0121 s^{-1} at a shear stress of 55.11 Pa (point *a*). Point *B* represents approximately the end of the creep region, after which a slight increase in stress leads to even a larger increase in shear rate, corresponding to the region *B-C* (fracture) where the structure is expected to be completely destroyed, being the stress at point *B* the static limit yield stress. The curve segment between *C* and *D* (the flow curve after yielding) corresponds to a shear-thinning (pseudoplastic) behavior, following a power law model.

Dynamic yield stresses are describing the oil properties at the final sheared state were the structure of the oils are finally broken through sustained shear (after point *C*). However as it was not possible to estimate the values of dynamic yield stress using the power law model (Herschel Bulkely model) because of the complex behavior of these oils, i.e. the mathematical solution provides zero values for some cases, such as Bouri and Faregh oils. Dynamic yield stresses were instead estimated by extrapolating the flow curves in the region *C-D* to zero shear rate and used as stress value to get more information about the liquid-like behavior of the broken gelled crude oils (viscous behavior). As mentioned above, the Faregh oil also showed a slightly different yielding pattern (Figures 3.26 and 3.27). Under the test conditions used, there was not possible to identify the creep region before the fracture, thus a primary yield stress was not calculated. This behavior is probably related to a different structure of the wax crystals aggregates.

Qualitatively similar flow and yielding behaviors were observed for the other oils at the studied temperatures. The yield stress values obtained and also the shear stress corresponding to the end of fracture (point *C*) are shown in **Table 3.2**.

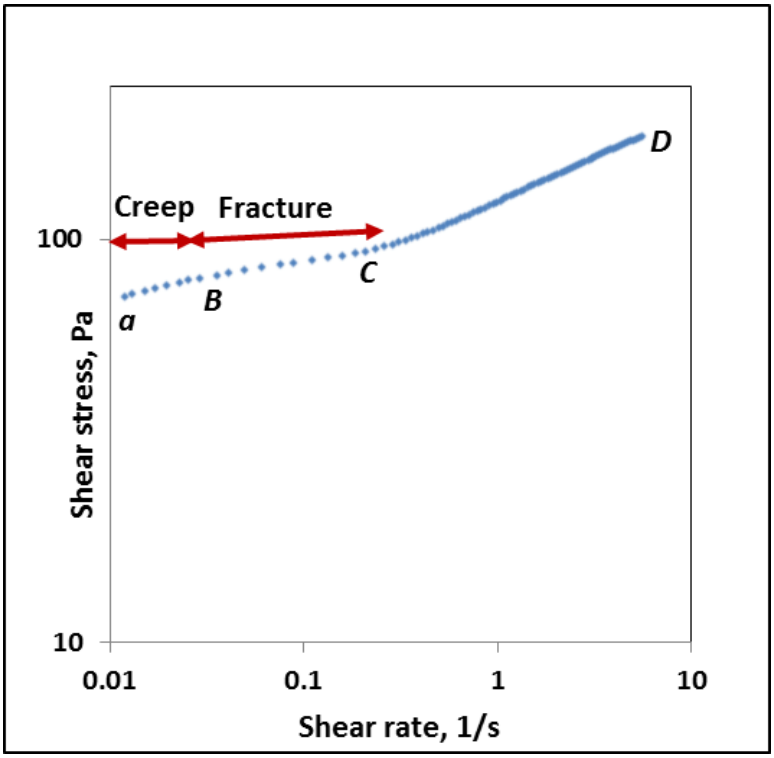

Figure 3.21 - Flow curve for Bouri oil: Shear stress vs shear rate during the yielding process at 7 °C [stress loading rate=18 Pa/min].

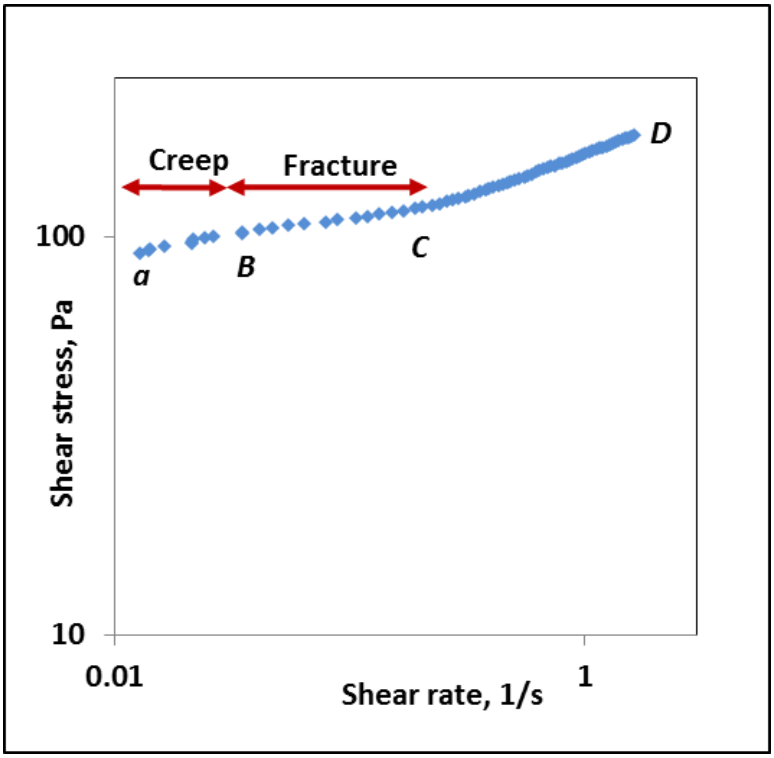

Figure 3.22 - Flow curve for Bouri oil: Shear stress vs shear rate during the yielding process at 3 °C [stress loading rate=18 Pa/min].

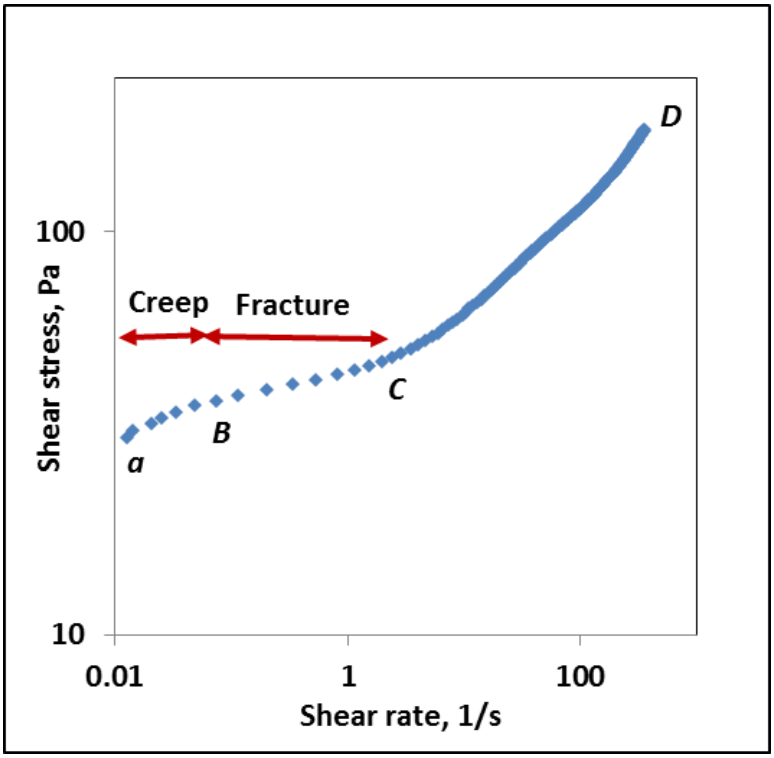

Figure 3.23 - Flow curve for Sarir oil: Shear stress vs shear rate during the yielding process at 21 °C [stress loading rate=18 Pa/min].

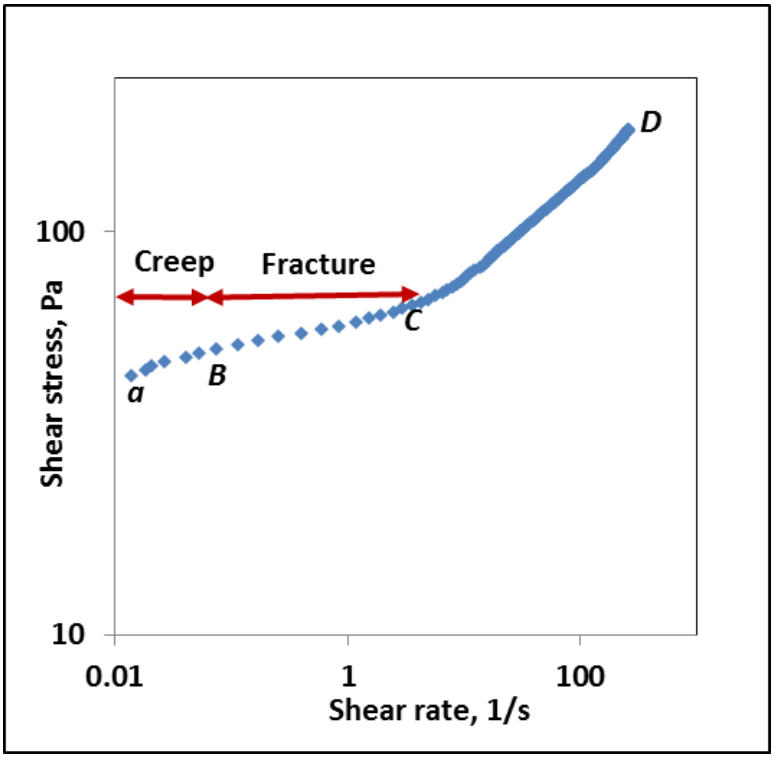

Figure 3.24 - Flow curve for Sarir oil: Shear stress vs shear rate during the yielding process at 19 °C [stress loading rate=18 Pa/min].

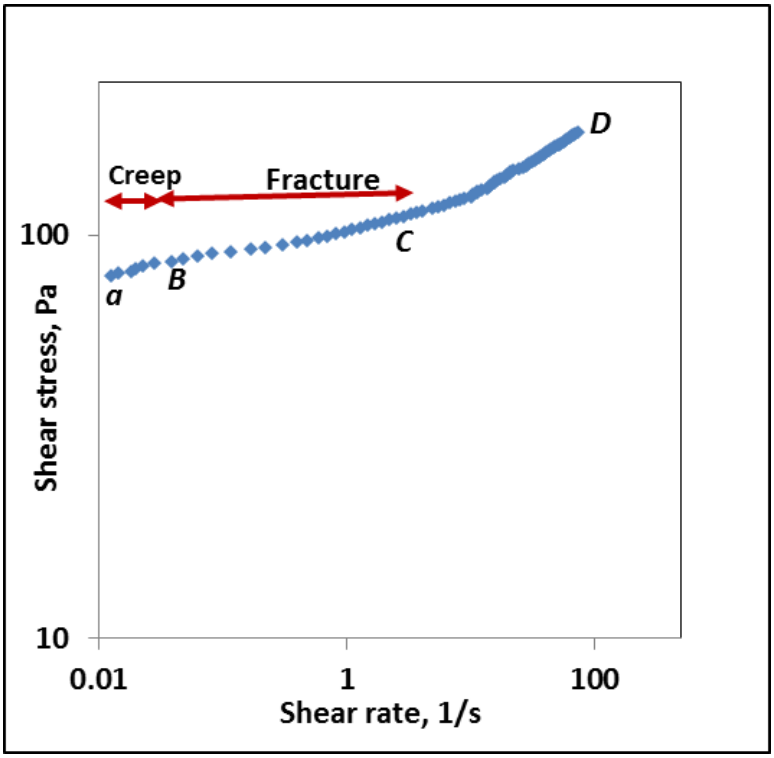

Figure 3.25 - Flow curve for Sarir oil: Shear stress vs shear rate during the yielding process at 15 °C [stress loading rate=18 Pa/min].

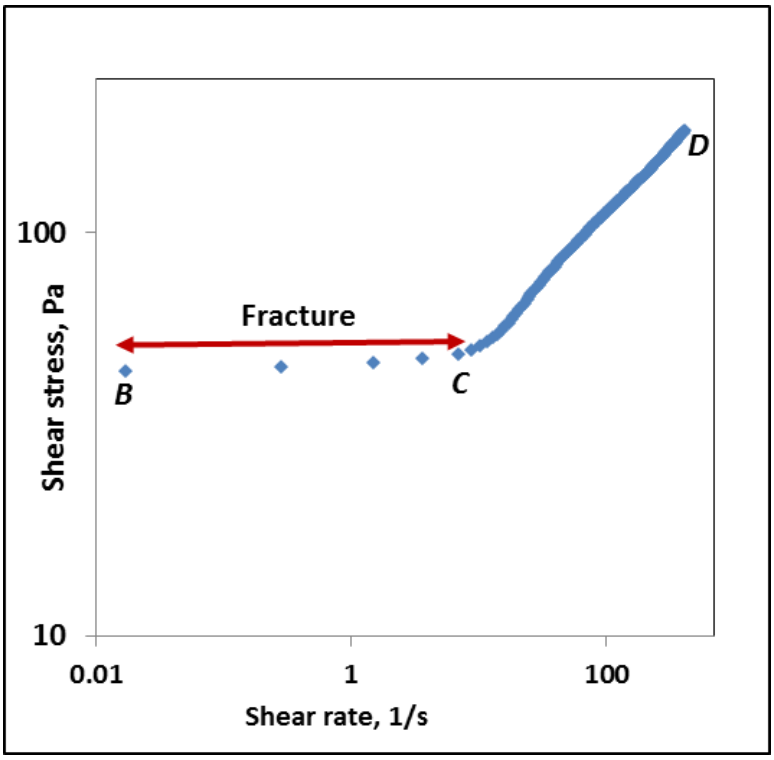

Figure 3.26 - Flow curve for Faregh oil: Shear stress vs shear rate during the yielding process at 18 °C [stress loading rate=18 Pa/min].

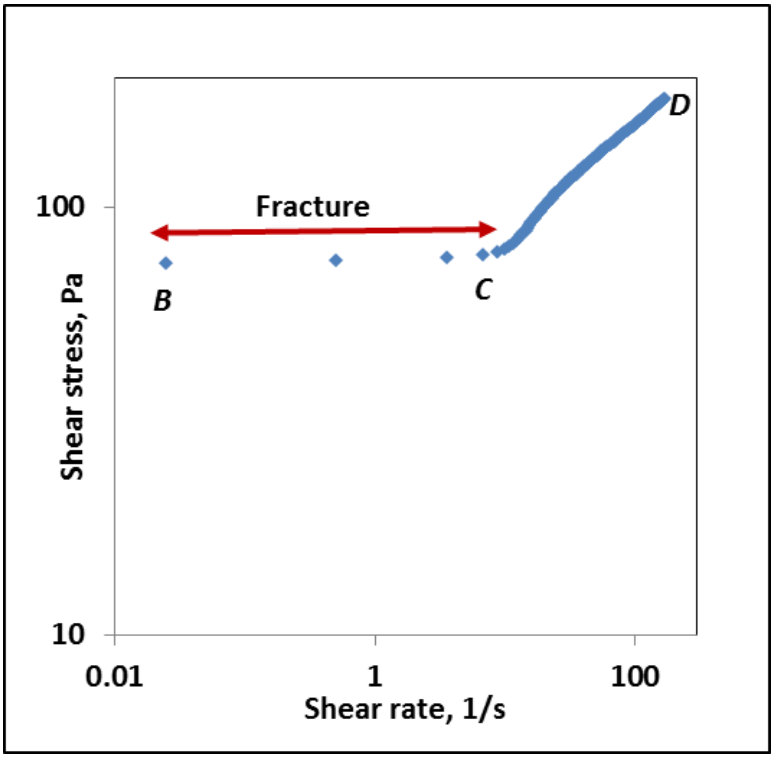

Figure 3.27 - Flow curve for Faregh oil: Shear stress vs shear rate during the yielding process at 16 °C [stress loading rate=18 Pa/min].

To obtain some information about the shear-thinning flow behavior of the gelled oils after fracture, we have applied the Herschel-Bulkley model (section 3.7.1), Equation 3.1, to the shear stress – shear rate data corresponding to the flow region *C-D*, by keeping τ_0 as a constant value, equal to the extrapolated dynamic yield stress. The Herschel-Bulkley equation describes the flow behaviour of shear thinning fluids that require some stress to initiate flow (dynamic yield stress). This kind of fluid will not flow until the applied shear stress exceeds a certain minimum value (τ_0) which is interpreted as yield stress. **Table 3.1** shows the Herschel-Bulkley parameters obtained from the fitting of Equation 3.1 to the flow curves (region *C-D*) of the three oils at the temperatures under study.

Table 3.1. Rheological parameters and correlation coefficients values of Herschel-Bulkley model for the investigated Libyan oils

Oil sample	Temperature /°C	*K*	*n*	τ_0 ([a])	R^2
Bouri	9	31.42	0.514	65	0.991
	7	39.86	0.546	83	0.993
	3	52.68	0.769	107	0.994
Sarir	21	5.97	0.524	47	0.997
	19	6.5	0.525	60	0.996
	15	7.00	0.570	101	0.995
Faregh	18	4.37	0.545	41	0.993
	16	9.72	0.599	59	0.990
	12	.....	.....	([b])	.....

([a]) Values of Dynamic yield stress (Pa)
([b]) Yield stress higher than 180 Pa

Table 3.1 reports very high regression correlation coefficient, R^2, for all oils, meaning that within the region C-D the flow follows the expected power law behavior. Values of *n* for the three oils are lower than one meaning that the oils exhibit similar flow behavior (shear-thinning behavior is taking place after fracture). However, the consistency index (*K*) and the flow behaviour index (*n*) are increasing with decreasing temperature for the three oils which means higher values of viscosities of the oils with decreasing temperature.

The important observation in all this data is that there is a significant difference between the *K* values with decreasing temperature for Faregh than for the other oils, which confirms the significant difference in viscosity with deceasing temperature for this oil leading to very high yield stresses at lower temperatures (greater than 180 Pa at 12°C).

Bouri oil displays higher *K* values (31.4-52.68) than Sarir (5.28-6.47) and Faregh oil (4.37-9.72) falls in between them, which indicates that a higher stress is necessary to break the structure of aggregated wax crystals. As previously discussed Bouri oil has the highest values of viscosities at the investigated conditions (with exception of Faregh oil at a temperature far from PP, T=12°C). This can be seen clearly in **Table 3.2** in the values of static yield stress.

Table 3.2 Yield stress values for the studied oils measured under a loading rate of 18 Pa/min.

Oil sample	Temperature, (° C)	Primary yield stress/ τ_p, Pa	Static yield stress/ τ_s, Pa	Fracture yield stress/ τ_f, Pa ([a])	Dynamic yield stress/ τ_d, Pa
Bouri	9	55	62	75	65
	7	72	80	96	83
	3	91	102	117	107
Sarir	21	31	38	51	45
	19	44	53	68	60
	15	79	88	112	101
Faregh	18	.....	46	51	41
	16	.....	74	80	59
	12	([b])	([b])	([b])	([b])

([a]) Stress at the end of fracture, starting of viscous (shear-thinning) flow
([b]) Yield stress higher than 180 Pa

As shown in **Table 3.2**, the fracture yield stress is an alternative to the yield stress here proposed to be used to describe the required stress for the oils after initial flow i.e.

the essential stress to continue and guarantee flow instead of dynamic yield stress for such complex crude oils.

The values of static yield stress of theses oils are inferior to the values of dynamic yield stress for Bouri and Sarir oils. This behavior is probably due to some factors that affect waxy crude oils during yielding process; from solid like to viscous like fluid; such as shear and thermal histories, thixotropic effects as well as the gel composition of the oils. It is also shown in **Table 3.2** that the values of fracture yield stress are higher than static yield stress which means that after fracture a higher stress is necessary to keep the oil flow due to this complex behaviour, as discussed above.

Yield stresses of waxy crude oils are known to be strongly influenced by the degree of interlocking structure developed by waxing and instability of the network [109]. As expected, the results of the yield stresses in **Table 3.2** indicate that the waxy structure strongly depends on the temperature of the oil. As the temperature decreases, a higher stress must be applied in order for the yielding to occur. For example, for Bouri oil, the static yield points, decrease with temperature from 102 Pa at 3°C to 62 Pa at the temperature of 9°C. Similar trends were observed for the other oils.

Comparing the three oils for a similar decrease in temperature below the pour point, Bouri oil shows the highest static yield stresses and Sarir oil the lowest (not considering the particular behavior of Faregh oil far from the pour point, at T=12°C). The static yield stress, corresponding to the shear stress required to start flow, is dependent on the nature of the micro-structure of the wax crystals in the oils before the structure is disturbed [57]. Therefore we may expect that for Bouri oil the interactions between wax crystals are more extensive. The existence of some heavy paraffins from C_{36} to C_{40} as well as the percentage of non-alkanes, above 20 wt% in Bouri oil may contribute to more rigidity for this oil than Faregh and Sarir oils, where the aggregate structures of Bouri oil are much more stable against the applied stress than those present in Faregh or Sarir oils.

Figure 3.28 shows the variation of static yield stress with temperature for the three oils. Lower temperatures lead to the formation of stronger aggregates, hence increasing

the gel strength. It is important to recall that for Bouri and Sarir oils a similar dependence of the static yield stress on temperature was observed, but Faregh oil showed a more pronounced temperature effect on the yielding, probably related to a different micro-structure and interactions between the crystals.

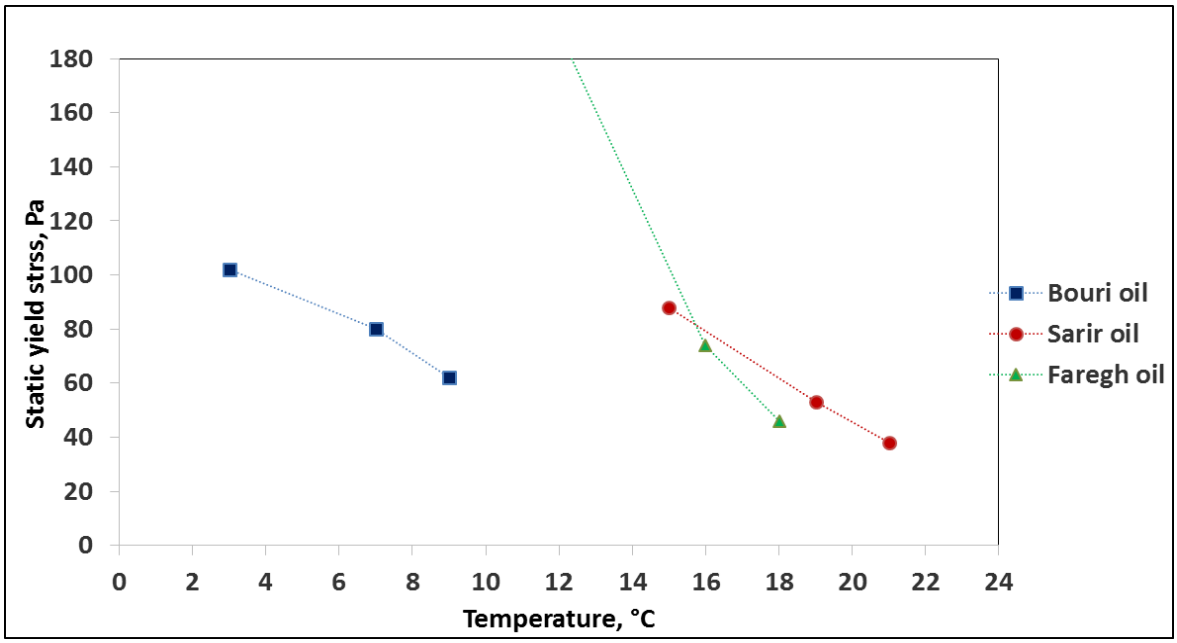

Figure 3.28- The effect of temperature on static yield stress of the investigated oils

Sarir presents the highest n-paraffin content, 92.66%, but its static yield stress is inferior to Bouri oil. This is a clear indication that the gel strength is not only dependent upon the n-paraffin content as previously suggested [47, 53]. Similarly, Faregh at 18 & 16°C (temperatures close to PP) and Sarir while presenting higher wax contents, of 24 and 15% respectively, their static yield stresses are inferior to that of Bouri oil. This is a clear indication that the gel strength is dependent upon other factor than just the wax content as previously proposed [48, 52]. It is thus important to investigate more carefully the gel strength dependence on the nature of the wax precipitates at temperatures near pour point.

Controlled stress tests enable the direct measurement of the yield stress in order to obtain the true yield stress (static yield stress value during fracture process) which is the value of most interest to pipeline engineers and the one most often used as the yield point [31,57]. In fact, for a gelled crude oil inside the pipeline, solving the start-up problem

implies applying a constant pump pressure greater than that required to overcome the static yield stress of the gelled oil. Although the static yield stress could be easily obtained from the simple direct measurements using the controlled stress test, as discussed above, its practical application to pipeline design is not straightforward since this measured static yield stress strongly depends on the time scale of the measurement, i.e., the stress loading rate applied during the test. The wax crude oils are time-dependent materials and therefore the static yield stress is dependent on the time scale of the test.

The flow curves presented in this Section illustrate the complex rheological characteristics of the waxy crude oils below their pour point temperatures. Creep and oscillatory tests at low deformation temperatures will be valuable complementary techniques to characterize the time-dependent and solid-like behavior of these gelled oils, namely in the elastic region, and will be discussed below.

In order to get further information regarding this aspect, the yielding behavior was also studied using different stress loading rates, as discussed in the next subsection.

3.10.1.3 The Effect of different time scales on the strength of waxy crude oils

It is important to carry out flow experiments at different stress loading rates to capture the effect of shearing time on the viscosity and yielding. In order to select the best conditions of applied stress and loading time, i.e. when starting a gelled pipeline, it may be that much lower stresses (pressures) are required but for a comparatively longer time, but not excessively long to justify not going for very high stresses, even so they necessarily would require shorter loading times to start up the pipeline, and vice-versa. It is also useful to analyze the variation of apparent viscosity under an applied stress ramp while the stress loading rate is varied. Such information will provide a complete picture of the oil behavior and will enable to provide the pipeline operators the required data regarding stress and viscosity. Predicting those rheological behaviors are important for evaluating the flow development and the time to re-establish steady state flow, i.e. how time affects the oil apparent viscosity, what parameters impact the yield stress development in a pipeline shutdown, and how those properties will behave during the

flow restart for the successful design/operation of pipelines and pumping of waxy crude oils, which is very costly if not carried out wisely.

The objective of this section was to study the effect of stress loading rate on the strength of the two gelled oils (yield stress and apparent viscosity as a function of the applied stress), in order to better understand what conditions may be more appropriated for the re-start of a pipeline. The shear stress ramp in these experiments also ranged from 0 Pa up to 180 Pa, applied over a period of 5 and 20 minutes (stress loading rate of 36 and 9 Pa/min, respectively), for two different temperatures, 9 and 21 °C for Bouri and Sarir oils, respectively (3 °C below the pour point of each oil). Once data for the two different loading rates, 9 and 36 Pa/min were obtained, they were compared with the previous results obtained at a stress loading rate of 18 Pa/min, at the same temperature. The measurements were carried out three times for repeatability.

Figures 3.29 - 3.30 display the data of viscosity as function of applied stress, at constant temperature and the three different stress loading rates, for Bouri and Sarir oils, respectively.

A similar dependency of the viscosity on the stress loading rate is observed for the two oils. The crude oils show non-Newtonian shear thinning behavior over the range of shear stresses studied.

Concerning the discussion in the previous section, two different regimens can be seen: rapid decline regime (*b*-*c*) corresponding to an infinite viscosity, and lower gradual decrease in viscosity variations as the shear stress increases, in the second regime (*c*-*d*).

As shown in Figure 3.29 for Bouri oil at a stress loading rate of 9 Pa/min, during the first regime the increasing applied stress causes the viscosity to drop drastically, falling from approximately 4782 Pa.s (point *b*) to a low value of 338.8 Pa.s (point *c*) within a stress range of (64 to 79) Pa. Lower gradual decrease of viscosity was observed during the second regime, decreasing to a lower value of 8.74 Pa.s (point *d*) at the end of the measurement. Similar qualitative behavior can be observed at a stress loading rate of 36 and 18 Pa/min for Bouri oil, and also for the other oil.

The time scale of the measurements has a strong effect on the oil's viscosity. The apparent viscosity increases with increasing time scale, i.e. viscosity expressing more resistance to deformation with decreasing stress loading rate. For example at (point *c*) when the stress loading rate decreases from 18 Pa/min to 9 Pa/min the viscosity of Bouri oil increases from 4551 Pa.s to 4782 Pa.s.

The observed viscosity variation with stress loading rate indicates that the slower the loading rate the stronger the structures. This is attributable to waxes and some other components in the crude oils. At lower stress loading rates (longer time scale), the structure of some destroyed aggregates of these chemical components will have a chance to rebuild up structures of aggregates, hence increasing the oil viscosity with more time. This behaviour is easily explained in relation to the significant time dependent properties throughout the time scale of the test, i.e. these waxy crude oils have a structure, their yield stress itself is time dependent.

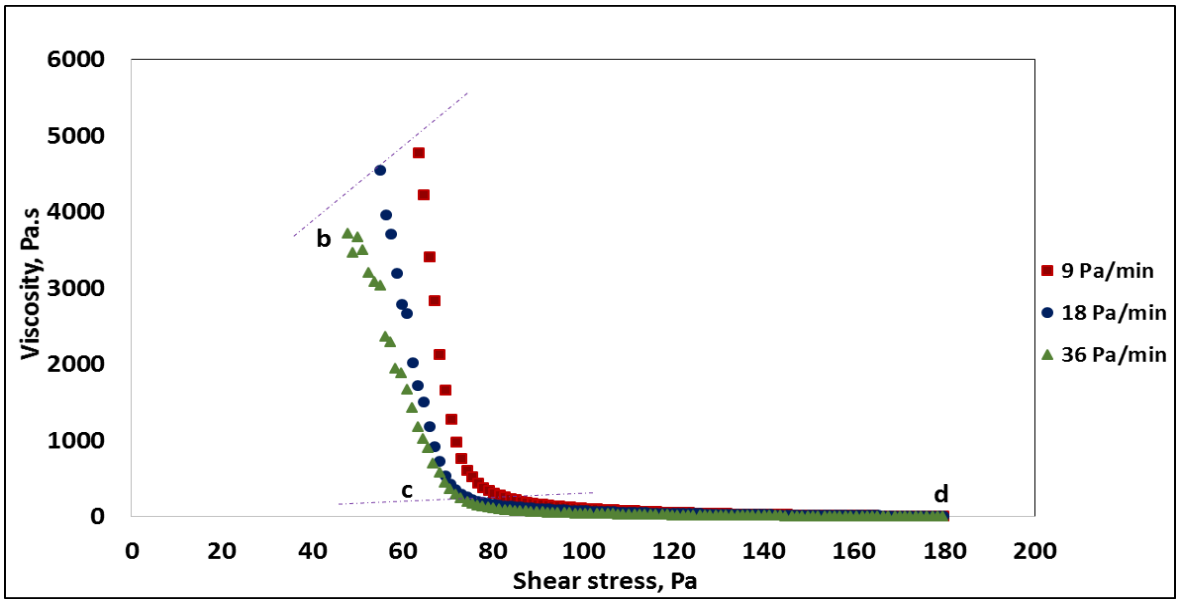

Figure 3.29 The effect of stress loading rate on viscosity for Bouri oil (T=9°C).

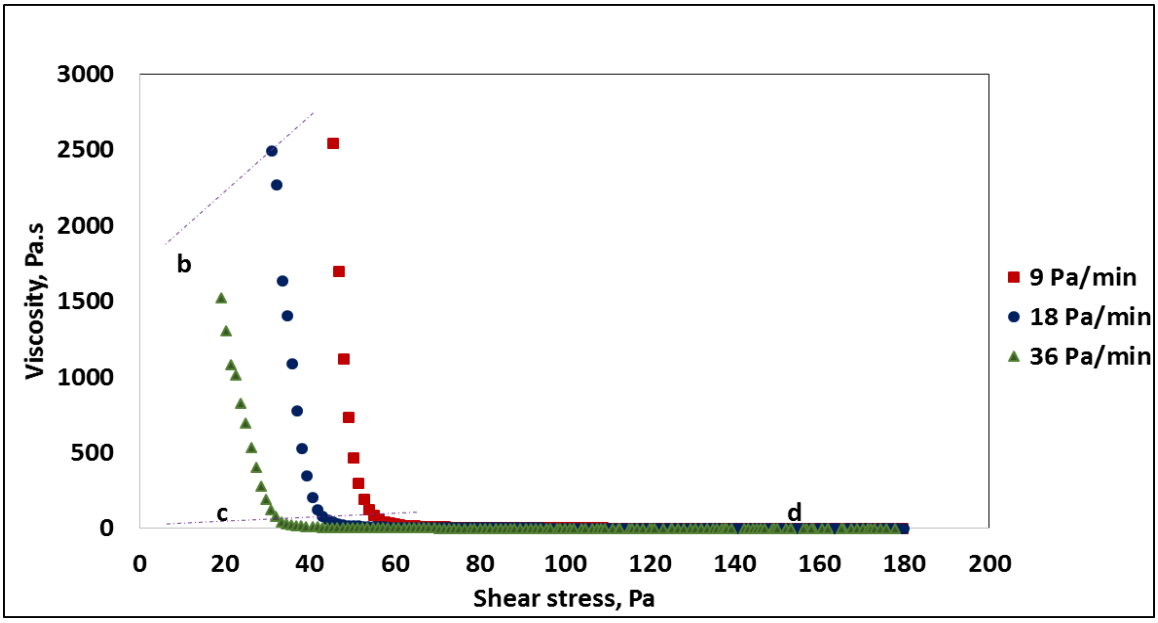

Figure 3.30 the effect of stress loading rate on viscosity for Sarir oil (T=21°C).

Figure 3.31 displays the effect of time scale on the apparent viscosity at shear stress of 70 Pa. Comparing the apparent viscosity of the two oils, we can observe that Bouri oil has higher viscosity values than Sarir oil at the three different time scales. As discussed above the time scale of the measurements has a strong effect on the oil's viscosity. For example the viscosity of Sarir oil was decreased by about 52 % with decreasing the time scale from 20 to 10 min.

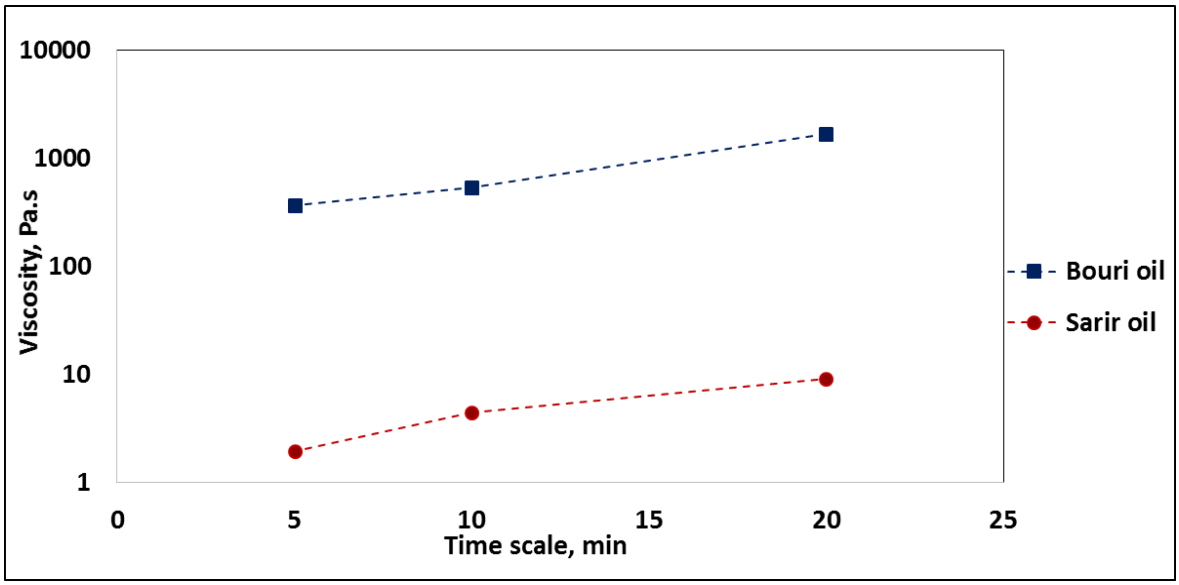

Figure 3.31 The effect of time scale on the apparent viscosity for Bouri and Sarir oils [shear stress =70 Pa]

Clearly the time scale of the measurements is important in order to characterize the time-dependent behavior of these gelled crude oils, as this kind of complex systems are known to show a thixotropic behavior, dependent on shear history, what is an important feature of waxy crude oils [104, 105, 110].

As previously discussed regarding the yield stresses of the crude oils (**See Table 3-2**), these parameters depend on the nature of the oil, temperature. Below pour point, the wax in the oil will precipitate and gradually build up a layer of agglomerates on the wall of the pipe which grows in time. The key information to restart the pipe is to know the minimum stress required to overcome the structure and induce flow. The data here obtained will be used to discuss the effect of the time scale on the static and fracture yield stresses. Dynamic stresses, which describe oils property after fracture were also considered at the different times scales.

Figures 3.32 to 3.35 display the flow curves for the two oils obtained at different loading rates at the investigated temperatures. At a stress loading rate of 36 Pa/min, a similar pattern in the yielding process of Bouri and Sarir oils was observed (Figures 3.33 and 3.35 respectively). As discussed earlier in the previous subsection, the data recorded before point B show that the shear rate increases gradually with the increasing shear stress during creep process, therefore the increasing pattern of shear rate following point *B* represents the fracture process or the static limit yield stress, hence point *B* and *C* is describing the static and fracture yield stresses of the oil.The curves becomes finally a sharply rising incline, segment (*C-D*), which represents the shear process after the yielding as the microstructure of the oil is destroyed. The curve segment between *C* and *D* corresponds to a shear-thinning behavior, following a power law model.

As already argued in the previous subsection, here it also was not possible to estimate the values of dynamic yield stress using Herschel-Bulkely model for Bouri oil. Dynamic yield stresses were instead estimated by extrapolating the flow curves in the region (*C-D)* to zero shear rate and then used as stress value to assess more information about the liquid like behavior of the broken gelled crude oils.

At a stress loading rate of 9 Pa/min, another representative pattern in the yielding process was observed for the two oils, a slightly different yielding pattern (Figures 3.32 and 3.34). Under these conditions it was not possible to identify the creep region before the fracture. As discussed before, the region (*B*-*C*) represents the fracture process followed by the final fracture of the samples, region (*C*-*D*). Point *B* is defined as static yield stress and point *C* is the fracture yield stress.

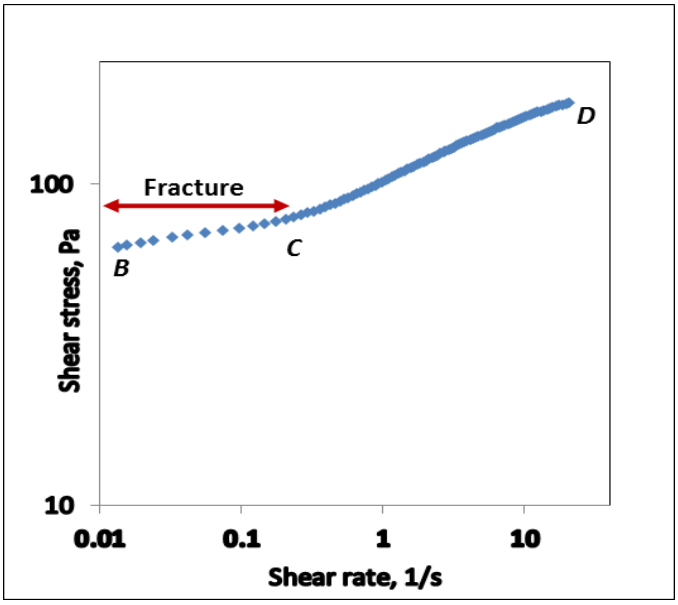

Figure 3.32 Flow curve for Bouri oil (Stress loading rate=9Pa/min, T=9°C).

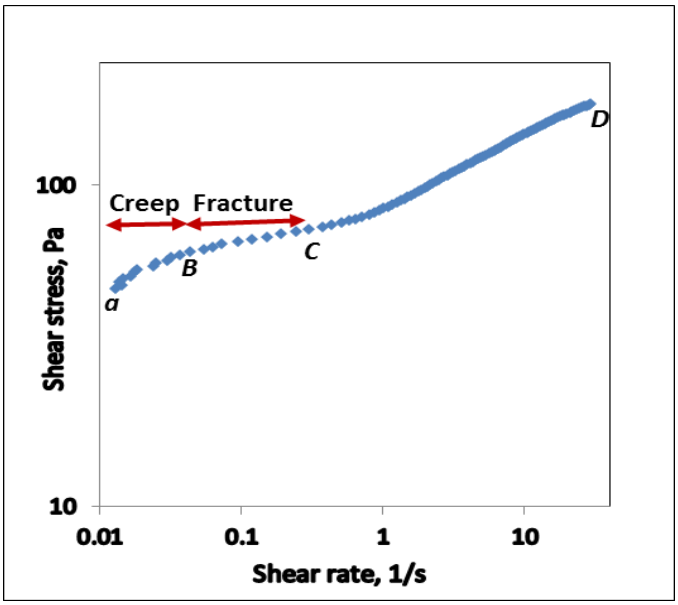

Figure 3.33 Flow curve for Bouri oil (Stress loading rate=36Pa/min, T=9°C).

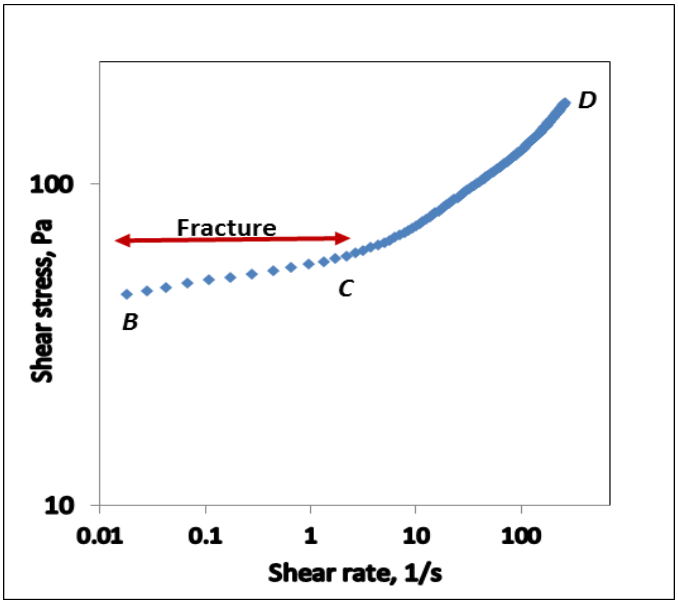

Figure 3.34 Flow curve for Sarir oil (Stress loading rate=9 Pa/min, T=21°C).

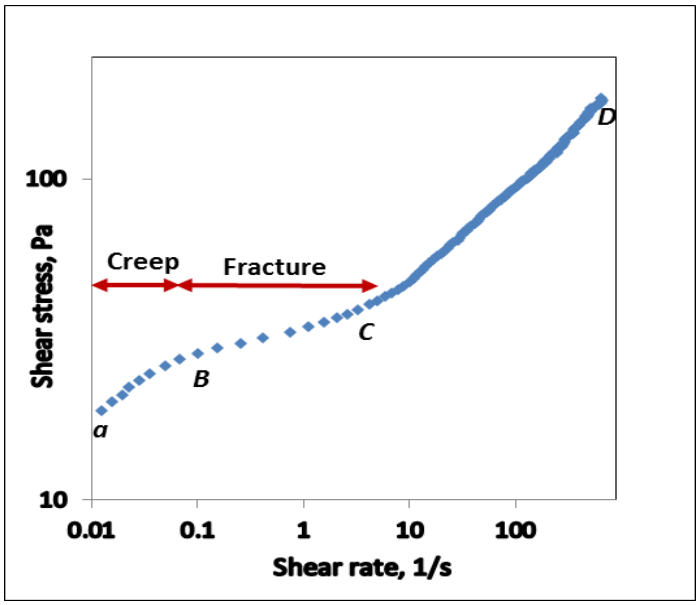

Figure 3.35 Flow curve for Sarir oil (Stress loading rate=36 Pa/min, T=21°C).

Having explained the information obtained from the Figures 3.32 to 3.35, they are now discussed specifically in relation to the stress loading rate for each oil, how it varies with time scales and a comparison made between them.

Here we have applied the Herschel-Bulkley model (Equation 3.1) to obtain some information about the shear-thinning flow behavior of the two gelled oils after fracture. The parameters of the Herschel-Bulkley model and correlation coefficients values as well

as the values of dynamic yield stresses, at three different loading rates, obtained from the flow curves for each oil are displayed in **Table 3.3**.

Table 3.3. Rheological Parameters and Correlation Coefficients values of Herschel-Bulkley model for the investigated Libyan oils at different stress loading rates.

Oil sample	Loading rate, Pa/min	K	n	τ_0 [(a)]	R^2
Bouri(T=9°C)	9	34.43	0.548	71	0.986
	18	31.42	0.514	65	0.991
	36	24.44	0.481	67	0.991
Sarir(T=21°C)	9	6.01	0.540	56	0.999
	18	5.97	0.524	47	0.997
	36	5.74	0.497	35	0.997

(a) Dynamic yield stress (Pa).

Table 3.3 reports very high regression correlation coefficient, R^2, for the two oils, meaning that Herschel-Bulkley model describes adequately the flow behavior of the crude oils within the region *C-D*. This observation suggests that the two oils exhibit similar flow behavior, pseudo-plastics ($n < 1$) under the conditions used.

The consistency index (*K*) and the flow behaviour index (*n*) decrease with increasing stress loading rate for the two oils which means lower values of viscosities with increasing stress loading rate.

Bouri oil displays higher values of the consistency index (*K*) than Sarir which indicates that a higher stress is necessary to breakdown the structure of aggregated wax crystals as previously suggested. This can also be clearly seen in **Table 3.4** in the values of static yield stress.

Table 3.4 Comparison of the yield stresses of Bouri and Sarir oils at different loading rates.

Oil sample	Loading rate, Pa/min	Static yield stress/ τ_s, Pa	Fracture yield stress/ τ_f, Pa	Dynamic yield stress/ τ_d, Pa
Bouri(T=9°C)	9	64	79	71
	18	62	75	65
	36	56	76	67
Sarir (T=21°C)	9	46	64	57
	18	38	53	47
	36	25	42	35

The results of the static yield stresses in Table 3.4 indicate that the gelled waxy structure is influenced by the stress loading rate. In general, for the same crude oil, with the increase in the stress loading rate of the oil the static yield stress decreases. For instance, the static yield stress of Bouri oil increased about 13% with decreasing the loading rate from 36 to 9 Pa/min and increased about 80% for Sarir oil with decreasing the loading rate from 36 to 9 Pa/min respectively.

As stated above, the increasing of the static yield stress with decreasing stress loading rate for the two oils suggests the development of stronger crystals that agglomerate together into a more rigid network structure. It's important to recall that Sarir oil shows a more pronounced dependence of yielding on the loading rate, probably related to a different micro-structure and interactions between crystals.

The important observation in all data above is that, crude oils are not just affected by the gel strength but also by the time scale of the measurements available for the microstructure of the gelled oil. Slow loading rates produce stronger structures requiring higher stresses for flow to commence. This may indicate that the pump pressure required to initiate a pipeline flow not only is controlled by the strength of the wax structure of the

oil in the pipeline but also is dependent on how quickly the pipeline is started. Since a lower time scale leads to both a lower static and a lower dynamic yield stress.

These results are the opposite of Chang et.al and Ronningsen's observations [35, 57], who ascertained that reducing the time scale of the measurements leads to both a higher static and a higher dynamic yield stress. Different characterization of different waxy oils can be seen in terms of the effect of stress loading rates. These observations suggest that, each waxy crude oil should be characterized individually to determine its yielding properties as a function of stress loading rate before any design or computation is carried out for re-start-up prediction.

The implication for the actual restarting pipeline of these oils is clear. For these Libyan waxy crude oils these results suggest that the pump pressure to restart a pipeline should be increased as high as possible, since lower operation will require long time scale that improves robust structure of crude oils requiring higher stress to initiate flow.

Flow characterization tests tell how a material is likely to flow under an imposed constant shear rate or shear stress and provide important information on yield stresses. Flow characterization do not however give complete information on viscoelastic properties of crude oils. To measure material viscoelastic properties, time dependent (creep) testing and oscillatory techniques are used. Consequently, some work is reported in the next two sections to clarify the behavior by further studies, and to develop and extended rheology knowledge on these particularly complex fluids.

3.10.2 Creep recovery test measurements at different constant stresses and different time scales

As discussed in the previous subsection, the elastic limit yield stress cannot be determined from steady increasing the applied stress (stress ramp in a flow test) since in the elastic region the corresponding shear rates would be very small and below the instrument resolution. Consequently, in this subsection we are concerned with two yield stresses, elastic yield stress and static yield stress limits, which are the ones most important for the initial fracture of gels in pipeline restarting flow.

As explained in the experimental method, the oil samples were first conditioned to remove all their shear and thermal memory and processed from a fluid state (39 °C for Bouri, 59 °C for Sarir and 53 °C for Faregh oil) and cooled down to a set temperature of 9 °C for Bouri oil, 21°C for Sarir oil and 18°C for Faregh oil at a pre-specified cooling rate. A subsequent holding time was then applied at the desired test temperature before each experiment.

In the creep experiments, the measurement of static and elastic yield stress limits was achieved by applying different shear stresses. If this shear stress is sufficient to get fracture at a specified time then the observed behaviour corresponds to the yielding of a solid, with the initial deformation being similar to an elastic solid followed by creep and fracture, after which the gelled oil begins to flow as a liquid. In this case, in order to measure the elastic and static yield stresses the stress must be reduced below this value. Therefore in this sub-section, different constant shear stresses were imposed over a specific period of time and then removed abruptly while recording the resulting strain recovery over time, in order to study the yielding behavior. Constant stress was also applied over different times to obtain a clear picture of the time dependent behaviour associated to the yielding process under constant applied stress.

3.10.2.1 Creep - recovery tests under different constant stresses

Creep - recovery tests were performed under different applied stresses, 8, 16, 25 and 32 Pa, maintained at a constant temperature mentioned above (3°C below pour point of each crude oil). Measurements of strain were then recorded over 1 minute under the applied stress (creep), and then during further 20 minutes after the stress was abruptly reduced to zero (recovery).

Figures 3.36 to Figure 3.38 present typical creep-recovery curves obtained for the three oils, Faregh, Sarir and Bouri, respectively. The data presented in these figures reveal that the recovery depends on the stress applied to the oil. For example the data displayed in Figure 3.36, which are those for Faregh oil, show complete strain recovery after the stress is removed for an applied stress of 8 Pa, indicating that the applied stress is below

the elastic limit and the crude oil responds as an elastic solid, with no irreversible deformation. Partial recoveries of the strain after the stress is removed for applied stresses of 16 and 25 Pa indicate that both elastic and plastic deformations are involved in the creep. However, after the stress is removed at 16 and 25 Pa, the gelled oil only recovers about 90 and 68% respectively. This indicates that the microstructure in the gelled oil upgrades gradually from viscoelastic state to the solid like state faster by lowering the stress. The applied stresses were below the static yield stress values.

The results, obtained after one minute creep at 8, 16 and 25 Pa show how strain decays with time during 20 minutes recovery. Again, from a microscopic perspective, the results illustrate how the structure of the gelled oil that have had the same time to reform, lead to different strain decays over time depending on the applied strain.

Finally with the stress of 32 Pa it is observed an abrupt increase of the strain during the transition from the viscoelastic state to the liquid regime. This rapid destructuring is describing the fracture of Faregh oil with a completely unrecoverable state as the strain increases dramatically in short time exceeding the static yield stress of the crude. The structure of the oil degrades from the initial elastic solid like state to the viscoelastic state and finally to the viscous state in less than 5 seconds.

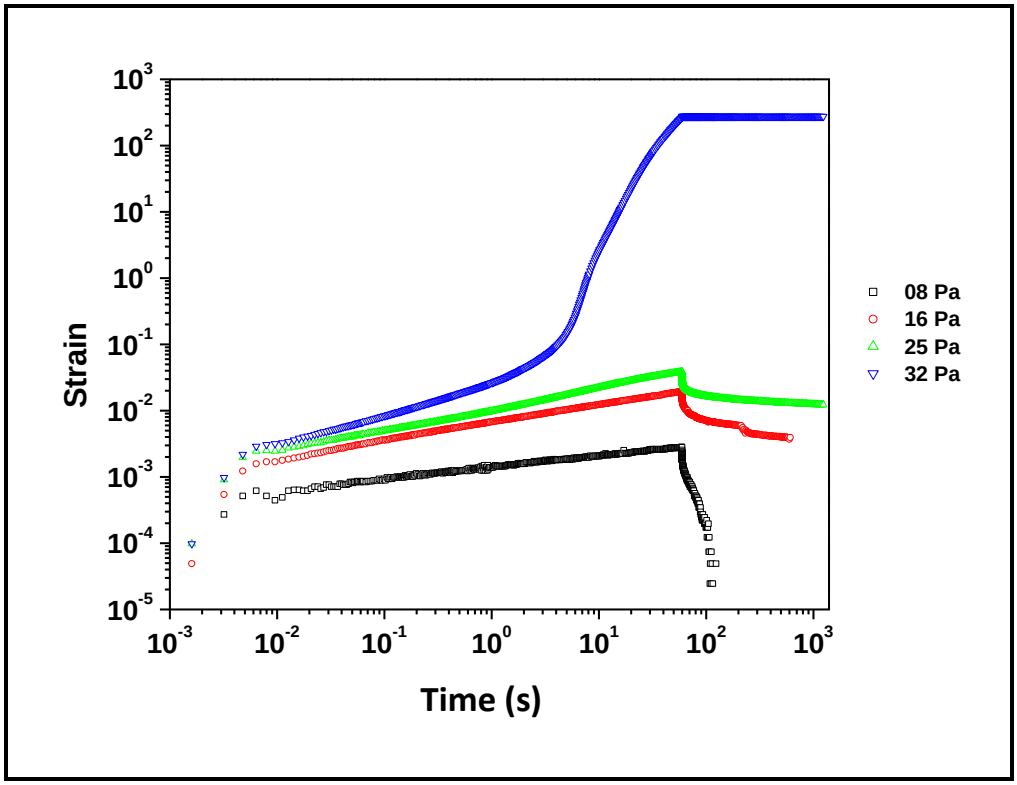

Figure. 3.36 Creep-recovery test: Faregh oil under different stresses [T=18°C].

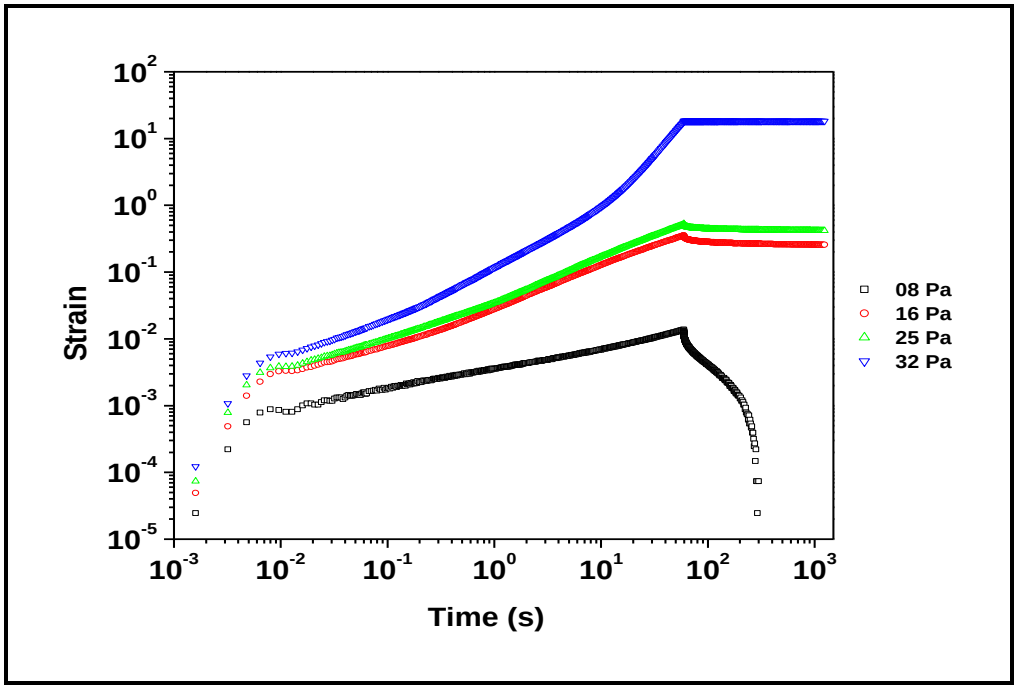

Figure 3.37 Creep-recovery test: Sarir oil under different stresses [T=21°C].

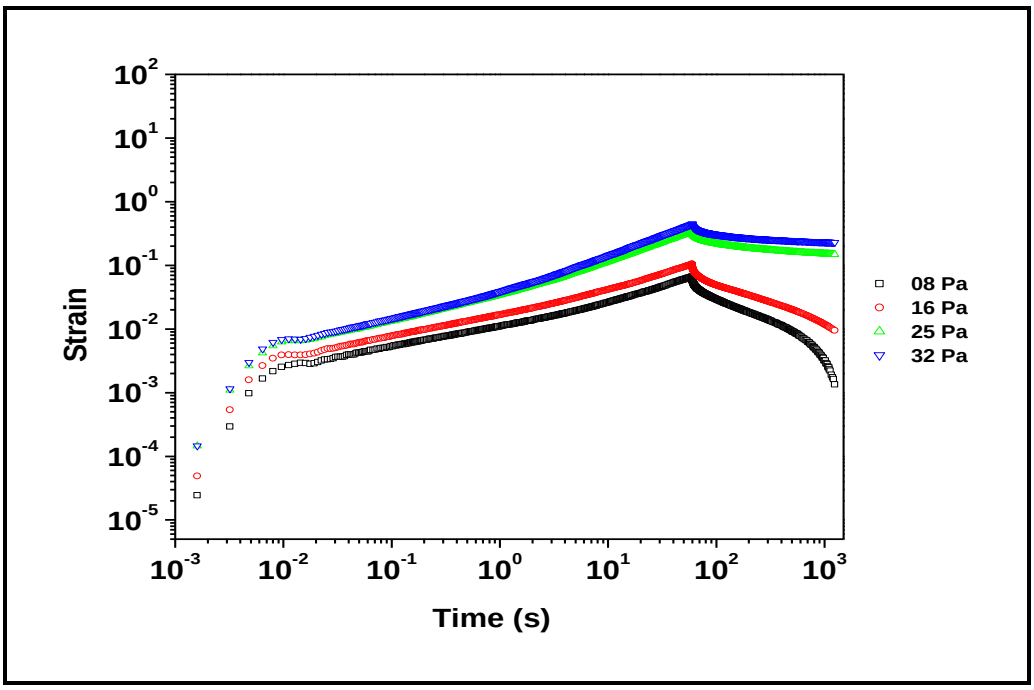

Figure 3.38 Creep-recovery test: Bouri oil under different stresses [T=9°C].

Two stress transitions can be defined from the results in the creep-recovery test. The first is between curves at stresses of 8 and 16 Pa, and the other is between curves at stresses of 25 and 32 Pa. The first transition may be described as the elastic limit yield stress, τ_e. The elastic-limit yield stress may be predicted to be in the 8-16 Pa range. An applied stress lower than this will only produce an elastic recoverable deformation, a stress higher than the elastic limit yield stress will cause creep, which will partially damage the waxy structure, if the stress is not sufficiently high to produce fracture.

The other transition is essentially the static yield stress, τ_s. A stress higher than the static yield stress limit will destroy the waxy structure completely. The oil after the destruction displays a typical viscous behaviour, with very high strain. A lower stress will not destroy the structure in a reasonable time. Therefore, the static limit yield stress value is in the range of 25-32 Pa.

For the sake of comparison, the same stresses have been determined for Sarir and Bouri oils. Similar features were observed for Sarir oil, as shown in Figure 3.37. A complete strain recovery was also observed after removal of an initial applied stress of 8 Pa, indicating that the wax structure was completely reformed, i.e. the applied stress is

below the elastic limit and the crude oil responds as an elastic solid. Partial recovery of the strain after the stress is removed at 16 Pa and 25 Pa indicates that both elastic and plastic deformations are involved in the creep. However the gel of Sarir oil at 16 and 25 Pa, only recovers about 28 and 20% of the total strain, respectively. Comparing the (% recovery) of the total strain for the two oils we can observe that Faregh has stronger partially recoils back recovery values than Sarir oil, indicating stronger gel strength. However, as for Faregh oil these two stresses are below the static yield stress values.

Once again, with subsequent increase of the stress to 32 Pa, a fracture was observed after which the gelled oil begins to flow as a liquid with unrecoverable strain. Based on measurements with an applied stress time of 1 min, the elastic-limit yield stress, τ_e, may be predicted to be in between 8-16 Pa and the static limit yield stress value, τ_s, in the range of 25-32 Pa. Consequently, the yielding process for both Sarir and Faregh oils may be recognised to follow the sequence of elastic deformation, viscoelastic creep, and final fracture. However, despite the fact that the results suggests similar range of elastic and static yield stresses limits for Faregh and Sarir, it would be desirable to measure further values of stresses in between 25 and 32 Pa. For instance Sarir oil may develop breaks in the structure, at stresses below 32 Pa, as the recovery of the strain after the stress is removed was of just 20 % at a stress of 25 Pa. A similar behavior observed for the elastic yield stress limit, suggesting values of stress less than 16 Pa may approximate the elastic yield stress limit more accurately.

In the graph of Figure 3.38 for Bouri oil, partial recovery of the oil after the stress is removed was observed at all the suggested stresses. The oil recovered about 98, 91, 55 and 48% of the total strain imposed at the stresses of 8, 16, 25 and 32 Pa respectively. Partial recovery of the oil at stress of 8 Pa indicates that the elastic yield stress is expected to be less than 8 Pa. A similar partial recovery of the oil observed at stress of 32 Pa indicates that the static yield stress is expected to be higher than 32 Pa.

A higher stress is then necessary to produce a fracture with a creep of time of 1 minute for Bouri oil. This characteristic, which is observed for Bouri oil, refers to the nature of the breakage of the wax crystals. Comparing the three oils at a similar stress

applied, Bouri oil shows relatively stronger partially recoils and back recovery values than the other oils, indicating a stronger gel strength. The results of creep tests confirm the results obtained in the previous subsection.

Having highlighted the importance of a sequence of creep tests using a varied range of shear stresses, we now must consider the effect of the creep time on gelled oil at a specified stress. We would expect the yielding to be sensitive to time as considered by some authors [21, 23], and therefore the possibility for the gel to recover partially or completely will depend on the stress magnitude and loading time.

3.10.2.2 The effect of creep time

The measurements here described seek to mimic the gradual development of strain at different time scales, i.e. the evaluation of the time dependency of crude oils under a definite applied stress. Two crude oils were chosen, Faregh and Bouri at 18 and 9 °C respectively (3 °C below pour point for each oil). The two oils were subjected to 5 and 20 minutes of creep under a stress of 16 Pa, and then to a recovery of further 20 minutes. Sarir oil measurements were rejected as we could not get reproducible and reliable results for this oil.

Figures 3.39 and Figure 3.40 display the effect of creep time on Faregh and Bouri oils respectively. Accordingly the final 20 minutes of each curve give the recovery as the microstructure of the oils is upgraded by about 62 and 64 % with 5 min creep for Faregh and Bouri oils respectively. Also partial recoils of the microstructure with 20 minutes creep, after stress removed, were observed. The gel recovered about 34 and 36 % of the total strain imposed during creep for Faregh and Bouri oils respectively. The results prove that the final strain response is influenced by the creep time: higher strain values are observed with a longer creep time.

Although, the two gelled oils cannot be said to be flowing even with 16 Pa and a time of creep of 20 min, fracture may occur at a stress of 16 Pa and 3°C below pour points for the two oils if the creep time is longer since the magnitude of the permanent deformation depends on length of time, amount of stress applied as well as temperature.

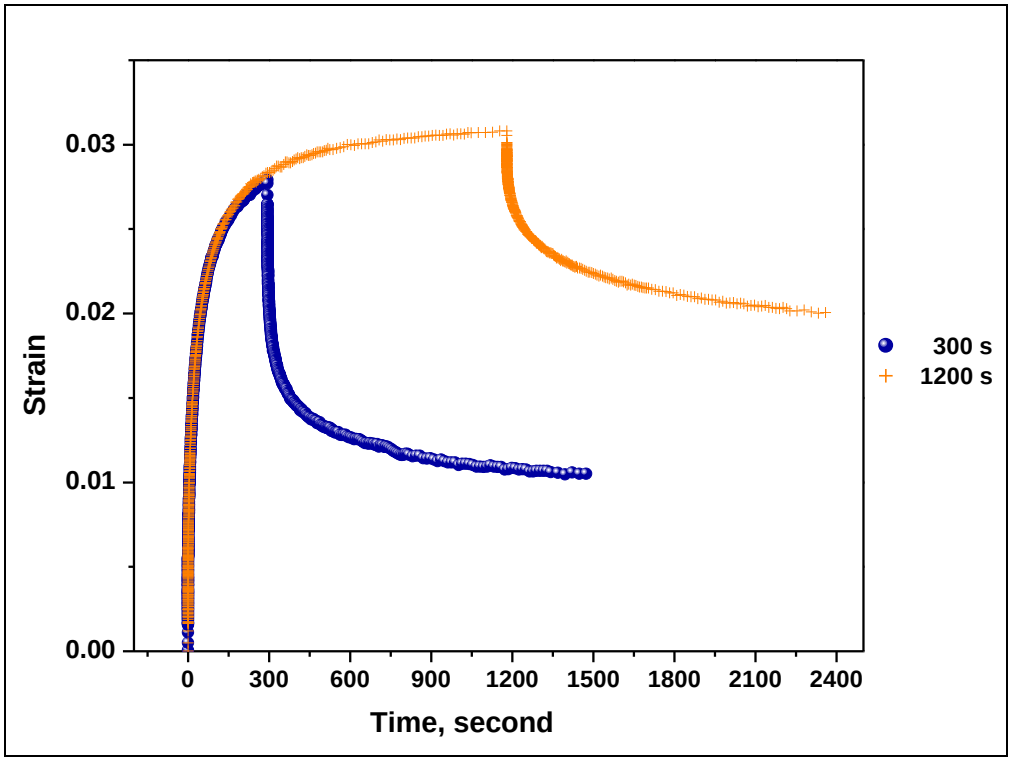

Figure 3.39 Creep-recovery test: effect of creep time [Faregh oil, T=18°C].

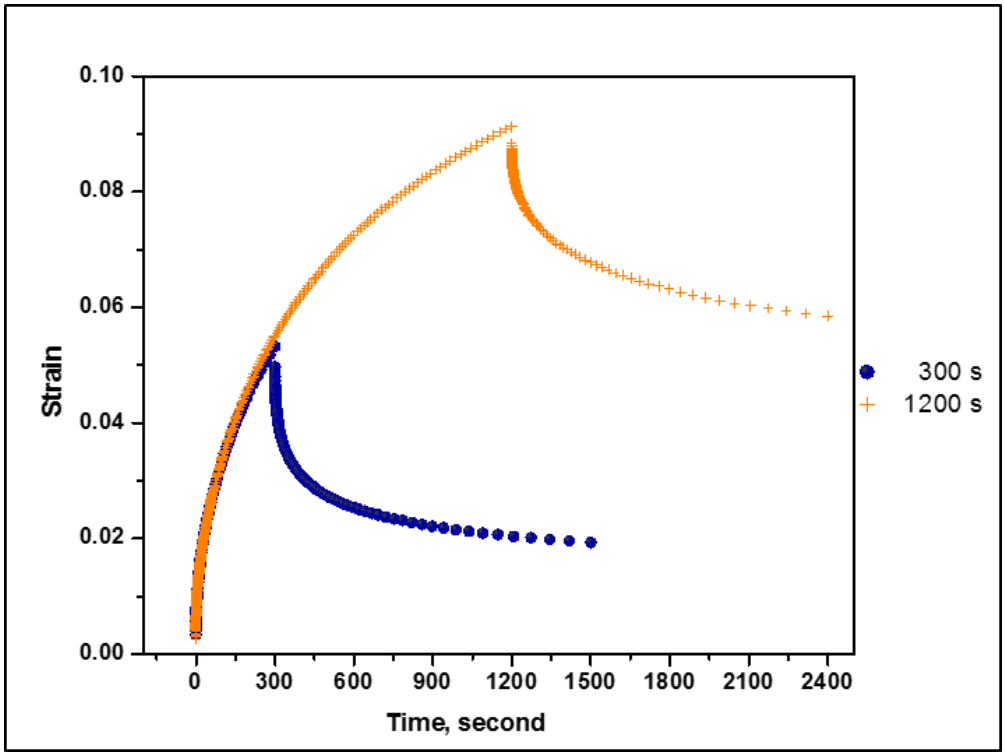

Figure 3.40 Creep-recovery test: effect of creep time [Bouri oil, T=9°C].

In summary, creep test is a direct technique for measuring the yield stress value. A shear stress is imposed to the oil and then observed if it flows or not. When a series of creep tests is performed, as already discussed, the yield stresses can be defined as the stress values below which there is no flow. But performing several tests is a time consuming task due to the time it takes to get to a good approximated values of yield stresses after several runs. Thus, despite the accuracy of creep tests and the observation of the creep flow, which characterises the gelled oil dynamics while it is in the solid state, the creep test is not a much practical technique for determining waxy oils yield stress. A more important practical technique to study the mechanical behavior of waxy oil is to be applied (Oscillatory rheology) as it provides information about both the viscous-like and the solid-like properties to understand the structural and dynamic properties of crude oil.

3.10.3 Characterization of the viscoelastic behavior of the gelled waxy crude oils near pour point temperature

As clarified earlier, oscillatory measurements are used extensively to study the materials' viscoelastic behavior. In this part, the results obtained from the oscillatory tests and their discussion are structured and conducted under two subsections, i.e.:

1. **Isothermal structure development**

Isothermal curing experiments (time sweep tests at constant frequency and temperature) were performed at different temperatures above and below pour points to evaluate how temperature influences structure development within the crude oils. Then frequency sweep tests were performed to characterize the viscoelastic behavior of the gels, after a selected holding time (60 min).

2. **Oscillatory stress sweep experiments to measure yield stress**

As mentioned in section (3.7.4), in these tests the stress was varied and the resulting strain was measured in both linear and nonlinear regions. The data obtained, namely the storage modulus (G') and the loss modulus (G''), were used to calculate yield stresses.

3.10.3.1 Isothermal structure development and viscoelastic behavior of the formed gels

Isothermal structure development at different temperatures was evaluated by measuring the viscoelastic moduli, G', and loss angle, δ, as a function of time, at constant oscillatory frequency, performing time sweep oscillatory tests at different temperatures around the pour point for each oil. After selected curing times, the viscoelastic behavior of the gels was studied by frequency sweep tests within the linear viscoelastic region.

As stated in the experimental methods, in all cases the oils were first heated to 10 °C above WAT (39 °C for Bouri, 53 °C for Faregh and 59 °C for Sarir) to avoid prior thermal memory effects. After heating to these temperatures for 20 min, each oil was loaded onto the rheometer plate, pre-heated at the same temperature, and then cooled to the desired test temperature at 0.5 °C/min.

Figures 3.41 -3.43 show the changes of storage modulus G' and loss angle δ with holding time at 6 different temperatures for Bouri, Faregh and Sarir oils respectively (the differences from these temperatures to each oil's pour point were the same, i.e., 5°C, 3°C and 1°C, below and above pour points). The variation trend of G'and δ with isothermal holding time were similar for each oil.

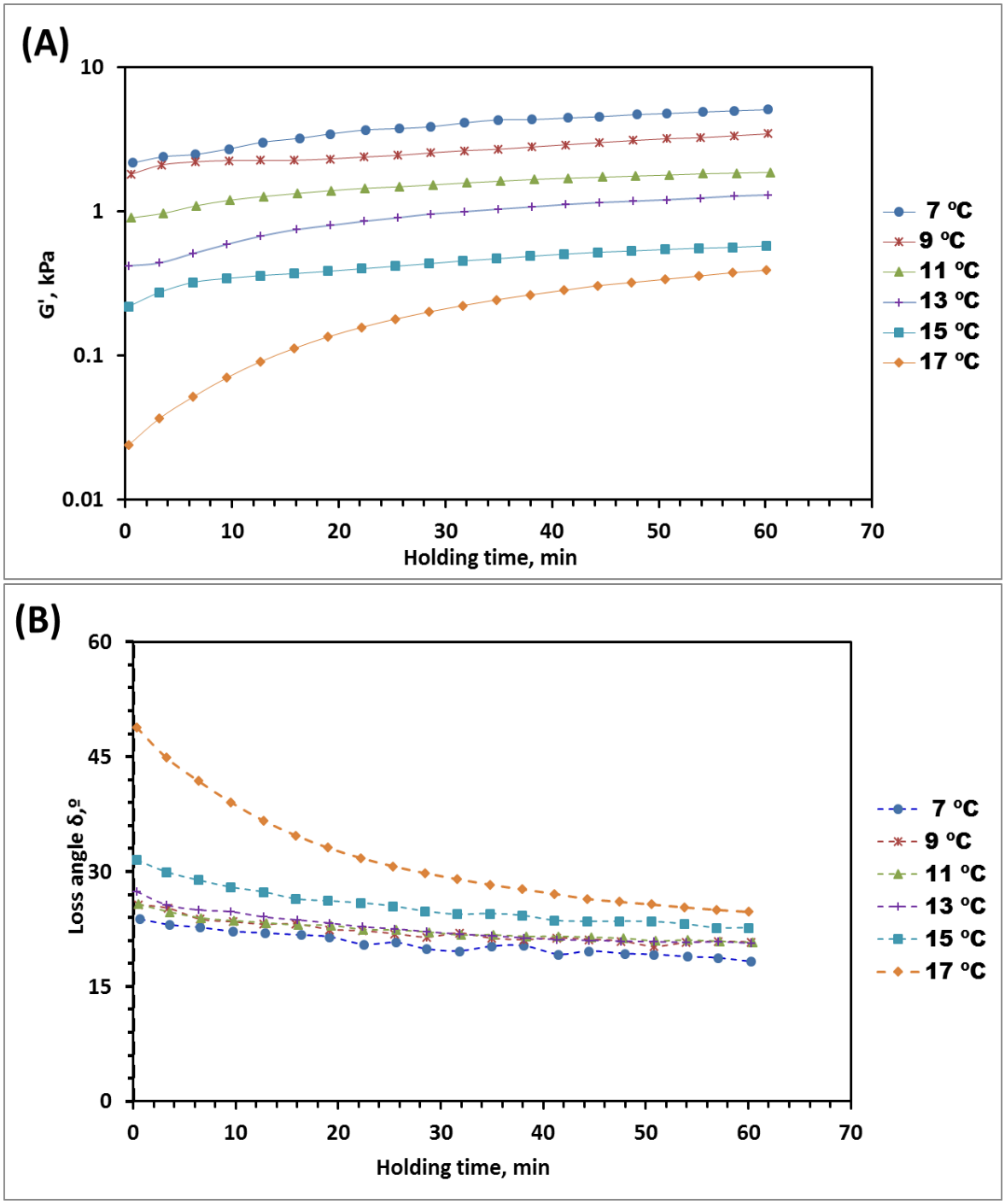

Figure 3.41. The isothermal structure development of Bouri oil; (A) variation of G' with holding time, (B) variation of δ with holding time [Oscillatory frequency 2 rad/s, Strain 0.1%].

Figure 3.41 displays the time dependence of G' and tan δ for Bouri oil. The modulus has a positive slope, being a function of the holding time during the initial ageing period at temperatures above pour point (13, 15 and 17° C), and then slowed down and tended

to an asymptotic value. For example at the temperature of 17°C, the value of G' increased from $2.3*10^{-2}$ KPa to 13.4 $*10^{-2}$ KPa for the period of 18 minutes of holding time. The characteristic of these gels are known to undergo a change to become, stronger, richer in heavier paraffins as well as a decreased fraction of entrapped oil in the deposit with time [83, 113].

At temperatures below pour point (11, 9 and 7° C), the storage modulus, G', keeps increasing very slightly with the increase of holding time, also indicating that the structure of the oil improves and formed a more elastic gel structure.

For most samples, the storage modulus (*G*') was already higher than the loss modulus (*G*'') at the beginning of the time sweep experiments, unsurprisingly since the temperatures analysed were below the pour point. The gelation temperature according to a rheological criterium is expected to be below the cloud point (WAT) but above the pour point [28]. This characteristic temperature associated to the sol–gel transition was defined as the point at which *G*' (elastic response) became greater than *G*'' (viscous response) [61].

The sol-gel transition was observed only for the isothermal curing at 17 °C as the value of δ became less than 45° after 3 minutes of holding time meaning that the gelation of the oil has occurred, since the storage modulus becomes higher than the loss modulus. While the initial values of loss angle, δ, at other temperatures were small (less than 45°) meaning that the oil has previously formed a gel structure and the structure has already a predominant elastic character before isothermal measurement.

Changes on G' and loss angle slow down as the time increased, attaining almost constant values, i.e. the structure development rate decreased as the time increased as a result of the reinforcement of the gelled network by slower rearrangement of the waxy crystals and increased interactions among them.

However, at the early period of holding time, the modulus G' and loss angle, δ, develop more quickly at temperatures above pour point than at temperatures below the pour point. It's clear that the structure development of the oil is in direct relation to the

temperature and holding time. The isothermal structure development is attributed to the active small crystals. At constant temperatures, the active small crystals take part in the rearrangement of wax crystal structures, so as to enhance the strength of the structure over the passage of time [49].

The structure of the oil becomes stronger with decreasing test temperature; the lower the temperature, the stronger the interactions among the crystals of wax due to increasing amount of crystalized paraffin, and the stronger the aptitude of the wax crystals to resist elastic and viscous deformation.

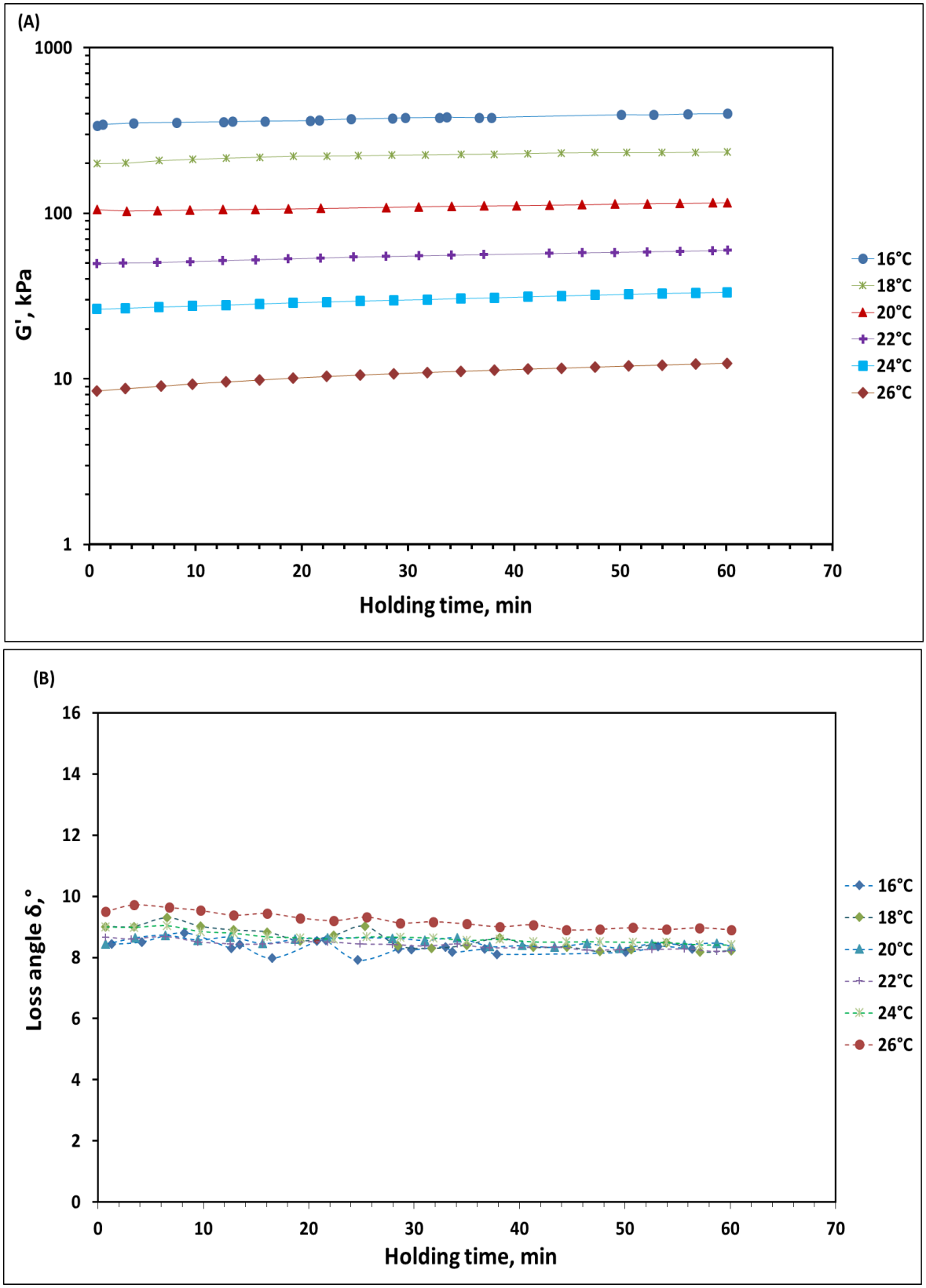

Figure 3.42. The isothermal structure development of Faregh oil; (A) variation of G' with holding time, (B) variation of δ with holding time [Oscillatory frequency 2 rad/s, Strain 0.1%].

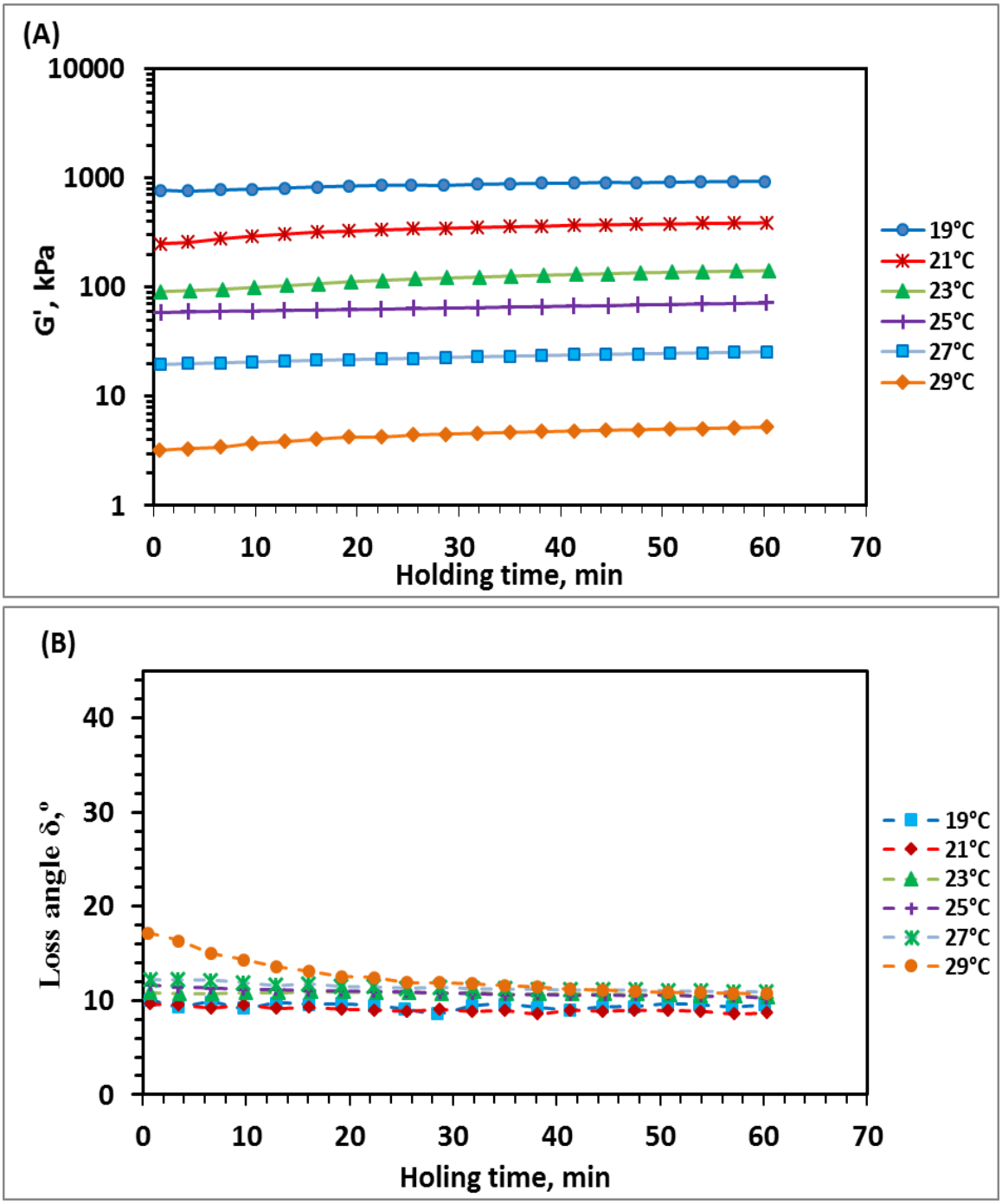

Figure 3.43. The isothermal structure development of Sarir oil; (A) variation of G' with holding time, (B) variation of δ with holding time [Oscillatory frequency 2 rad/s, Strain 0.1%].

The two other waxy oils, Faregh and Sarir, revealed a qualitatively similar behavior. For instance Faregh oil (Figure 3.43) shows that, increasing time did not have any remarkable effect on the storage modulus, G' and loss angle (8° <δ< 10°) . Both values, G' and δ, remain fairly constant during one hour holding time at temperatures above and

below pour point, indicating stagnant gel structure within the suggested holding time at the six different temperatures; the oil has already formed a gel structure and the structure is elastic-dominant before starting the measurement($\delta<45°$). The more pronounced changes observed for Bouri oil at the higher temperatures were probably due to the higher proximity to the sol-gel transition temperatures.

In general, there was no particular behaviour change in the suggested range of temperatures around the pour point. The results stated above illustrate that the influence of isothermal holding time on the structure developments of waxy crude oils depend on temperature and the nature of the oil.

After the holding time the final viscoelastic properties of the gels were evaluated by frequency sweep experiments at the same curing temperature. The Storage modulus, G', and loss modulus, G'', for the three oils, Bouri, Faregh and Sarir are plotted as a function of frequency in Figures 3.44 (A, B) to 3.46 (A, B) respectively. These data provide precise information on how at a given temperature, and after a certain curing time, the structure changes as function of frequency.

Figure 3.44 (A, B) represents the spectrum of frequencies of Bouri oil. Both moduli showed essentially the same pronounced frequency dependence over the time range analyzed, meaning that the rearrangement of the particulate network is taking place within the gelled oil and is responsible for important dissipative processes within the deformation period, although solid like G' dominates over G'' through the whole suggested spectrum. This behaviour may result from a high degree of porosity of the gelled network, which traps a large fraction of oil and non-crystallised material, contributing to the relatively high viscous character of the gel.

Similar spectrum of frequencies were observed for the other oils, Faregh and Sarir [Figures 3.45 (A, B) and 3.46 (A, B)] respectively. The increasing frequency had a lower effect on G' and G'' comparing to Bouri oil. However, both moduli, G' and G'', still keep increasing slightly but continuously, meaning that some rearrangements of the wax crystals within the network are still allowed.

On a comparison of the mechanical spectra obtained for the three oils, Bouri showed lower values of storage and loss modulus. For example, at frequency of (100 rad/sec) Bouri oil reaches the lower values of the order of (10^{-1}-10^{1} KPa) at the range of temperatures from 17 to 7 °C than Sarir (10^{0}-10^{3} KPa) at temperatures from 29 to 19 °C and Faregh oil (10^{0}-10^{2} KPa) fall in between at the range of temperature from 26 to 16 °C (the same temperature differences around PP for each oil). The lower structured network of Bouri oil seems to be related to the lower crystallinity and lower wax content and also to the presence of other materials that may reduce the crystallinity of the structure as discussed in chapter 2 (section 2.4.2.1). It can be seen in (Figure 2.7, chapter2) that the X-ray diffraction patterns obtained for the waxes show a lower degree of crystanillity for Bouri oil than for the other oils.

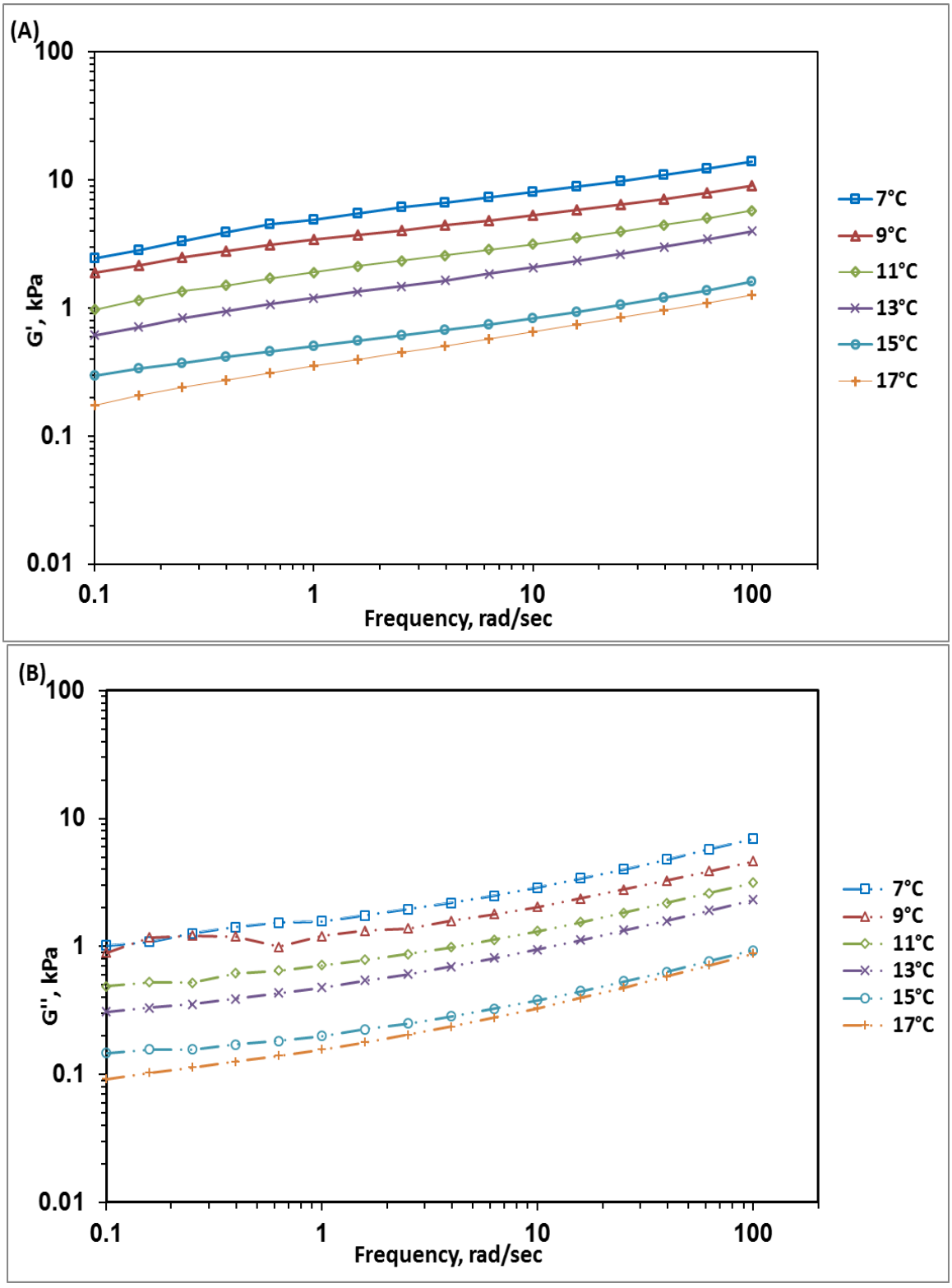

Figure 3.44. Mechanical spectra (storage and loss modulus as a function of oscillatory frequency) at different temperatures for Bouri oil: (A) storage modulus, G', (B) loss modulus, G'' [Strain = 0.1%].

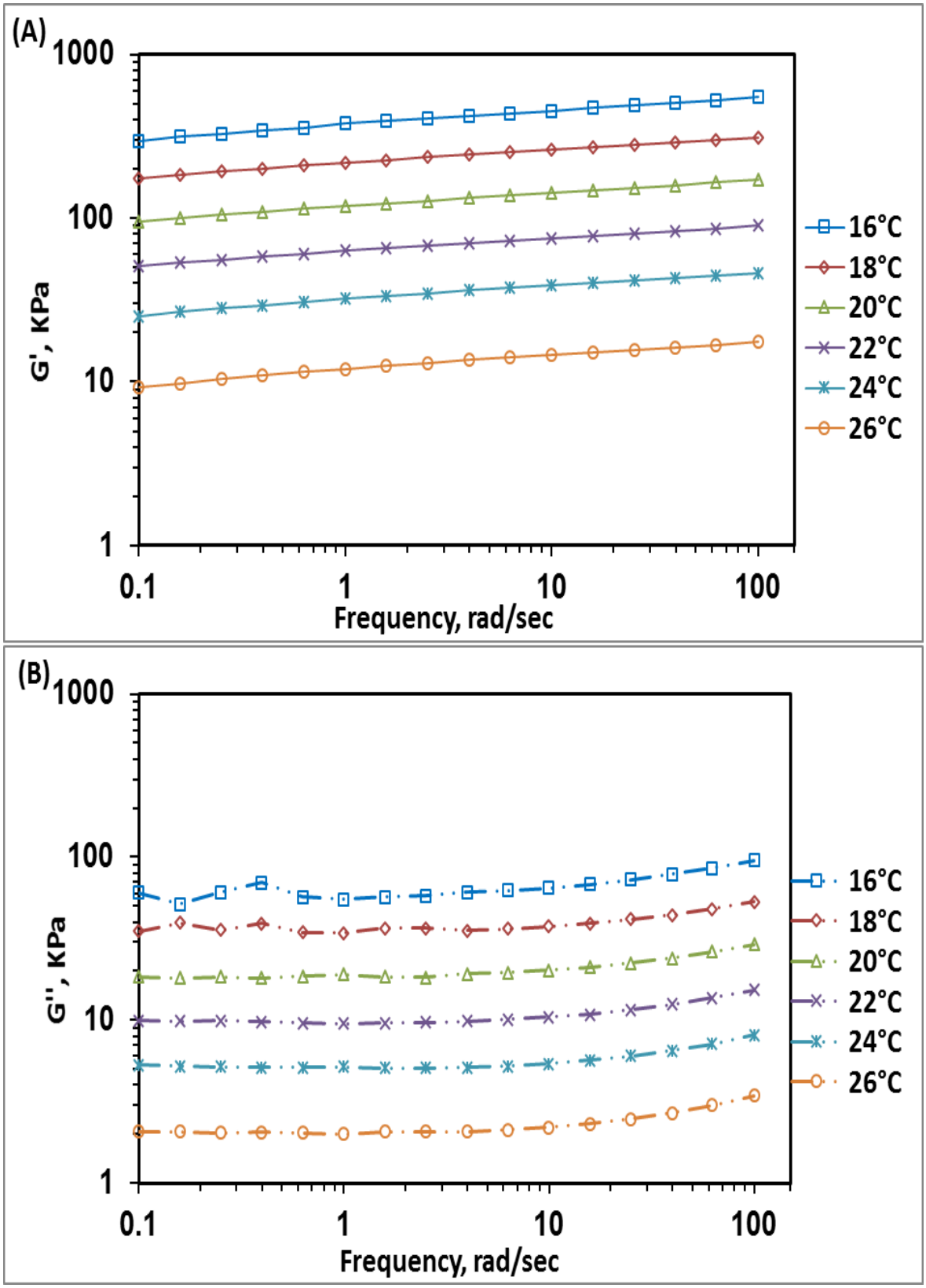

Figure 3.45. Mechanical spectra (storage and loss modulus as function of oscillatory frequency) at different temperatures for Faregh oil: (A) storage modulus, G', (B) loss modulus, G'' [Strain = 0.1%].

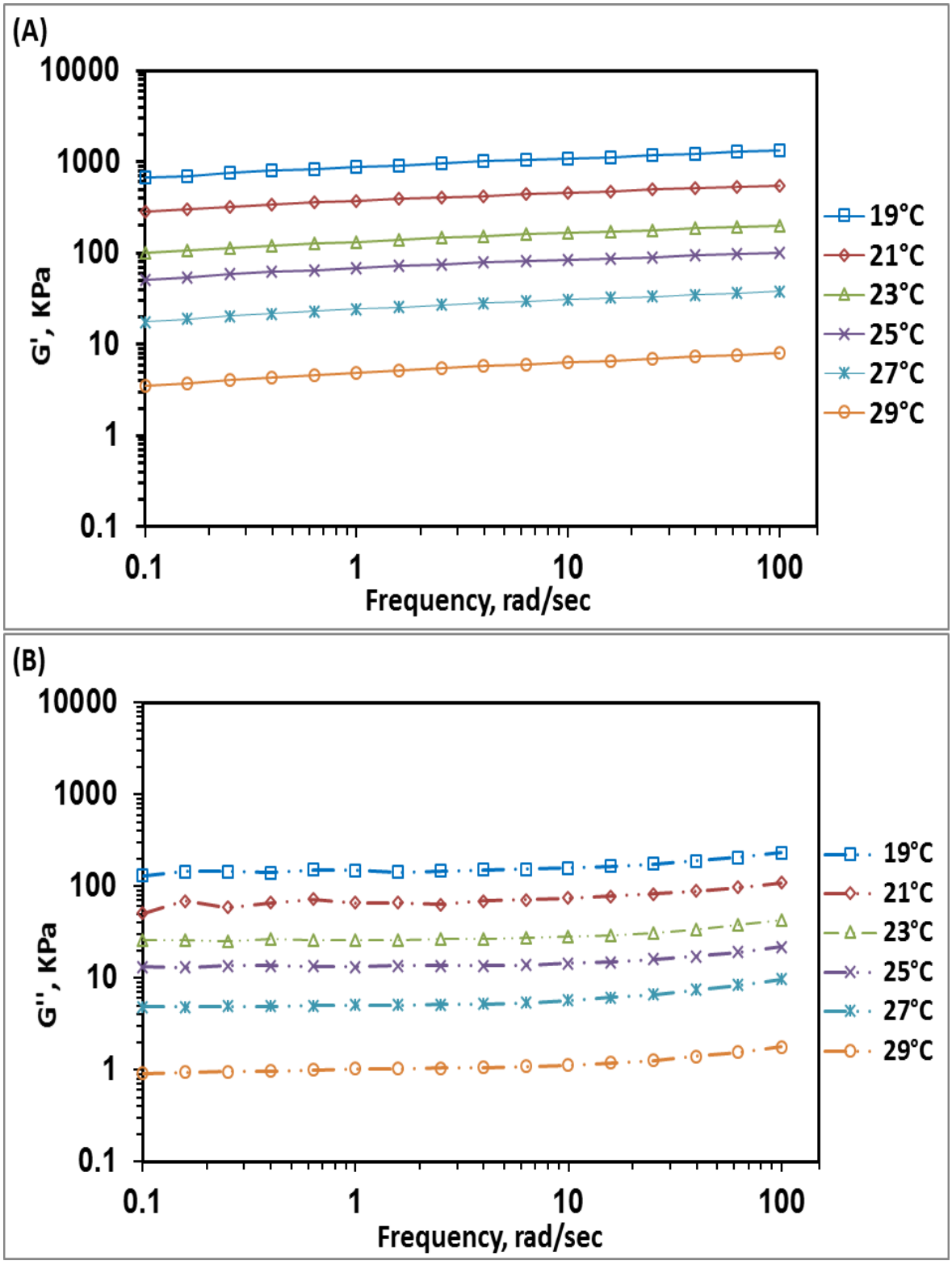

Figure 3.46. Mechanical spectra (storage and loss modulus as function of oscillatory frequency) at different temperatures for Sarir oil: (A) storage modulus, G', (B) loss modulus, G'' [Strain = 0.1%].

To verify what we suggested above, the relationship between the tangent of phase angle and temperatures as well as the storage and loss modulus are drawn for the three oils at the angular frequency of 1 rad/sec. Figures 3.47 (A, B) to 3.49 (A, B) represent the values of G', G'' and tangent of the phase angle (tan δ) at the different investigated temperatures for Faregh, Sarir and Bouri respectively.

The temperature had a strong effect on the modulus, but the relative solid (elastic) character of the gelled oils (tanδ) was only slightly affected, except for Bouri oil and for the higher temperatures, closer to the sol-gel transition point, where naturally the system is less structured and the dissipative processes are still important.

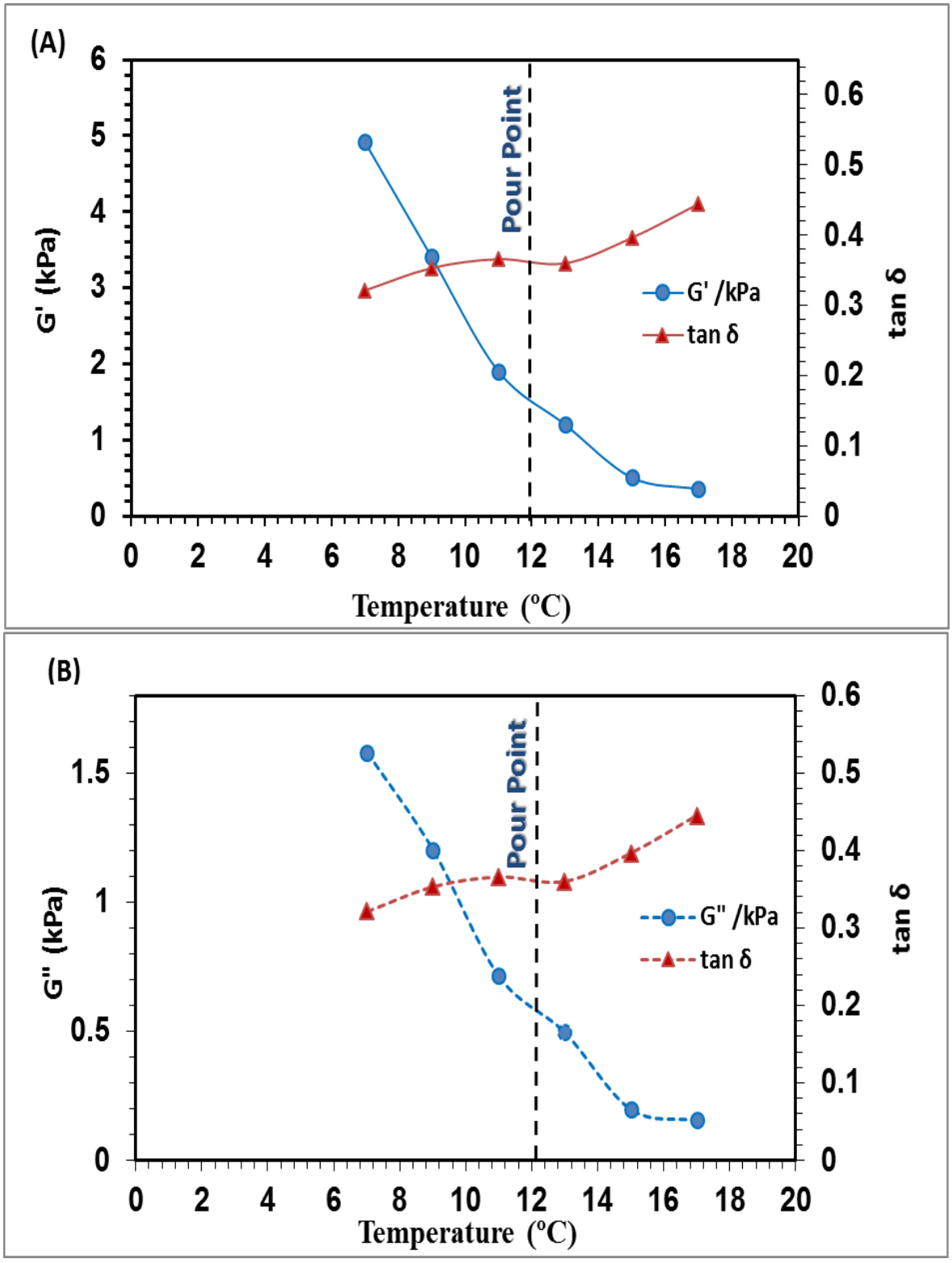

Figure 3.47. Storage modulus and tangent of phase angle (A); loss modulus and tangent of phase angle (B) for Bouri oil at different temperatures [angular frequency, ω = 1 rad/s].

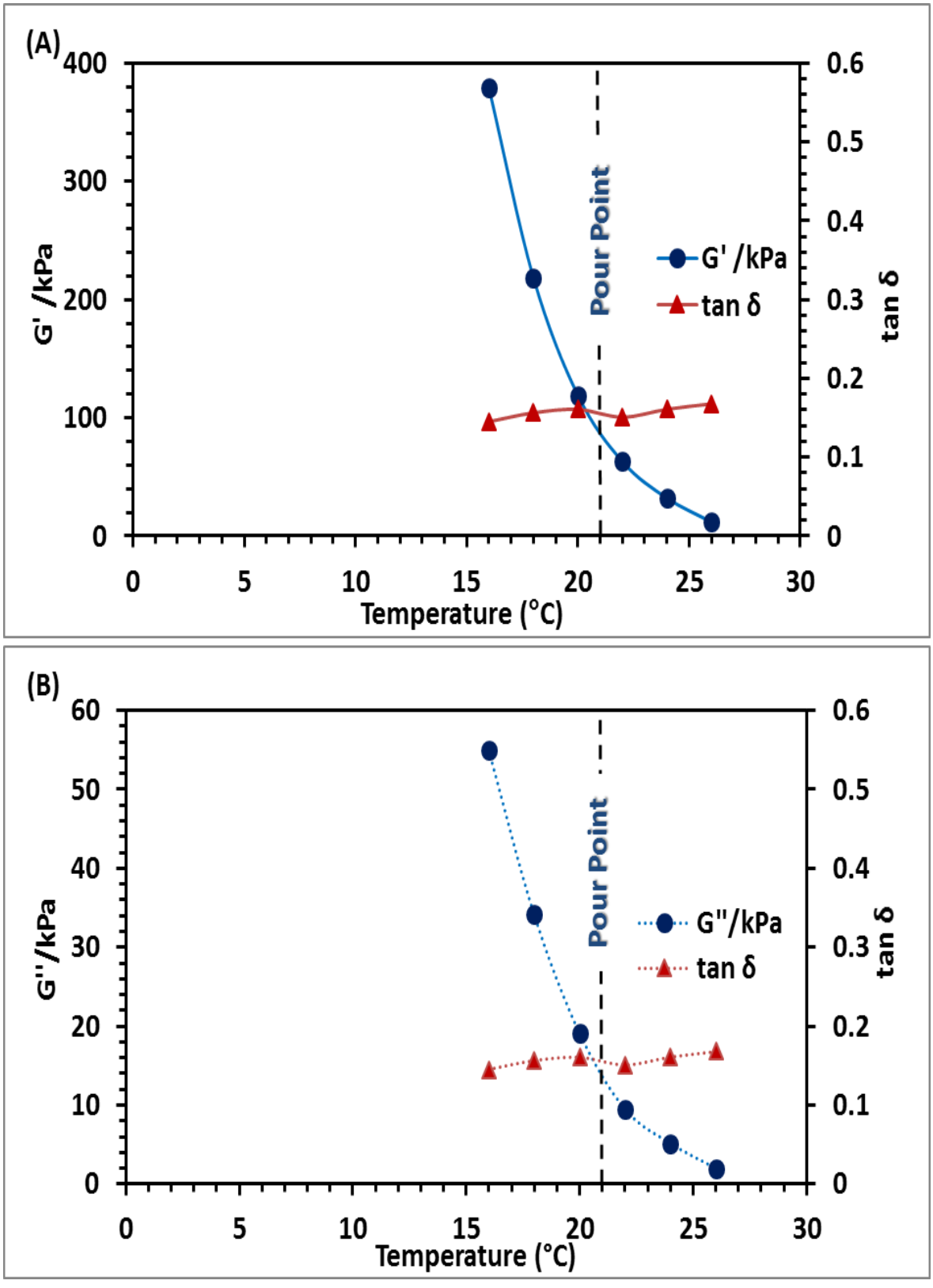

Figure 3.48. Storage modulus and tangent of phase angle (A); loss modulus and tangent of phase angle (B) for Faregh oil at different temperatures [angular frequency, ω = 1 rad/s].

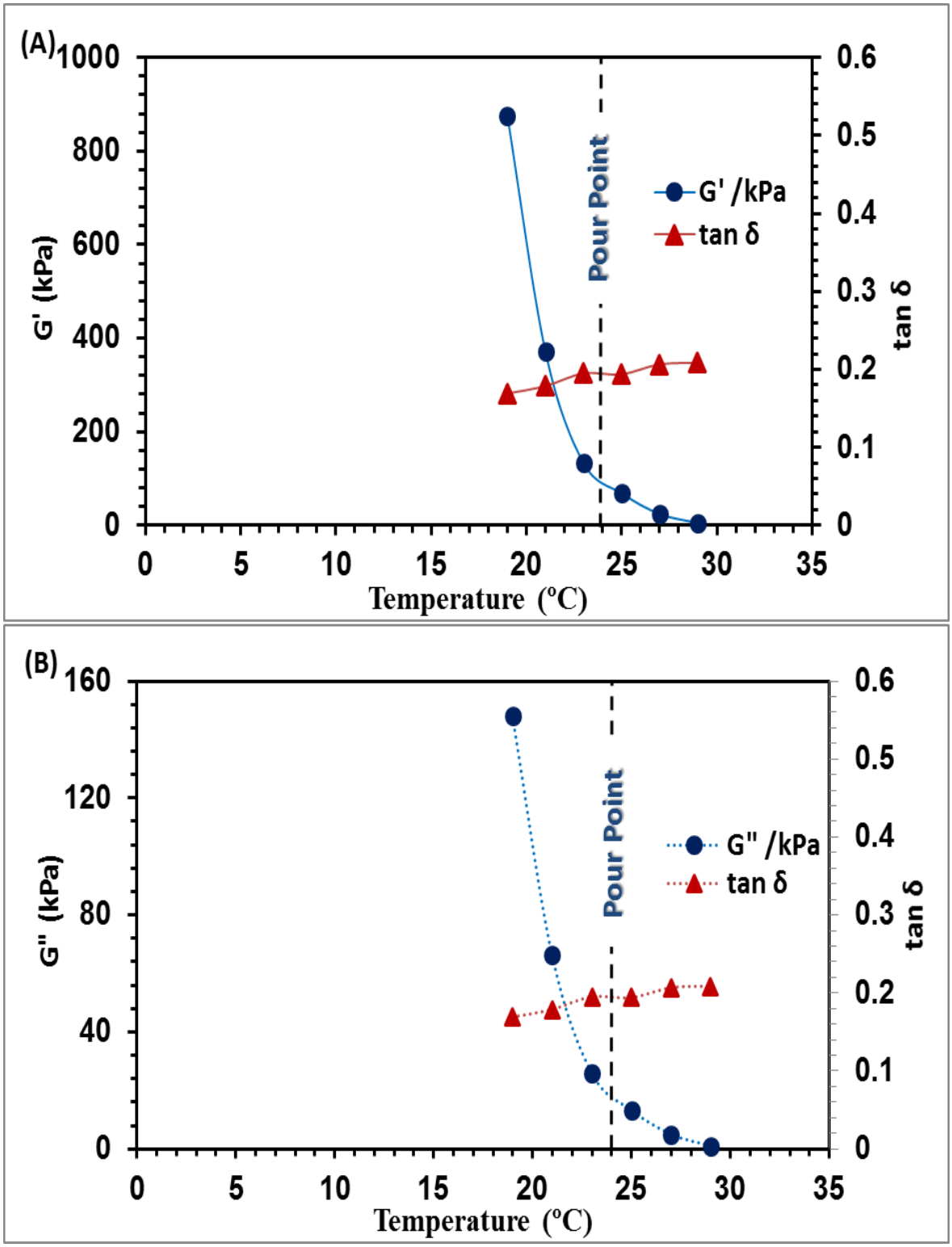

Figure 3.49. Storage modulus and tangent of the phase angle (A); loss modulus and tangent of phase angle (B) for Sarir oil at different temperatures [angular frequency, ω = 1 rad/s].

Although similar characteristics were observed, the shear modulus degradation was not as drastic as the observed at lower temperatures (below PP). In effect, this suggests that a different correlation between temperature and modulus at temperatures above and below PP takes place, signifying crystallisation kinetics at temperatures above pour points different from crystallisation kinetics at temperatures lower PP. At temperatures below PP, the crystals are well established so the difference between the values of modulus is increasing as the temperature increases (above PP).

In summary, in the three samples used during these experiments the outcomes observed and recorded are very similar and congruent; i.e. the rigidity or solid like behavior dominates over viscous behavior at temperature near PP. The structure development over the time range analyzed have been found to be underpin temperature and the nature of crude oil.

3.10.3.2 Oscillatory stress sweep experiments and yield stresses

As explained in section 3.8.4, oscillatory tests (shear mode) are very well suited to the measurement of the yield stress because if carried out accurately, they approach the yield region very progressively from the solid state. Measurement of how the shear storage modulus G' and loss modulus G'' varies with increasing stress can then detect the end of the solid deformation and the entire yielding region until fracture of the material occurs. This is what was tested with the three oil samples, Faregh, Bouri and Sarir, gelled at different temperatures as described in the previous section, in an effort to explore the stability and strength of the gelled oils, and estimate the various yielding stresses using oscillatory stress sweep measurements, from 0 to 100 Pa, at a constant oscillatory frequency of 1 rad/s.

The measurements were performed at temperatures of 9 and 7 °C for Bouri oil, 18 and 16 °C for Faregh oil and 21 and 19 °C for Sarir oil (3 and 5 °C below pour point temperature for each oil), after the curing steps described in the previous section.

Results are shown in Figures 3.50 (*a*, *b*) to 3.55 (*a, b*) for Faregh, Bouri, and Sarir oils, obtained for the temperatures under consideration, using two graphical representations

for a more clear definition of the yield stress values of interest: Figures *a* present the data of strain as a function of applied stress and Figures *b* present G' and G'' variations with increasing the stress.

The dynamic rheological tests performed, at a frequency of 1 rad/sec, involved both a linear viscoelastic region, in the low strain amplitude range where the true structural properties before yielding can be observed, and a nonlinear region at higher strain amplitudes, where the sample fracture can be analysed.

The range of stress amplitude that keeps G' and G'' constant determines the linear viscoelastic region (LVR). This region characterizes the unperturbed structure of the gelled oil and thus corresponds to the elastic response of the material. This is very important to determine how the waxy oil yields from an elastic state into a viscous state and therefore to define the elastic-limit yield stress (τ_e). Here our main purpose was to determine the elastic and static yield stresses, those that were not accurately measured by the flow tests described in the previous section.

The data in Figure 3.50 (*a*, *b*) obtained for Faregh oil at 18 °C are taken here as a basis of discussion.

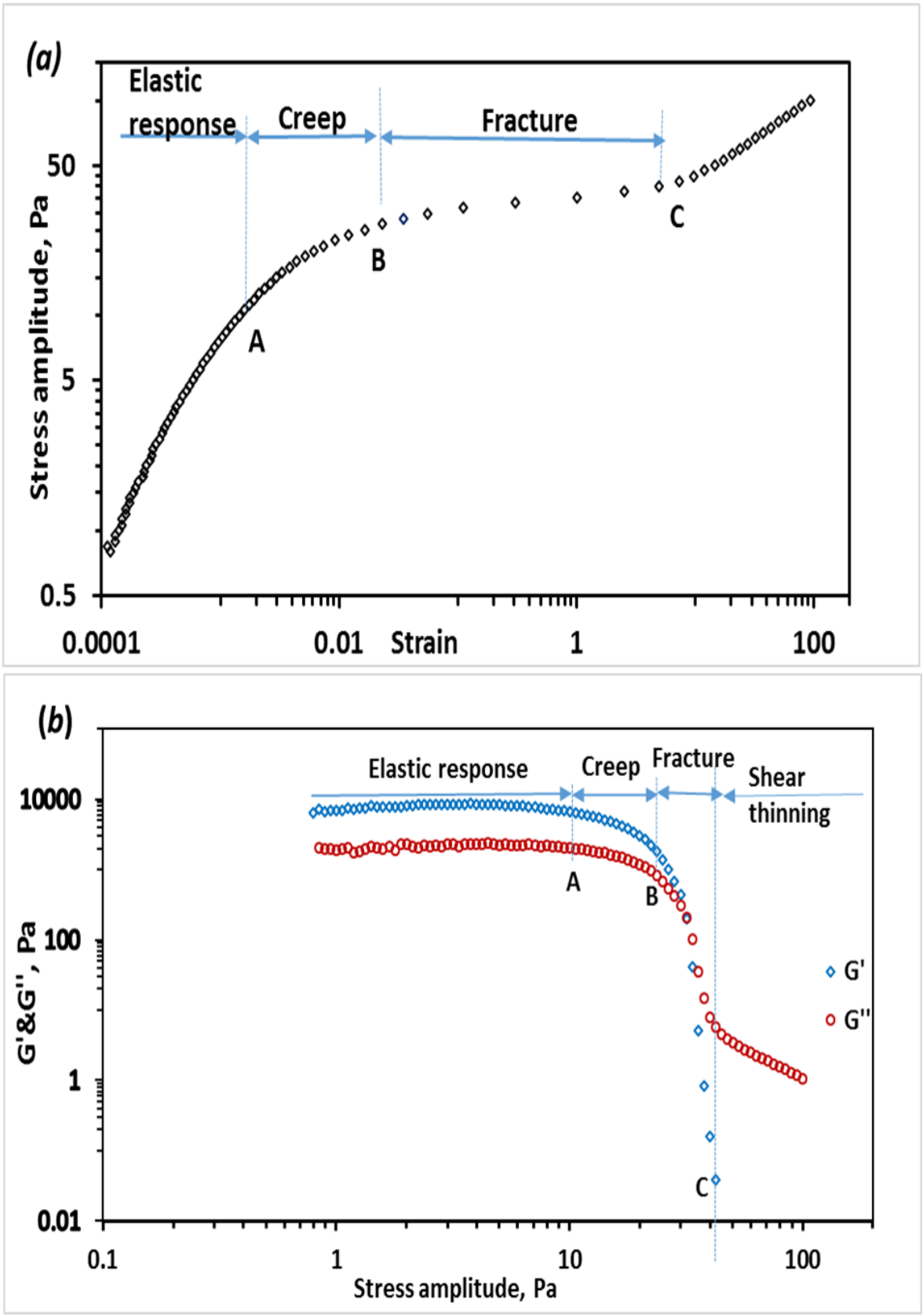

Figure 3.50. Oscillatory test: (a) stress vs strain relationship during the yielding process; (b) G' and G'' during yielding; ω = 1 rad/s [Faregh oil, T=18 °C, 3 °C below PP].

The initial linear stress-strain relationship, before point A, for a stress amplitude lower than 10 Pa, indicates an elastic response. The stress-strain relationship follows the Hooke's law. The storage modulus, G', is higher than the loss modulus, G'', indicating a predominance of gel-like structures (predominant elastic character). The region before point A in Figure 3.50 (b) where G' and G'' are almost constant and independent of the applied stress correspond to the linear viscoelastic region where the microstructure of the waxy network in the gelled oil is not destroyed. When the stress amplitude increases above 10 Pa, G' and G'' decrease gradually with increasing the stress amplitude, representing a creep response in which both elastic and plastic strains are implicated, characterized also by the deviation of stress-strain curves from the linear relationship. Point A is characterized as the elastic yield stress, τ_e.

An oscillatory stress with an amplitude higher than the elastic limit yield stress will cause creep, which will incompletely damage the waxy structure, if the stress is not sufficiently high to break the gel structure. After point B, another increasing pattern of the strain follows together with sharp drops of G' and G'', indicating the fracture process of the waxy network structure. Another important change around B is that G' becomes lower than G'' after B, which also indicates a change of the oil from solid-like to liquid-like state. Point B is identified as the static yield stress of the oil, τ_s.

When G' becomes lower than G'', that is when the fluid part of the oil overtakes the solid part at a stress of 33.5 Pa, is considered as another point of yielding and is defined as flow yield stress, τ_F. The final range of the curve after point C shows viscous behavior, and G' much lower than G''.

Qualitatively similar yielding behaviors were observed for Faregh oil at 16 °C as well as the other two oils.

Having defined three different yield stresses obtained from oscillatory measurements using stress amplitude mode, they are discussed in relation to the strength for each oil, how it varies with temperature and a comparison made between them.

The values of yield stresses, τ_e, τ_s, and τ_F at the different temperatures obtained from Figures 3.50 to 3.55 are displayed for each oil in **Table 3.5**.

Table 3.5 Yield stress values for the studied oils measured at a frequency of 1 rad/sec.

Oil sample	Temperature, °C	Elastic yield stress, τ_e(Pa)	Static yield stress, τ_s(Pa)	Flow yield stress, τ_F(Pa)
Bouri	9	13	33.5	59.6
	7	28	56.3	94.5
Sarir	21	7.9	22.4	50.2
	19	18	35.5	59.6
Faregh	18	10	26.6	31.6
	16	22	53.1	66.9

The linear viscoelastic range, LVR, for Sarir oil is shorter than for the other two oils at the two temperatures under consideration, for instance, at 3 °C below pour point for each oil, the reduction of G' for Sarir oil, started at stress of 7.9 Pa comparing with a reduction of G' at stresses of 13 and 10 Pa for Bouri and Faregh respectively. Similar differences in the LVR limits can be seen at the temperatures 19° C for Sarir, 16° C for Faregh and 7° C for Bouri (5° C below pour point). This indicates that the interactions between the wax crystals building up the gelled networks are less sensitive to the applied stress for Bouri and Faregh than for Sarir oil. In general, Bouri oil showed higher values of elastic, static and flow yield stresses than the two other oils, in accordance to what was previously observed with the flow tests (section 3.10.1.2), indicating a stronger gel.

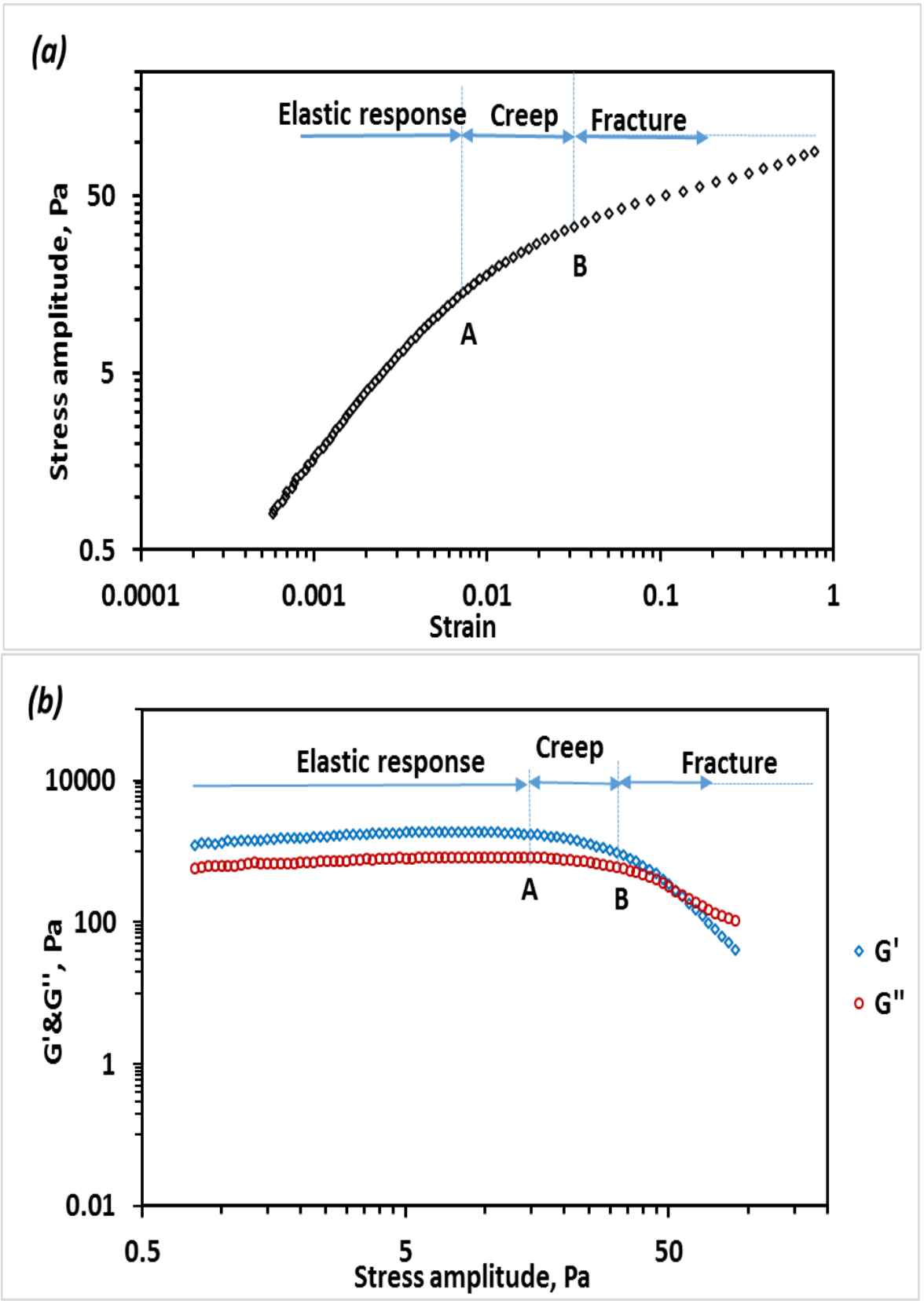

Figure 3.51. Oscillatory test: (a) stress vs strain relationship during the yielding process; (b) G' and G'' during yielding; ω = 1 rad/s [Bouri oil, T=9 °C, 3 °C below PP].

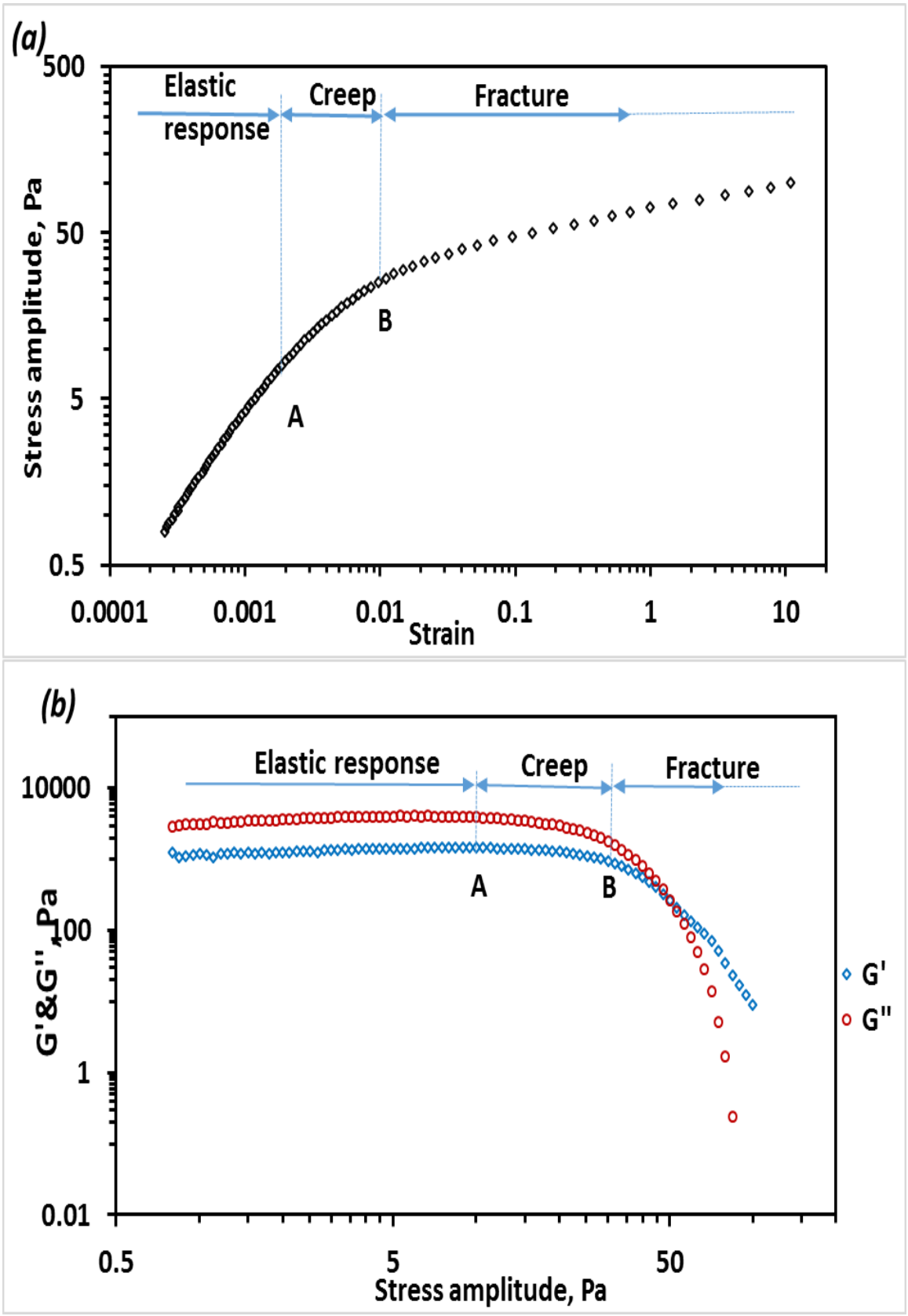

Figure 3.52. Oscillatory test: (a) stress vs strain relationship during the yielding process; (b) G' and G'' during yielding; ω = 1 rad/s [Sarir oil, T=21 °C, 3 °C below PP].

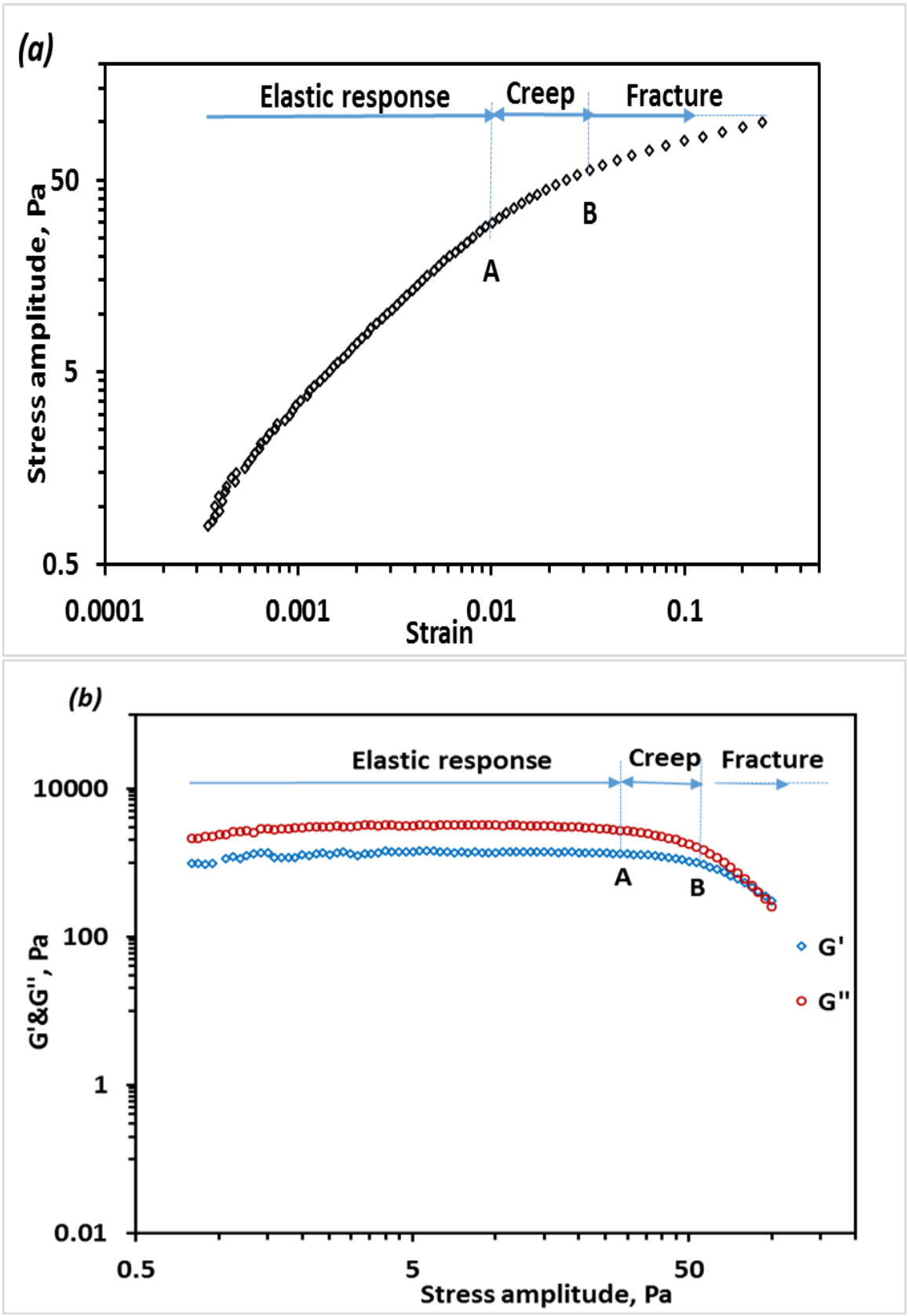

Figure 3.53. Oscillatory test: (a) stress vs strain relationship during the yielding process; (b) G' and G'' during yielding; ω = 1 rad/s [Bouri oil, T=7° C, 5 °C below PP].

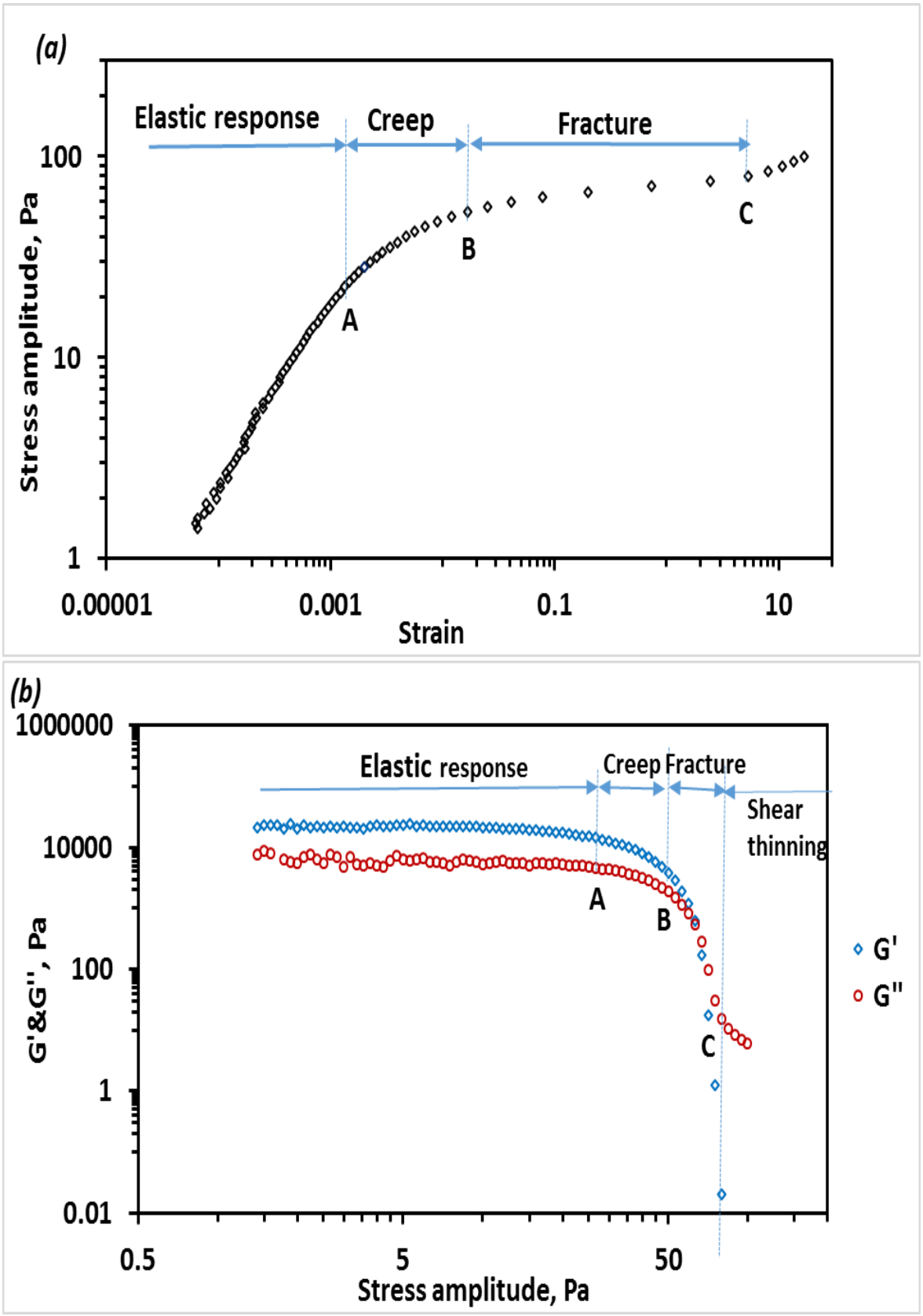

Figure 3.54. Oscillatory test: (a) stress vs strain relationship during the yielding process; (b) G' and G'' during yielding; ω = 1 rad/s [Faregh oil, T=16 °C, 5 °C below PP].

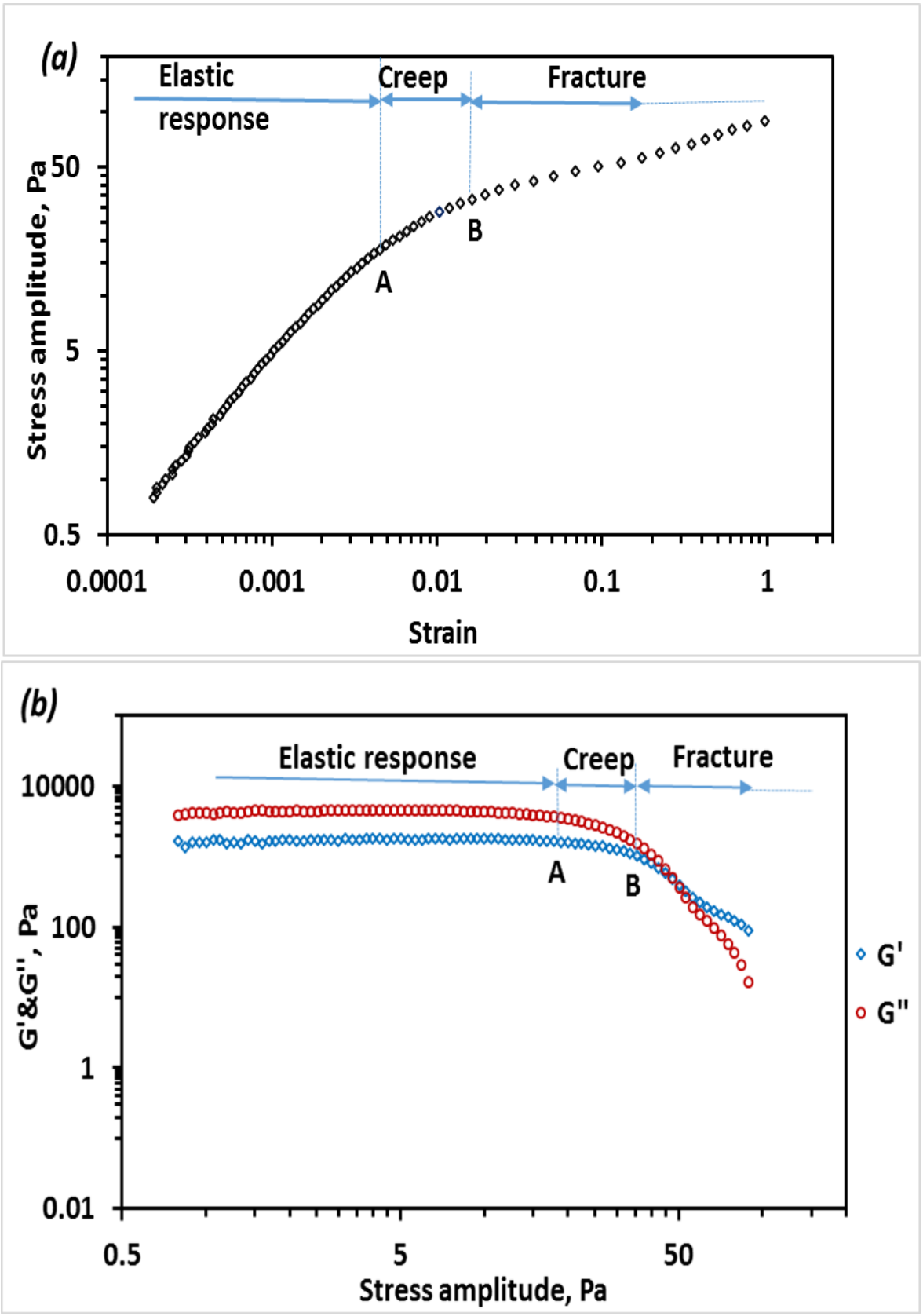

Figure 3.55. Oscillatory test: (a) stress vs strain relationship during the yielding process; (b) G' and G" during yielding; ω = 1 rad/s [Sarir oil, T=19°C, 5 °C below PP].

Clearly because of the direct dependence of yield stress on the temperature, the decrease in the yield stresses are proportional to the increasing in temperature. Lower temperatures produce stronger structures requiring higher stresses to fracture and flow .The range of LVR depends on the nature of the crude oil and temperature applied. More elasticity can be observed at lower temperatures.

3.10.4 Comparison of data obtained by the three rheological tests

The results given in the previous sections from three different rheological tests for three Libyan waxy crude oils were obtained with identical thermal and shear histories. The values of τ_s were determined from each testing. The values of τ_e, were determined from two tests, creep-recovery and oscillatory testing, as in the shear flow tests, only the fracture process and partial creep process were observed, and so are the values of τ_f that can be determined from shear flow tests and oscillatory testing. Consequently, it will be desirable to compare the results of these yield stresses for the three techniques.

However, because of the time scale dependency of static and fracture yield stresses, it is meaningless to compare directly the measured static and fracture yield stresses determined from shear flow tests with other techniques since the time scale is totally distinct in the different tests. The measured elastic yield stress from different tests, however, can be comparable since it is not influenced by the characteristic time of the tests. So from the argument above, what is comparable are the results of elastic and static yield stresses measured by creep-recovery tests at 21 and 18 °C of Sarir and Faregh oils respectively, with the results given by oscillatory measurements.

The elastic limit yield stress by creep measurements was determined for Faregh and Sarir oils between 8 and 16 Pa and the elastic yield stress for Faregh and Sarir oils by oscillatory tests is 7.9 and 10 Pa respectively. The static limit yield stress by creep measurements was determined between 20 to 32 Pa and the static yield stress for Faregh and Sarir oils by oscillatory tests is 26.6 and 31.6 Pa respectively. The results from the two different techniques are in reasonably agreement.

3.11 Conclusions

In this chapter, characterization of the rheological behavior for three Libyan waxy crude oils, Bouri, Faregh and Sarir, has been presented by means of three experimental techniques.

The central focus of this thesis has been on the development of a better understanding and description of the flow behavior of some Libyan waxy oils using controlled stress tests in order to improve the prediction of flow properties. Then creep and oscillatory techniques has been used to measure the viscoelastic properties. Therefore the following are the conclusion of this chapter, set against the information obtained by the three experimental techniques used:

- **Flow behavior of the crude oils using controlled stress testing**

The flow behavior of three waxy crude oils produced from Libyan crude oils has been investigated. The measurement test was conducted under controlled stress mode and the values of shear rate were obtained. The effect of temperature and stress loading rate on the flow behavior and yield process were analyzed.

1. The viscosity dependence on temperature of waxy crude oils below pour point has been analyzed using viscosity-temperature data. It was found that Libyan crude oils display shear thinning behavior, revealing their non-Newtonian character. Moreover it was observed that the higher the content of heavy n-paraffin in the crude oil, as is the case of Bouri oil, the more viscous the crude oil is.

2. The gel strength of the three oils has been characterized by studying their yield behavior. The observed flow behaviour is very complex and, most importantly, the yield stress of the gelled waxy oils is a complex function of gel composition and shear and thermal histories under which the gel has been formed. The results demonstrated that these crude oils can exhibit more complex behaviour when deformation undergo complete fracture. This powers us to re-define or suggest another important yield stress for the oil industry which assess such complex oils, by taking the importance of the stress at the end of the fracture process into account; we have defined it as *the fracture yield*

stress. Consequently a four-yield-stresses model is suggested to describe the different stages of the yielding process for these oils at low temperatures. The primary, static, fracture and dynamic yield stresses are describing the complete process. The yielding development of these oils occurs in three stages. Initial elastic limit, at which elastic limit yield stress value (τ_e) can be defined, although this yield value is ignored since this limit cannot be recorded by rheometer using controlled stress mode. The second stage is viscoelastic creep at which primary yield stress (τ_p) are descried for the sake of simplifying the comparison between oils; for instance this range did not appear in the yielding process of Faregh oil sample. Primary yield stress is the first point observed by rheometry in the creep region, it is an approximation to the beginning of the creep region. And finally the fracture process region, which is described by two limits of yield stresses: One which is the stress at the starting point of fracture process, defined as static yield stress value (τ_s) then the crude oil will break and flows at the end of this region; The other is the yield stress at the end of the fracture region which is described as the fracture yield stress, (τ_f). The two values (the static yield stress and fracture yield stress) are the stress values relating to the yielding process and may be considered to be the two true and most important yield values to be considered and measured to help restart plugged pipelines as well as continue flow after restart. Static yield stress, the stress value when the fracture occurs, as this stress value determines the pump capacity required to initiate flow and ensure pipeline restart while fracture yield stress, and the stress value determines the pump capacity required to guarantee flow after fracture. However the stress value, (τ_f) to guarantee flow is higher than the stress values (τ_s) to break structure and initiate flow for such complex waxy oils. Dynamic yield stress in this work were used to obtain information about the shear thinning flow behaviour after fracture using the HB model, by keeping dynamic yield stress as constant value and the two parameters of the equation, the consistency index, *K* and the flow-behavior index, *n*, were estimated to give an idea on the viscosity of the oil after fracture and the shear thinning degree.

3. The effect of different stress loading rates has been considered in this study at different temperatures below pour point. The results of these tests showed that slow stress loading rates produce stronger structures requiring higher stresses to fracture and

induce flow. However, the strength of the structure of the three oils studied have been found to underpin temperature and loading rates.

- **Creep recovery measurements at different constant stresses and time scales**

Creep- recovery tests were performed. A sequence of creep tests using a varied range of shear stresses were prepared at constant time to investigate the yielding characteristics of the oils and to analyze the structure. Two yield stresses were measured, static and elastic. Also constant stress was applied at different time period to study the effect of time scale on the viscoelastic behavior of gelled waxy oils. The measurements were carried at 3 °C below the Pour point temperatures for each oil. The obtained results lead to the following conclusions:

1. The yielding process of the crude oils is occurring in three distinct stages: elastic deformation which is a rapid elastic increase in strain, followed by viscoelastic creep with a slower linear rise in strain, and finally fracture creep range with the deformation of gel structure.
2. No flowing of the crude oil samples at stresses of 8, 16, 25 Pa as well as at 32 Pa for Bouri oil sample, since these stresses were below the static yield stress. Faregh and Sarir oils flowed at stress of 32 Pa. The possibility for the oil to recover partially or completely or even fracture is time and stress dependent. In particular, depending upon the imposed stress value and time applied each oil will respond differently.

- **The viscoelasticity of the gelled waxy crude oils near pour point temperature**

In this research the oscillatory measurements were used in order to explore the stability and strength of the three crude oil gels. We have experimentally described the static conditions at very low deformation (linear viscoelastic range) at two temperatures below the pour points through the stress sweeping tests. The results of these tests have shown that the existence of LVR depends on the nature of the crude oils and temperature applied. Three yield stresses have been described during the stress sweep tests, named as elastic yield stress, τ_e, static yield stress, τ_s, and flow yield stress, τ_F.

The effect of holding time on the isothermal structure development of the three oils has been investigated at different temperatures above and below the pour point by means of Oscillatory frequency measurements. It is observed that, the impact of isothermal holding time on the structure developments of waxy crude oils depends on temperature and the nature of the oil; the structure under isothermal condition has become stronger with increasing holding time for Bouri oil, while the effect of holding time on the structure development of Sarir and Faregh oils is less pronounced. However a stronger structure was observed at lower temperatures. The obtained data from frequency sweep measurements showed that the suggested frequency spectrum has a little effect on the structure deformation of the three oils at all proposed temperatures.

The data presented in this thesis provide a rheological characterization of waxy oils that we hope can contribute to improve their understanding of their complex flows and have implications for flow assurance strategies as well as a better understanding of the physical phenomena of Libyan waxy oils underlying the rheology.

In general, it cannot be assumed that the conclusions of this thesis are valid for all waxy crude oils since there are many differences between oils produced from different areas in the world. But the same qualitative tendencies of the rheological behavior could be predicted, as they origin is in the basic behaviour between wax molecules. Moreover, the information developed here is itself a useful guideline for evaluating the rheological behavior of other waxy oils. Still the challenges faced by flow assurance specialists in the oil industry are certainly varied and complex.

3.12 References

1. Singh, P., Venkatesan, R., Fogler, H.S. and Nagarajan, N., 2000. Formation and aging of incipient thin film wax-oil gels. *AIChE Journal*, *46*(5), pp.1059-1074.

2. Chin, W.C., 2001. *Computational Rheology for Pipeline and Annular Flow: Non-Newtonian Flow Modeling for Drilling and Production, and Flow Assurance Methods in Subsea Pipeline Design*. Gulf Professional Publishing.

3. Sharma, S., Mahto, V., Sharma, V.P. and Saxena, A., 2016. An emperical correlation for estimating the viscosity of non-Newtonian waxy crude oils. *Petroleum Science and Technology*, *34*(6), pp.523-530.

4. Roenningsen, H.P., Bjoerndal, B., Baltzer Hansen, A. and Batsberg Pedersen, W., 1991. Wax precipitation from North Sea crude oils: 1. Crystallization and dissolution temperatures, and Newtonian and non-Newtonian flow properties. *Energy & Fuels*, *5*(6), pp.895-908.

5. Alghanduri, L.M., Elgarni, M.M., Daridon, J.L. and Coutinho, J.A., 2010. Characterization of Libyan waxy crude oils. *Energy & Fuels*, *24*(5), pp.3101-3107.

6. Zheng, S., Saidoun, M., Mateen, K., Palermo, T., Ren, Y. and Fogler, H.S., 2016, May. Wax Deposition Modeling with Considerations of Non-Newtonian Fluid Characteristics. In *Offshore Technology Conference*. Offshore Technology Conference.

7. Barnes, H.A., 1999. The yield stress—a review or 'παντα ρει'—everything flows?. *Journal of Non-Newtonian Fluid Mechanics*, *81*(1), pp.133-178.

8. Ahmadpour, A., Sadeghy, K. and Maddah-Sadatieh, S.R., 2014. The effect of a variable plastic viscosity on the restart problem of pipelines filled with gelled waxy crude oils. *Journal of Non-Newtonian Fluid Mechanics*, *205*, pp.16-27.

9. Betancourt, S., Davies,T., Kennedy, R., Dong, C., Elshahawi, H., Mullins, O. C., Nighswander, J., and O'Keefe, M. 2007. Advancing fluid-property measurements Schlumberger Oil field Review. 19:56-70.

10. Blue, M.E., Jackson, R.E., Ottomanelli, M.J. and George, D.S., Harris Corporation, 2015. *Hydrocarbon fluid pipeline including RF heating station and related method*. U.S. Patent 9,198,234.

11. Li, S., Huang, Q., Fan, K., Zhao, D. and Lv, Z., 2016. Transportation technology with pour point depressant and wax deposition in a crude oil pipeline. Petroleum Science and Technology, 34(14), pp.1240-1247.

12. Nguyen, D.A., Fogler, H.S. and Chavadej, S., 2001. Fused chemical reactions. 2. Encapsulation: Application to remediation of paraffin plugged pipelines. *Industrial & engineering chemistry research*, *40*(23), pp.5058-5065.

13. Nguyen, D.A., Iwaniw, M.A. and Fogler, H.S., 2003. Kinetics and mechanism of the reaction between ammonium and nitrite ions: experimental and theoretical studies. *Chemical engineering science*, *58*(19), pp.4351-4362.

14. Nguyen, D.A. and Fogler, H.S., 2005. Facilitated diffusion in the dissolution of carboxylic polymers. *AIChE journal*, *51*(2), pp.415-425.

15. Nguyen, D.A., Moraes, F.F.D. and Fogler, H.S., 2004. Fused chemical reactions. 3. Controlled release of a catalyst to control the temperature profile in tubular reactors. *Industrial & engineering chemistry research*, *43*(18), pp.5862-5873.

16. El-Gamal, I.M. and Gad, E.A.M., 1998. Low temperature rheological behavior of Umbarka waxy crude and influence of flow improver. *Colloids and Surfaces A: Physicochemical and Engineering Aspects*, *131*(1), pp.181-191.

17. Li, C., Yang, Q. and Lin, M., 2009. Effects of stress and oscillatory frequency on the structural properties of Daqing gelled crude oil at different temperatures. *Journal of Petroleum Science and Engineering*, *65*(3), pp.167-170.

18. Adeyanju, O. and Oyekunle, L., 2012. An experimental study of rheological properties of nigerian waxy crude oil. *Petroleum Science and Technology*, *30*(11), pp.1102-1111.

19. Kane, M., Djabourov, M., Volle, J.L., Lechaire, J.P. and Frebourg, G., 2003. Morphology of paraffin crystals in waxy crude oils cooled in quiescent conditions and under flow. *Fuel*, *82*(2), pp.127-135.

20. Chanda, D., Sarmah, A., Borthakur, A., Rao, K.V., Subrahmanyam, B. and Das, H.C., 1998. Combined effect of asphaltenes and flow improvers on the rheological behaviour of Indian waxy crude oil. *Fuel*, *77*(11), pp.1163-1167.

21. Visintin, R.F., Lockhart, T.P., Lapasin, R. and D'Antona, P., 2008. Structure of waxy crude oil emulsion gels. *Journal of Non-Newtonian Fluid Mechanics*, *149*(1), pp.34-39.

22. Japper-Jaafar, A., Bhaskoro, P.T., Sean, L.L., Sariman, M.Z. and Nugroho, H., 2015. Yield stress measurement of gelled waxy crude oil: Gap size requirement. *Journal of Non-Newtonian Fluid Mechanics*, *218*, pp.71-82.

23. Taraneh, J.B., Rahmatollah, G., Hassan, A. and Alireza, D., 2008. Effect of wax inhibitors on pour point and rheological properties of Iranian waxy crude oil. *Fuel processing technology*, *89*(10), pp.973-977.

24. Guo, L., Zhang, J., Sun, G. and Bao, Y., 2015. Thixotropy and its estimation of water-in-waxy crude emulsion gels. *Journal of Petroleum Science and Engineering*, *131*, pp.86-95.

25. Kumar, L., Skjæraasen, O., Hald, K., Paso, K. and Sjöblom, J., 2016. Nonlinear rheology and pressure wave propagation in a thixotropic elasto-viscoplastic fluids, in the context of flow restart. *Journal of Non-Newtonian Fluid Mechanics*, *231*, pp.11-25.

26. Bao, Y., Zhang, J., Wang, X. and Liu, W., 2016. Effect of pre-shear on structural behavior and pipeline restart of gelled waxy crude oil. *RSC Advances*, *6*(84), pp.80529-80540.

27. Malkin, A.Y. and Khadzhiev, S.N., 2016. On the rheology of oil (Review). *Petroleum Chemistry*, *56*(7), pp.541-551.

28. Lopes-da-Silva, J.A. and Coutinho, J.A., 2007. Analysis of the isothermal structure development in waxy crude oils under quiescent conditions. *Energy & Fuels*, *21*(6), pp.3612-3617.

29. Mortazavi-Manesh, S. and Shaw, J.M., 2014. Thixotropic rheological behavior of Maya crude oil. *Energy & Fuels*, *28*(2), pp.972-979.

30. Mortazavi-Manesh, S. and Shaw, J.M., 2016. Effect of diluents on the rheological properties of Maya crude oil. *Energy & Fuels*, *30*(2), pp.766-772.

31. Wardhaugh, L.T. and Boger, D.V., 1991. The measurement and description of the yielding behavior of waxy crude oil. *Journal of Rheology*, *35*, pp.1121-1156.

32. Zhang, J.J. and Liu, X., 2008. Some advances in crude oil rheology and its application. *Journal of Central South University of Technology*, *15*, pp.288-292.

33. Visintin, R.F., Lapasin, R., Vignati, E., D'Antona, P. and Lockhart, T.P., 2005. Rheological behavior and structural interpretation of waxy crude oil gels. *Langmuir*, *21*(14), pp.6240-6249.

34. Li, H., Zhang, J. and Yan, D., 2005. Correlations between the pour point/gel point and the amount of precipitated wax for waxy crudes. *Petroleum science and technology*, *23*(11-12), pp.1313-1322.

35. Rønningsen, H.P., 1992. Rheological behaviour of gelled, waxy North Sea crude oils. *Journal of Petroleum Science and Engineering*, *7*(3), pp.177-213.

36. Barbato, C., Nogueira, B., Khalil, M., Fonseca, R., Gonçalves, M., Pinto, J.C. and Nele, M., 2014. Contribution to a more reproductible method for measuring yield stress of waxy crude oil emulsions. *Energy & Fuels*, *28*(3), pp.1717-1725.

37. He, C., Ding, Y., Chen, J., Wang, F., Gao, C., Zhang, S. and Yang, M., 2016. Influence of the nano-hybrid pour point depressant on flow properties of waxy crude oil. *Fuel*, *167*, pp.40-48.

38. Davidson, M.R., Nguyen, Q.D., Chang, C. and Rønningsen, H.P., 2004. A model for restart of a pipeline with compressible gelled waxy crude oil. *Journal of non-newtonian fluid mechanics*, *123*(2), pp.269-280.

39. Sun, G., Zhang, J. and Li, H., 2014. Structural behaviors of waxy crude oil emulsion gels. *Energy & Fuels*, *28*(6), pp.3718-3729.

40. Cheng, C., Boger, D.V. and Nguyen, Q.D., 2000. Influence of thermal history on the waxy structure of statically cooled waxy crude oil. *SPE Journal*, *5*(02), pp.148-157.

41. Chang, C., Nguyen, Q.D. and Rønningsen, H.P., 1999. Isothermal start-up of pipeline transporting waxy crude oil. *Journal of non-newtonian fluid mechanics*, *87*(2), pp.127-154.

42. Marchesini, F.H., Alicke, A.A., de Souza Mendes, P.R. and Ziglio, C.M., 2012. Rheological characterization of waxy crude oils: Sample preparation. *Energy & Fuels*, *26*(5), pp.2566-2577.

43. Zhu, Y., Zhang, J., Li, H. and Chen, J., 2007. Characteristic temperatures of waxy crude oils. *Petroleum Science*, *4*(3), pp.57-62.

44. Tinsley, J.F., Jahnke, J.P., Dettman, H.D. and Prud'home, R.K., 2009. Waxy gels with asphaltenes 1: Characterization of precipitation, gelation, yield stress, and morphology. *Energy & Fuels*, *23*(4), pp.2056-2064.

45. Aiyejina, A., Chakrabarti, D.P., Pilgrim, A. and Sastry, M.K.S., 2011. Wax formation in oil pipelines: A critical review. *International journal of multiphase flow*, *37*(7), pp.671-694.

46. Alcazar-Vara, L.A., Garcia-Martinez, J.A. and Buenrostro-Gonzalez, E., 2012. Effect of asphaltenes on equilibrium and rheological properties of waxy model systems. *Fuel*, *93*, pp.200-212.

47. Oh, K., Jemmett, M. and Deo, M., 2009. Yield behavior of gelled waxy oil: effect of stress application in creep ranges. *Industrial & Engineering Chemistry Research*, *48*(19), pp.8950-8953.

48. Venkatesan, R., Nagarajan, N.R., Paso, K., Yi, Y.B., Sastry, A.M. and Fogler, H.S., 2005. The strength of paraffin gels formed under static and flow conditions. *Chemical Engineering Science*, *60*(13), pp.3587-3598.

49. Jia, B. and Zhang, J., 2012. Yield behavior of waxy crude gel: Effect of isothermal structure development before prior applied stress. *Industrial & Engineering Chemistry Research*, *51*(33), pp.10977-10982.

50. Zhao, Y., Kumar, L., Paso, K., Safieva, J., Sariman, M.Z.B. and Sjöblom, J., 2012. Gelation behavior of model wax–oil and crude oil systems and yield stress model development. *Energy & Fuels*, *26*(10), pp.6323-6331.

51. Singh, P., Fogler, H.S. and Nagarajan, N., 1999. Prediction of the wax content of the incipient wax-oil gel in a pipeline: An application of the controlled-stress rheometer. *Journal of Rheology (1978-present)*, *43*(6), pp.1437-1459.

52. Oh, K. and Deo, M., 2009. Characteristics of wax gel formation in the presence of asphaltenes. *Energy and Fuels*, *23*(3), pp.1289-1293.

53. Paso, K.G. and Fogler, H.S., 2004. Bulk stabilization in wax deposition systems. *Energy & fuels*, *18*(4), pp.1005-1013.

54. Venkatesan, R., Östlund, J.A., Chawla, H., Wattana, P., Nydén, M. and Fogler, H.S., 2003. The effect of asphaltenes on the gelation of waxy oils. *Energy & fuels*, *17*(6), pp.1630-1640.

55. Kriz, P. and Andersen, S.I., 2005. Effect of asphaltenes on crude oil wax crystallization. *Energy & fuels*, *19*(3), pp.948-953.

56. de Oliveira, M.C.K., Carvalho, R.M., Carvalho, A.B., Couto, B.C., Faria, F.R. and Cardoso, R.L., 2009. Waxy Crude Oil Emulsion Gel: Impact on Flow Assurance†. *Energy & Fuels*, *24*(4), pp.2287-2293.

57. Chang, C., Boger, D.V. and Nguyen, Q.D., 1998. The yielding of waxy crude oils. *Industrial & engineering chemistry research*, *37*(4), pp.1551-1559.

58. Singh, P., Venkatesan, R., Fogler, H.S. and Nagarajan, N.R., 2001. Morphological evolution of thick wax deposits during aging. *AIChE Journal*, *47*(1), pp.6-18.

59. Coutinho, J.A., Lopes da Silva, J.A., Ferreira, A., Rosário Soares, M. and Daridon, J.L., 2003. Evidence for the aging of wax deposits in crude oils by Ostwald ripening. *Petroleum science and technology*, *21*(3-4), pp.381-391.

60. Schou Pedersen, K., Skovborg, P. and Roenningsen, H.P., 1991. Wax precipitation from North Sea crude oils. 4. Thermodynamic modeling. *Energy & Fuels*, *5*(6), pp.924-932.

61. da Silva, J.A.L. and Coutinho, J.A., 2004. Dynamic rheological analysis of the gelation behaviour of waxy crude oils. *Rheologica Acta*, *43*(5), pp.433-441.

62. Mirante, F.I. and Coutinho, J.A., 2001. Cloud point prediction of fuels and fuel blends. *Fluid Phase Equilibria*, *180*(1), pp.247-255.

63. Coutinho, J.A., Knudsen, K., Andersen, S.I. and Stenby, E.H., 1996. A local composition model for paraffinic solid solutions. *Chemical engineering science*, *51*(12), pp.3273-3282.

64. Yang, F., Zhao, Y., Sjöblom, J., Li, C. and Paso, K.G., 2015. Polymeric wax inhibitors and pour point depressants for waxy crude oils: A critical review. *Journal of Dispersion Science and Technology*, *36*(2), pp.213-225.

65. Rao, I.J. and Rajagopal, K.R., 2000. Phenomenological modelling of polymer crystallization using the notion of multiple natural configurations. *Interfaces and free boundaries*, *2*(1), pp.73-94.

66. Rao, I.J. and Rajagopal, K.R., 2001. A study of strain-induced crystallization of polymers. *International Journal of Solids and Structures*, *38*(6), pp.1149-1167.

67. Akinade, A. and Ajediti, O., 2015. Tool for Predicting Wax Deposition Rate at Different Operating Conditions: A Penetration Theory Approach. *Tool for Predicting Wax Deposition Rate at Different Operating Conditions: A Penetration Theory Approach*, *4*(5), pp.278-283.

68. Hou, L. and Zhang, J.J., 2007. Viscoelasticity of gelled waxy crude oil. *Journal of Central South University of Technology*, *14*, pp.414-417.

69. Letoffe, J.M., Claudy, P., Kok, M.V., Garcin, M. and Volle, J.L., 1995. Crude oils: characterization of waxes precipitated on cooling by dsc and thermomicroscopy. *Fuel*, *74*(6), pp.810-817.

70. Hansen, A.B., Larsen, E., Pedersen, W.B. and Nielsen, A.B., 1991. Wax Precipitation from North Sea Crude Oils. 3. Precipitation and Dissolution of Wax Studied by Differential Scanning Calorimetry. *Energy & Fuels*, *5*(6), pp.914-923.

71. Pedersen, W.B., Hansen, A.B., Larsen, E. and Nielsen, A.B., 1991. Wax Precipitation from North Sea Crude Oils. 2. Solid-Phase Content as Function of Temperature Determined by Pulsed NMR. *Energy & Fuels*, *5*(6), pp.908-913.

72. Webber, R.M., 2001. Yield properties of wax crystal structures formed in lubricant mineral oils. *Industrial & Engineering Chemistry Research*, *40*(1), pp.195-203.

73. Guo, X. and R. K. Prud'homme. 2005. Crystal structure of mixed paraffins and rheological behavior of model waxy oils. *J. American Chemical Society, 50*(1), pp.81-83.

74. Bagdat, M. and Masoud, R., 2015. Control of Paraffin Deposition in Production Operation by Using Ethylene–TetraFluoroEthylene (ETFE). In *ICIPEG 2014* (pp. 13-21). Springer Singapore.

75. Azevedo, L.F.A. and Teixeira, A.M., 2003. A critical review of the modeling of wax deposition mechanisms. *Petroleum Science and Technology*, *21*(3-4), pp.393-408.

76. Sanjay, M., Simanta, B. and Kulwant, S., 1995. Paraffin problems in crude oil production and transportation: a review. *SPE Production & Facilities*, *10*(01), pp.50-54.

77. Wardhaugh, L.T. and Boger, D.V., 1991. Flow characteristics of waxy crude oils: application to pipeline design. *AIChE Journal*, *37*(6), pp.871-885.

78. Weingarten, J.S. and Euchner, J.A., 1988. Methods for predicting wax precipitation and deposition. *SPE Production Engineering*, *3*(01), pp.121-126.

79. Wardhaugh, L.T. and Boger, D.V., 1987. Measurement of the unique flow properties of waxy crude oils. *Chemical engineering research & design*, *65*(1), pp.74-83.

80. Merino-Garcia, D., Margarone, M. and Correra, S., 2007. Kinetics of waxy gel formation from batch experiments. *Energy & fuels*, *21*(3), pp.1287-1295.

81. Brown, T.S., Niesen, V.G. and Erickson, D.D., 1995. Measurement and Prediction of the Kinetics of Paraffin Deposition. *Journal of Petroleum Technology*, *47*(4), pp.328-329.

82. Ribeiro, F.S., Mendes, P.R.S. and Braga, S.L., 1997. Obstruction of pipelines due to paraffin deposition during the flow of crude oils. *International journal of heat and mass transfer*, *40*(18), pp.4319-4328.

83. Creek, J.L., Lund, H.J., Brill, J.P. and Volk, M., 1999. Wax deposition in single phase flow. *Fluid Phase Equilibria*, *158*, pp.801-811.

84. Ribeiro, F.S., Mendes, P.R.S. and Braga, S.L., 1997. Obstruction of pipelines due to paraffin deposition during the flow of crude oils. *International journal of heat and mass transfer*, *40*(18), pp.4319-4328.

85. Svendsen, J.A., 1993. Mathematical modeling of wax deposition in oil pipeline systems. *AIChE Journal*, *39*(8), pp.1377-1388.

86. Ramirez-Jaramillo, E., Lira-Galeana, C. and Manero, O., 2004. Modeling wax deposition in pipelines. *Petroleum science and technology*, *22*(7-8), pp.821-861.

87. Agrawal, K.M., Khan, H.U., Surianarayanan, M. and Joshi, G.C., 1990. Wax deposition of Bombay high crude oil under flowing conditions. *Fuel*, *69*(6), pp.794-796.

88. Lee, H.S., 2008. *COMPUTATIONAL AND RHEOLOGICAL STUDY OF WAX DEPOSITION AND GELATION IN SUBSEA PIPELINES* (Doctoral dissertation, The University of Michigan).

89. Burger, E.D., Perkins, T.K. and Striegler, J.H., 1981. Studies of Wax Deposition in the Trans Alaska Pipeline. *Journal of Petroleum Technology*, *33*(6), pp.1075-1086.

90. Mehrotra, A.K. and Bhat, N.V., 2007. Modeling the effect of shear stress on deposition from "waxy" mixtures under laminar flow with heat transfer. *Energy & fuels*, *21*(3), pp.1277-1286.

91. Guozhong, Z. and Gang, L., 2010. Study on the wax deposition of waxy crude in pipelines and its application. *Journal of Petroleum Science and Engineering*, *70*(1), pp.1-9.

92. Coutinho, J.A. and Daridon, J.L., 2005. The limitations of the cloud point measurement techniques and the influence of the oil composition on its detection. *Petroleum Science and Technology*, *23*(9-10), pp.1113-1128.

93. Hamouda, A.A. and Davidsen, S., 1995, February. An Approach for Simulation of Paraffin Deposition in Pipelines as a Function of Flow Characteristics With a Reference to Teesside Oil Pipeline. In *SPE International Symposium on Oilfield Chemistry*.

94. Leiroz, A.T. and Azevedo, L.F., 2007. Paraffin deposition in a stagnant fluid layer inside a cavity subjected to a temperature gradient. *Heat transfer engineering*, *28*(6), pp.567-575.

95. Majeed A, Bringedal, B., and Overa, S. 1990. Model Calculates Wax Deposition for N. Sea Oils. *Oil and Gas J*. **88** (25): 63 - 89.

96. http://petrowiki.org/Models_for_wax_deposition_in_pipelines (accessed on 19/7/2016)

97. Dirand, M., Chevallier, V., Provost, E., Bouroukba, M. and Petitjean, D., 1998. Multicomponent paraffin waxes and petroleum solid deposits: structural and thermodynamic state. *Fuel*, *77*(12), pp.1253-1260.

98. Mózes, G. ed., 1983. *Paraffin Products* (Vol. 14). Elsevier.

99. Lee, H.S., Singh, P., Thomason, W.H. and Fogler, H.S., 2007. Waxy oil gel breaking mechanisms: adhesive versus cohesive failure. *Energy & Fuels*, *22*(1), pp.480-487.

100. Venkatesan, R. and Fogler, H.S., 2004. Comments on analogies for correlated heat and mass transfer in turbulent flow. *AIChE journal*, *50*(7), pp.1623-1626.

101. Vignati, E., Piazza, R., Visintin, R.F., Lapasin, R., D'Antona, P. and Lockhart, T.P., 2005. Wax crystallization and aggregation in a model crude oil. *J. Phys.: Condens. Matter*, *17*, pp.S3651-S3660.

102. Coussot, P., Nguyen, Q.D., Huynh, H.T. and Bonn, D., 2002. Viscosity bifurcation in thixotropic, yielding fluids. *Journal of Rheology*, *46*(3), pp.573-589.

103. Barnes, H.A., 1997. Thixotropy—a review. *Journal of Non-Newtonian fluid mechanics*, *70*(1), pp.1-33

104. Hou, L. and Zhang, J.J., 2007. New method for rapid thixotropic measurement of waxy crude. *Journal of Central South University of Technology*, *14*, pp.471-473.

105. Guo, L., Wang, Y., Shi, S., Yu, X. and Chen, X., 2015. Study on Thixotropic Properties of Waxy Crude Oil Based on Hysteresis Loop Area. *Engineering*, *7*(07), p.469.

106. Barnes, H.A., 1995. A review of the slip (wall depletion) of polymer solutions, emulsions and particle suspensions in viscometers: its cause, character, and cure. *Journal of Non-Newtonian Fluid Mechanics*, *56*(3), pp.221-251.

107. http://www.azom.com/article.aspx?ArticleID=2884 (accessed on 30/11/2016)

108. Khan, M.R., 1996. Rheological properties of heavy oils and heavy oil emulsions. *Energy Sources*, *18*(4), pp.385-391.

109. Phillips, D.A., Forsdyke, I.N., McCracken, I.R. and Ravenscroft, P.D., 2011. Novel approaches to waxy crude restart: Part 2: An investigation of flow events following shut down. *Journal of Petroleum Science and Engineering*, *77*(3), pp.286-304.

110. Mendes, R., Vinay, G., Ovarlez, G. and Coussot, P., 2015. Modeling the rheological behavior of waxy crude oils as a function of flow and temperature history. *Journal of Rheology*, *59*, pp.703-732.

111. Mitsoulis, E., 2007. Flows of viscoplastic materials: models and computations. *Rheology reviews*, *2007*, pp.135-178.

112. Hasan, S.W., Ghannam, M.T. and Esmail, N., 2010. Heavy crude oil viscosity reduction and rheology for pipeline transportation. *Fuel*, *89*(5), pp.1095-1100.

113. Seyssiecq, I., Ferrasse, J.H. and Roche, N., 2003. State-of-the-art: rheological characterisation of wastewater treatment sludge. *Biochemical Engineering Journal*, *16*(1), pp.41-56.

114. Pevere, A., Guibaud, G., Van Hullebusch, E., Lens, P. and Baudu, M., 2006. Viscosity evolution of anaerobic granular sludge. *Biochemical Engineering Journal*, *27*(3), pp.315-322.

115. http://www.welding-advisers.com/Creep-test.html (accessed on 20/11/2016)

116. Mezger, T.G., 2006. *The rheology handbook: for users of rotational and oscillatory rheometers*. Vincentz Network GmbH & Co KG.

4 Final conclusions and Future work

4.1 Final conclusion

The oil producers have currently large operating costs associated with flow assurance, in particular trying to minimize the problems caused by wax deposition. The ability to control wax deposition in pipelines is most important for planning their operation and design. This thesis was focused on Libyan waxy crude oils, and the characterization of their nature and behavior has been the object of this research during the last few years.

We aimed at obtaining information and improve the knowledge and understanding of the physico-chemical characteristics and rheological behavior of Libyan crude oils presenting wax deposition problems during their transportation, since the oil sector in Libya lacks studies of this type. Therefore, such task is of great interest and became all the more pressing with the instability in Libya during these last few years that led to prolonged stops in oil production, making the restarting a complicated and costly challenge.

In this work we focused on five Libyan crude oils known for their wax deposition problems. Initially a detailed physico-chemical characterization of the five oils and their waxes was made.

Our main goal in this work was to understand the rheological behavior of these crude oils upon precipitation of the wax. To achieve this goal a comprehensive rheological characterization at various temperatures around their pour point was done, including steady-shear flow tests, oscillatory tests at low strain amplitudes and creep-compliance tests.

The following are the main conclusions of this work, set against the objectives listed in chapter 1.

1. To characterize five Libyan oils and their waxes using a combination of various analytical techniques.

- The crude oils studied are medium or light crude oils with high wax content.

- Although the wax appearance temperature could be expected to increase with the oil wax content, the results obtained showed no direct correlation between these two variables. The WAT seems to be dependent upon not only the wax content but also on the paraffin distribution in the wax and the oils solvation ability.

- The pour point temperature of the oils shows a very good linear dependency upon the WAT for all crude oils.

- The results of all the analyses of the extracted waxes indicate that they are highly paraffinic macrocrystalline waxes.

Overall, all the studied Libyan crude oils present macrocrystalline waxes composed of essentially straight-chain saturated paraffinic hydrocarbons such as the n-alkanes.

2. To study the rheological characteristics of three waxy oils, Faregh, Sarir and Bouri.

- The flow properties, viscosity, shear rate and shear stress, were measured for the three oils at various temperatures below their pour point. The measurements showed that the observed flow behaviour is very complex, so there is no standard method to predict the yield stress of waxy crude oils to be adopted by the petroleum industry; the process of yielding is still challenging; a model with four yield stresses was suggested instead of model with three yield stresses which has an extensive range of application for waxy crude oils.

- Measurements of the viscoelastic behaviour were carried out using creep- recovery and oscillatory tests. This facilitated a better understanding of the structure of the gelled oils at low temperatures. Also stress sweep tests were used to study the yielding process and predict the yield stresses using oscillation. Bouri oil showed the lowest structured network although of its high values of yield stress. However Bouri oil has the lowest crystallinity and the lowest value of wax content which may contribute to this low structured gel; the higher values of yield stresses may be explained as result of the

interaction between the paraffin crystals that display a high stress resistance leading Bouri oil to be less sensitive against stress.

We do believe that the aims achieved and the impact of the results on the oil industry in Libya will be important contributions for the suitable solution for wax deposition problems and to reduce the operation and transportation costs due to line blockage.

4.2 Future work

The work developed in the characterization of wax deposition of some Libyan oils provided some new insights for their behavior. However, as an outlook for future developments, some investigations aiming at a better representation and some new contributions should be attempted for a complete characterization of those oils. More specifically, further future developments should include the following:

1. A set of measurements could be performed by other techniques which would maximize the knowledge and improve the opportunity to further advances by achieving more information about the chemical and physical nature of the Libyan paraffinic waxes. Further details about the nature of the waxes could be obtained from spectroscopic techniques such as FTIR, and Raman, and more details on its composition could be obtained from mass spectrometry, while the crystal size and shape could be measured by SEM or by light scattering.

2. A set of other rheological measurements could also be performed:

a) The flow behaviour tests could be used in future at more different loading rates and different cooling rates to get more insight of the parameters e.g. apparent viscosity, apparent yield stresses etc.

b) More detailed study on the viscoelastic behavior using creep - recovery tests. First, more creep tests are needed to improve the prediction of yield stresses. Recovery process needs to be researched more extensively. e.g. studying the apparent viscosity, with time to deepen understanding the behavior of the oil at rest.

c) Study of the rheological behaviour of Remal and Sedra crude oils.

In this work it was not possible to do the measurements for Remal and Sedra by AR100, TA instruments due to the very high / low values of pour point of Remal and Sedra, respectively, and the time required to carry out such measurements. It is here suggested that these analysis should be carried out on a more advanced rheometer in order to characterize these two oils, as well as to obtain information for ageing times of the waxes that would go considerably beyond the timeframe studied on this thesis, and that could provide more realistic data to what is happening on a pipeline shut down for long periods of time.

d) In principle the data obtained can be used as such and it provides a good basis to assess scaling up. More efforts concerning the use of real environments in the field would be useful to understand the behavior of these studied waxy crude oils under real conditions to help the oil companies to guide operation at the large scales.

3. Another interesting improvement would be to use the results from this thesis to develop reliable deposition models to describe wax precipitation in Libyan waxy oils and create tools to mitigate the associated flow assurance problems.

4. The main goal of this work would be to create another contribution to support the Libyan oil industry. The evaluation and parameterization of a suitable depositions model, comprising both the thermodynamic and kinetic aspects of the process, would help to avoid or minimize flow assurance problems related to wax deposition. The availability of this model could help in the design of flow lines and surface facilities, and in developing operating plans that anticipate and quantify the problems of wax deposition, saving time and helping to identify the appropriate solutions to alleviate production problems.

5 Appendix A

A-1 Technical information for Faregh crude oil

Faregh oil field is located at south of Gialo. It contains about 27 wells, seven still under construction.

1. The distance of crude oil pipeline from Faregh main station to Gialo station is approx. 62 Km. The diameter of the pipeline is 12'', the material is; carbon steel pipe, WT 0.330, insulated with 3" Thick Polyurethane covered with 6 mm High density Polyethylene.

2. The pipeline is buried approx. 3.5 feet above the top of the pipe, Elevation 140 ft.

3. The production rate which has been pumping through this pipeline is approx. 15,000 BOPD (until 2011), at temperature of 130-140 Deg. F.

4. There are 3 multistage vertical centrifugal pumps located at downstream of the crude storage tanks to transfer the crude to Gialo station.

5. The inlet of temperature and pressure of the crude to the pump is 130-140 Deg F, and 5-20 Psi.

6. The temperature of the crude oil is maintained either in winter or in summer by hot water heating pipes inside the storage tank and by electrical heat trace and insulation on pipes.

7. Hot water heating (used on vessels and tanks etc.), electrical tracing(used on piping and instrumentation)

8. The hot water circulation rate designed for approx. 900 US gallon/Min at 29 psi differential pressure and around 110 psi at Gialo side.

9. The crude oil pipe is regularly pigged from the launcher at Faregh station and received at Gialo station.

A-2 Technical information for Sarir crude oil

1. The pipeline length from Sarir field to Ahariqh port is about 513.7 km,Internal diameter = 33.25". The outer diameter 34", made of (carbon steel API 5L.x52 longitudinal seam welded) and enveloped by wrapping tape, thickness is about 6 mm.

2. All substations lines as well as the flow lines from wells have diameters between 6 inches and 24 inches, the shipping line to the Meslla field is 30 inches. All those lines are made of carbon steel and coated by wrapping tape.

3. The main line of Sarir – Tobruk's height and length (Figure A-1) covered by sand with a thickness of centimeters to about 2 meters.

4. There are 10 pumps at the beginning of the line, 5 buffered and 5 are working 24 hours.

5. The production rate to Tobruk = 150,000 barrels per day (until 2011).

6. The chemicals of removing wax deposition are not being injected continuously, sometimes is injected on winter or during a special operations such as replacement of pipeline parts, where the mechanical cleaning process (pigging) stopped.

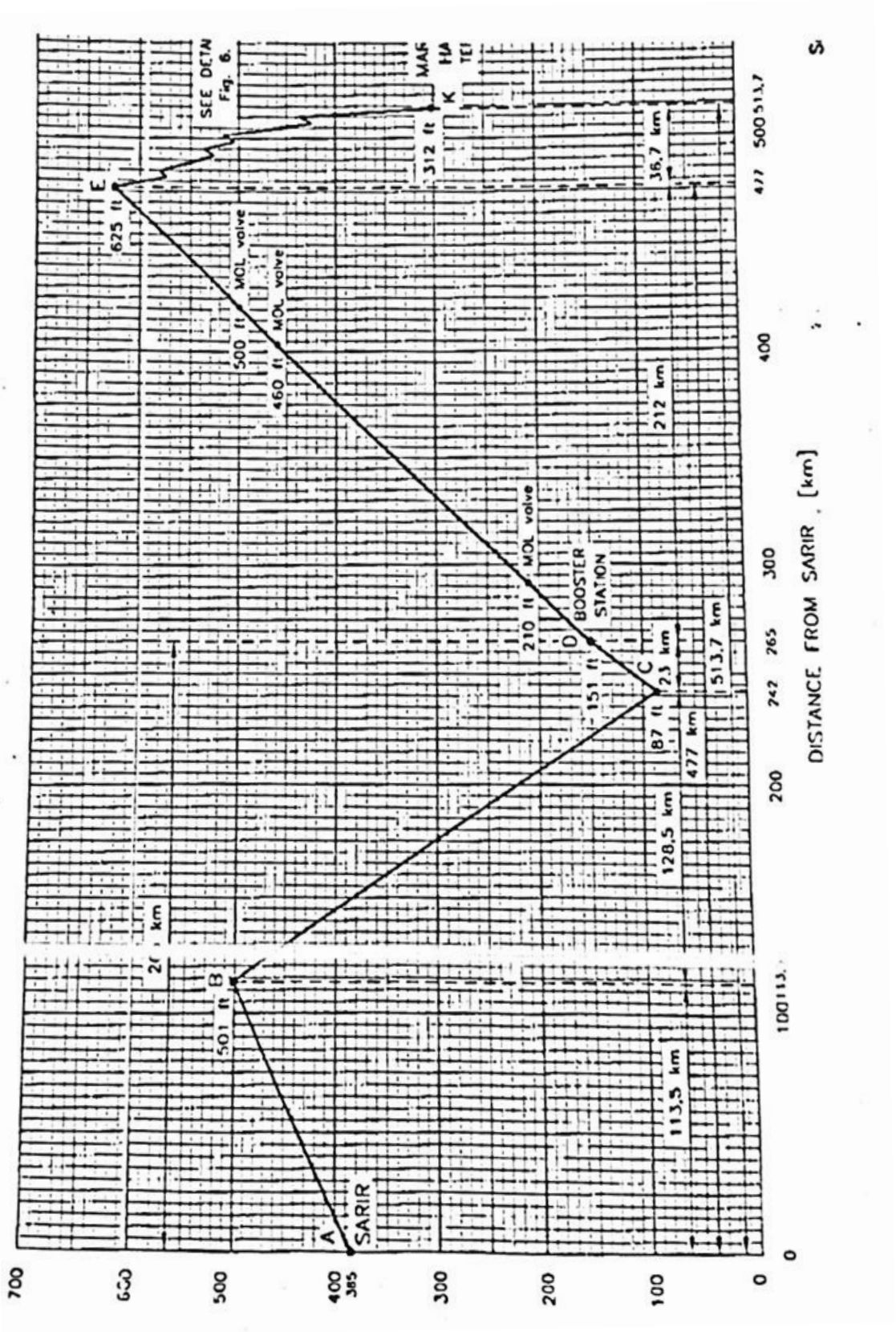

Figure A-1: The main line of Sarir–Tobruk's height and length

6 Appendix B

Energy Fuels **2010,** *24,* 3101–3107 · DOI:10.1021/ef1001937
Published on Web 05/04/2010

energy&fuels
article

Characterization of Libyan Waxy Crude Oils

Layla M. Alghanduri,[†,‡] Mohamed M. Elgarni,[†] Jean-Luc Daridon,[§] and Joao A. P. Coutinho*[,‡]

[†]*Libyan Petroleum Institute, Post Office Box 6431, Tripoli, Libya,* [‡]*Centre for Research in Ceramics and Composite Materials (CICECO), Departamento de Química da Universidade de Aveiro, 3810-193 Aveiro, Portugal, and* [§]*Laboratoire des Fluides Complexes, Université de Pau, 64000 Pau, France*

Received February 19, 2010. Revised Manuscript Received April 22, 2010

The prediction of wax formation and the understanding of the physicochemical characteristics of the wax phase are of major importance in flow assurance. The characterization of the oil and wax can provide useful estimates of the parameters and behavior required for operational engineering process developments and/or physical modifications to the processing of crude oils, aiming at the reduction of costs of production and transportation. Five Libyan crude oils and their waxes were characterized using various experimental techniques. Waxes were extracted using the Universal Oil Products (UOP) 46-64 method and purified by column chromatography. Differential scanning calorimetry (DSC) and cross polar microscopy (CPM) techniques were used to study the wax appearance temperature (WAT) for these crude oils. Waxes were characterized using gas chromatography (GC), nuclear magnetic resonance (NMR), and X-ray diffraction (XRD). The carbon number distribution was determined by gas chromatography−flame ionization detector (GC−FID). Extensive information about the structural composition of these waxes was performed using ^{13}C NMR, and information for the crystalline structure of these waxes was obtained using XRD. This study shows that the five Libyan crude oils studied have wax contents between 8 and 24 wt % with WAT in the range of 22.5−68.17 °C. The isolated waxes are shown to be paraffinic (macrocrystalline wax) with an orthorhombic structure.

Introduction

The heavy saturated fraction of crude oil, known as wax, tends to precipitate during the extraction and transport of crude oils as a result of the temperature (T) and pressure (P) drop of the fluid. As soon as the $P-T$ conditions fall within the solid region of the phase envelope, i.e., the temperature of the oil falling below the wax appearance temperature (WAT), there will be formation of deposits on the reservoir or pipelines. The wax deposition causes the plugging of pipelines and clogging of transport equipment, being a well-known and expensive problem in the petroleum industries.[1,2] A better understanding of the oil composition and the paraffinic hydrocarbons present in the crude oils can help face this problem both preventively and providing remediation whenever necessary. Several useful analytical techniques have been proposed in the petroleum industry to study the petroleum fluid characteristics in general, and they can provide adequate information concerning the wax formation to facilitate production developments and thus avoid shutdowns and operational problems, which cost billions of dollars per year during oil production and transportation.[3] Although predictive models are available today for wax formation[4,5] and deposition[6,7] in crudes, they always required detailed compositional knowledge of the oils for an adequate performance.

The purpose of this study is to evaluate the characteristics of five different Libyan crude oils, as well as their waxes. These oils, named Remal, Sarir, Sedra, Bouri, and Farigh, were supplied by three companies, Waha, Eni-Oil, and Arabian Gulf Oil, operating in Libya through the National Oil Corporation. The oils were chosen because of the wax problems that they present during transport. The location of these wells is presented in Figure 1, showing the sedimentary basins of Libya. The Bouri oilfield off Libya's western coast is the largest producing offshore oilfield, estimated to contain 2 billion barrels in proven recoverable crude oil. The Sirte basin contains around 80% of Libya's established oil reserves and production. Sedra provides the largest contribution to crude oils export, whereas Sarir is regarded as the second most important contribution for exportation.[8] These Libyan waxy crude oils present problems in transportation through pipelines because of thermal environmental changes. These crudes, mainly during wintry weather or at night, present a decreasing flow of crude oil because of the deposition of a solid phase that obstructs the pipeline, and as result of that, the flow handling becomes difficult. Because of the long distance that the oils travel through the pipelines from the field to the coast terminals (e.g., the distance from the Sarir field to

*To whom correspondence should be addressed. E-mail: jcoutinho@ua.pt.

(1) Misra, S.; Baruah, S.; Singh, K. *SPE Prod. Facil.* **1995**, *10* (Feb), 50–54.
(2) Merino-Garcia, D.; Correra, S. *Pet. Sci. Technol.* **2008**, *26*, 446–459.
(3) Department of Energy (DOE) and University of Tulsa embark on wax deposition study. *Oil Gas J.* **2001**, *99*, 56.
(4) Daridon, J. L.; Pauly, J.; Coutinho, J. A. P.; Montel, F. *Energy Fuels* **2001**, *15*, 730–735.
(5) Coutinho, J. A. P.; Daridon, J. L. *Energy Fuels* **2001**, *15*, 1454–1460.
(6) Coutinho, J. A. P.; Edmonds, B.; Moorwood, T.; Szczepanski, R.; Zhang, X. H. *Energy Fuels* **2006**, *20*, 1081–1088.
(7) Edmonds, B.; Moorwood, T.; Szczepanski, R.; Zhang, X. H. *Energy Fuels* **2008**, *22*, 729–741.
(8) Najah, T.; El-Moudir, W. Libyan crude oils, their characteristics and suitability for further processing. Presented at the Organization of Arab Petroleum Exporting Countries (OAPEC)/IFP Seminar, Rueil-Malmaison, France, June 2006.

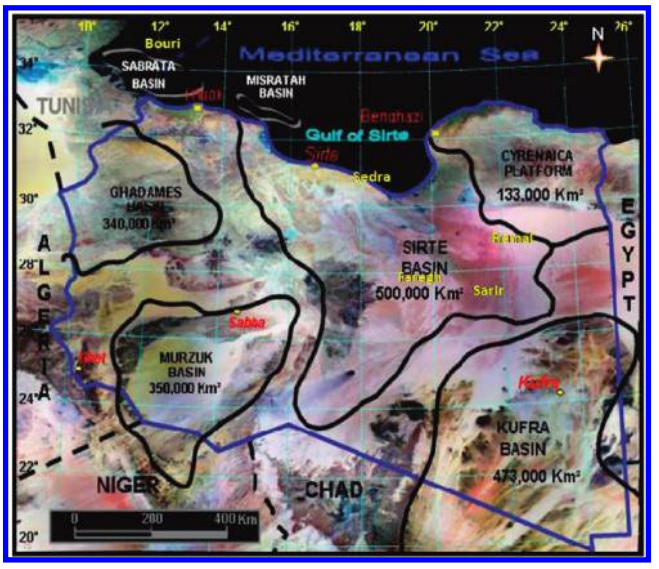

Figure 1. Map showing the location of the investigated oil wells.

the coast terminal is about 513.6 km), thermal or mechanical treatment and flow improvers are always applied to these crude oils to avoid the transportation problem, which severely increases their production costs.

In practice, the characterization of the oils and their waxes can be achieved through various physicochemical and compositional analyses, such as American Petroleum Institute (API) gravity and viscosity, WAT, wax content, and pour point, and further characterization of the waxes by gas chromatography (GC), differential scanning calorimetry (DSC), nuclear magnetic resonance (NMR), and X-ray diffraction (XRD), among others.[9,10] The information obtained by these techniques can be of great importance to explain the causes of wax deposition and to be able to understand, predict, and prevent it during transportation, production, and storage of petroleum.

In this work, a number of these techniques were used to characterize the five Libyan crudes under study. The WAT was measured by DSC; the wax content was measured by the Universal Oil Products (UOP) 46-64 method; and the waxes recovered were further purified by column chromatography. The purified waxes were then analyzed by GC, DSC, NMR spectroscopy, and XRD spectrometry for a full characterization of their nature, as discussed below.

Experimental Section

After a preliminary characterization of the crude oils under study, their waxes were extracted and also characterized. The techniques used for the oils and waxes are described below.

Oil Characterization. *Viscosity and Density*. The viscosity and density measurements were carried on an Anton Paar Viscometer, model SVM3000, according to ASTM D445-06 and ASTM D5002-99, respectively,[11] at the temperatures of 40 and 80 °C. The standard S3 from Paragon Scientific was used to calibrate the viscometer. The samples were heated above the WAT before the viscosity measurements to ensure that all wax particles are dissolved.

API Gravity. The API gravity is used to estimate the quality of a crude oil. The values of API gravity for each crude oil were estimated on the basis of the following equation using density values at 40 °C, except for Remal that used values at 80 °C:

$$\mathrm{API} = \frac{141.5}{\mathrm{SG}} - 131.5 \qquad (1)$$

WAT. The WAT was measured for the studied crudes using a Mettler DSC822e calibrated with indium and flushed with dry nitrogen. To measure the WAT, crude oil samples of about 10 mg were heated to 40 K above pour-point temperatures and then cooled with a cooling rate of 1 or 3 K/min to evaluate the effect of the cooling rate on the WAT. Three runs were carried for each oil, and average results are reported. The WAT was taken here as the onset temperature of the exothermal peak observed.

Pour Point. The pour point of a crude oil is the temperature at which the oil gels because of the crystallization of waxes. Pour-point temperatures of the crude oils were measured using the standard test method for the pour point, ASTM D97-06.[11]

Water Content. The water content of the crude oils studied was evaluated in the oil samples as received using a Metrohm 831 Karl Fischer (KF) coulometer.[12]

Wax Content. Because the composition, type, and properties of the waxes present in a crude oil differ with the crude oil source, it is important to extract them from the hydrocarbon matrix to evaluate their chemical composition and structural characteristics. The UOP 46-64 method[13] was used to extract the wax from the crude oil. A total of ca. 2 g of crude oil was dissolved in 500 mL of petroleum naphtha, and 15 g of Fuller's earth were added to the solution. The mixture was then filtered and evaporated. Finally, 200 mL of a mixture of 1:3 petroleum naphtha/acetone was added to the solution, and the liquid was chilled to about −17 °C and filtered by a cold filter funnel, after which the sample was washed with hot naphtha and the petroleum naphtha was evaporated to recover the wax. This was weighed, and the wax content was evaluated.

Molecular Weight. The average molecular weight of the crudes was determined by cryoscopic depression by the relation

$$M_w = \frac{1000 k_f m_{oil}}{\Delta T_{fus} m_{xyl}} \qquad (2)$$

using xylene as the solvent.

Wax Characterization. *Wax Purification*. Before characterization, the waxes extracted from the crudes according to the procedure described above were further purified by cleaning the waxes using a silica gel column to remove the polar material that remains after precipitation. The wax samples were dissolved in *n*-hexane and passed through a 50 cm silica chromatographic column. The procedure was based on the method described by Musser and Kilpatrick.[14]

GC. A Varian gas chromatograph (CP3800) with a flame ionization detector (FID) was used for the characterization of the wax composition. A capillary column CP-5, 30 m long and with 0.32 mm internal diameter and 0.25 μm film thickness, was used. The wax was dissolved in CS_2, and the samples were injected into the column using an auto-sampler, with the injector at a temperature of 250 °C, with a split/splitless ratio of 1:50. The detector temperature was 300 °C. Analysis was performed under a helium flow rate of 1.2 mL/min and a temperature program of 40−280 °C at 12 °C/min and held for 5 min at the highest temperature.

(9) Coutinho, J. A. P.; Daridon, J. L. *Pet. Sci. Technol.* **2005**, *23*, 1113–1128.
(10) Musser, B. J.; Kilpatrick, P. K. *Energy Fuels* **1998**, *12*, 715–725.
(11) American Society for Testing and Materials (ASTM). *Annual Book of ASTM Standards*; ASTM: West Conshohocken, PA, 2008; Vol. 05.01.
(12) Freire, M. G.; Gomes, L.; Santos, L. M. N. B. F.; Marrucho, I. M.; Coutinho, J. A. P. *J. Phys. Chem. B* **2006**, *110*, 22923–22929.
(13) Universal Oil Products (UOP). UOP Method 46-64, Paraffin Wax Content of Petroleum Oils and Asphalts, UOP Co., Des Plaines, IL, 1964.
(14) Musser, B. J.; Kilpatrick, P. K. *Energy Fuels* **1998**, *12* (4), 715–715.

Table 1. Physical Properties for the Libyan Crude Oils Studied in This Work

				kinematic viscosity ($mm^2 s^{-1}$)		density ($g cm^{-3}$)			
crude oil samples	UOP wax content (wt %)	pour-point temperature (°C)	M_w	at 40 °C	at 80 °C	at 40 °C	at 80 °C	API gravity (deg)	water content (ppm)
Remal	18.8	51	331.5		18.680		0.886	25.13	
Bouri	15.0	12	249.7	20.475	7.225	0.883	0.860	25.70	820
Sarir	13.6	24	244.7	13.563	5.270	0.829	0.810	35.64	1327
Sedra	8.0	0	200.7	5.253		0.827		36.03	206
Faregh	24.1	21	217.2	4.446	2.557	0.790	0.772	43.47	576

Table 2. WAT at the Two Cooling Rates for the Studied Oils[a]

crude oil samples	WAT (°C) at 3 K/min	WAT (°C) at 1 K/min
Remal	67.3 ± 1.92	68.2 ± 0.38
Bouri	29.2 ± 0.54	29.7 ± 0.28
Sarir	48.7 ± 0.36	49.6 ± 0.10
Sedra	22.5 ± 0.04	23.2 ± 0.88
Faregh	42.1 ± 0.22	43.1 ± 0.14

[a] Uncertainty assigned is 2 times the standard deviation of the measurements.

Elemental Analysis. Elemental analysis (C, H, N, and S) for the purified waxes were carried out at the Centro de Apoio Científico e Tecnolóxico á Investigación (CACTI) of the University of Vigo (Spain) using a CHNS analyzer.

DSC. Thermal characterization of the waxes (melting temperatures and enthalpies) was carried out on a Mettler DSC822e calibrated with indium and flushed with dry nitrogen. The melting point of the waxes is taken as their peak temperature.

^{13}C NMR Spectra. Carbon NMR was used to provide a value for the relative proportions of aliphatic and aromatic carbons in the wax. Quantitative ^{13}C NMR spectra were collected on a Bruker Avance 300 spectrometer operating at 75.47 MHz. Wax samples were diluted at 50% in $CDCl_3$, and the spectra were recorded at 295 K with tetramethylsilane (TMS) as the internal reference. The inverse gate decoupling sequence, which allows for quantitative analysis and a comparison of signal intensities, was used with the following parameters: pulse angle, 30°; acquisition time, 3.48 s; relaxation delay, 60 s; data points, 32 000; and scans, 5000. Information concerning the different types of carbon present is based on the works by Carman et al.[15] and Sperber et al.,[16] and the aromatic content is quantified according to ASTM D5292-99.[11]

XRD Spectra. Diffractograms of the waxes at room temperature were acquired on Philips X'Pert equipment, which operates in the reflection mode with Cu Kα radiation ($\lambda = 1.5406$ Å). Diffraction data were collected in a 2θ range from 2° to 60°, with a step of 0.02° and a time per step of 2 s, with incident and diffracted beam anti-scatter slits of 1°, divergence slit of 1°, and receiving slit of 0.1 mm, on a curved graphite diffracted beam monochromator.

Results and Discussion

Crude Oil Properties. Analyses were carried to characterize the five crude oils studied on this work. Specific gravity (SG), API gravity, viscosity, pour-point temperature, wax content, average molecular weight, and water content of each crude oil were measured as described above, and the results are reported in Table 1. The high pour point of Remal precluded the measurement of the viscosities and densities at 40 °C and also the water content.

The oil characterization shows that the crudes studied here are medium or light crude oils with high wax content. As expected, the wax content correlates well with the API gravity and the viscosity of the crudes at 40 °C. The crudes with a larger wax content present lower API gravities and higher viscosities.

Table 3. Composition (wt %) of the Waxes Studied

	Remal	Bouri	Sarir	Sedra	Faregh
C11		0.213			
C12		0.176			
C13		0.316			
C14		0.735			0.189
C15	0.405	1.763	0.460	0.394	0.480
C16	0.650	2.183	0.920	0.574	0.860
C17	1.030	2.865	2.065	1.148	1.233
C18	1.915	4.063	4.182	2.226	3.498
C19	3.598	5.083	7.054	4.831	4.543
C20	5.453	5.983	9.140	8.159	7.921
C21	7.679	6.207	10.443	10.489	11.267
C22	8.371	6.195	9.979	10.961	11.474
C23	8.804	5.392	9.577	10.300	9.834
C24	8.395	5.16	7.754	9.034	9.356
C25	8.331	4.203	7.040	7.670	6.949
C26	7.710	3.839	5.674	6.043	6.338
C27	7.378	3.297	4.662	5.503	5.058
C28	6.120	3.8	3.797	4.753	4.561
C29	5.477	2.816	3.236	4.070	3.427
C30	4.163	2.504	2.440	3.364	2.873
C31	3.126	2.259	1.713	2.646	1.928
C32	2.158	1.848	1.242	1.927	1.648
C33	1.595	1.554	0.989	1.535	1.127
C34	0.319	1.374		1.156	1.113
C35		1.228		1.006	0.896
C36		0.736			0.485
C37		0.653			
C38		0.546			
C39		0.354			
C40		0.351			
total *n*-alkanes	92.68	77.70	92.37	97.79	97.06
iso- and cycloalkanes	7.32	22.30	7.63	2.21	2.94

Table 4. Elemental Analysis and H/C Ratio of the Waxes Extracted from the Oils and Total Aromatic Carbon Content of the Waxes under Study Measured by ^{13}C NMR

	C (wt %)	H (wt %)	H/C	C(ar) NMR (wt %)
Remal	85.28	14.72	2.07	0.7
Bouri	85.52	14.48	2.03	1.1
Sarir	85.66	14.34	2.01	0.9
Sedra	86.02	13.98	1.95	1.8
Faregh	85.09	14.91	2.10	0.6

The WAT is the temperature at which some heavy paraffinic molecules start to precipitate from solution. WAT is considered as one of main guidelines for system design, production operations, and the planning of the exploration of a reservoir.[9] The WATs for the five oils have been measured using DSC as the onset temperature of the exothermal peak observed upon cooling. Results for the WAT measured at the two cooling rates used are reported in Table 2. Although the WATs measured at the lowest cooling rate are consistently higher, the difference between these are in general within the uncertainty of the measurements estimated as

(15) Carman, C. J.; Harrington, R. A.; Wilkes, C. E. *Macromolecules* **1977**, *10*, 536–544.
(16) Sperber, O.; Kaminsky, W.; Geissler, A. *Pet. Sci. Technol.* **2005**, *23*, 47–54.

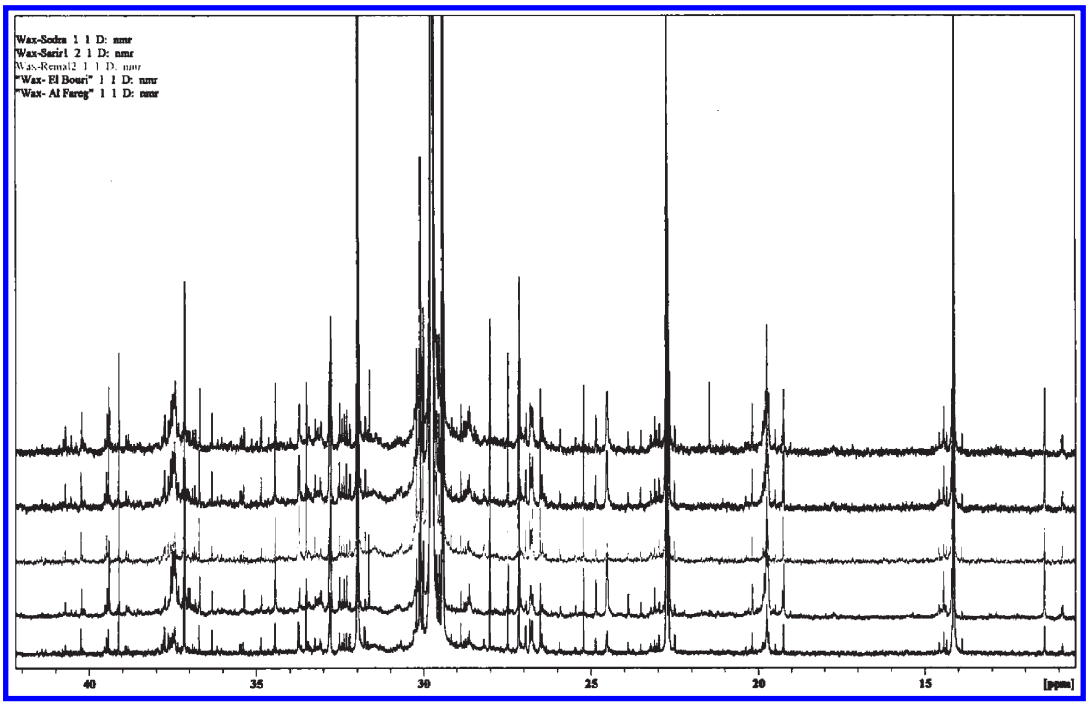

Figure 2. ^{13}C NMR spectra for the waxes studied in the aliphatic region. The spectra correspond, from top to bottom, to Sedra, Sarir, Remal, Bouri, and Faregh.

2 times the standard deviation. It can thus be assumed that the WATs measured at the two cooling rates are statistically identical. It is also quite remarkable that, although the WAT would be expected to increase with the wax content of the oil, there seems to be no straight relation between the two, with Faregh presenting one of the highest wax contents, while its WAT is inferior to those of Remal and Sarir. This is a clear indication that the WAT is dependent upon not only the wax content but also the wax composition, as previously suggested.[9] The pour point, however, displays a very good linear dependency upon the WAT for all fluids of 23 ± 3 K below the measured WAT. The WAT is thus, for these crudes, a good indicator of their pour point.

Wax Composition. The wax composition was determined by means of a GC−FID analysis according to the procedure described above. The *n*-alkane distributions and the content of non-*n*-alkanes on the oil are reported in Table 3. The results indicate that all of the waxes extracted are highly paraffinic macrocrystalline waxes. They vary from being essentially made up of *n*-alkanes, as is the case for Sedra and Faregh, to oils, such as Bouri, that, although highly paraffinic, present a non-*n*-alkane content slightly above 20 wt %. The two other oils, Remal and Sarir, present waxes very rich in *n*-alkanes, with the *n*-alkane content above 90 wt %.

To obtain more detailed information on the composition of the waxes, in particular, to evaluate the amount of tertiary and aromatic carbons present in the wax, elemental analysis and ^{13}C NMR were used. The peaks on the NMR spectra were assigned to carbon types according to the suggestion of Carman et al.[15] and Sperber et al.[16]

The elemental analysis, reported in Table 4, presents H/C ratios higher than 2 for all waxes, except Sedra, with a H/C ratio of 1.95. These values are typical of macrocrystalline paraffinic waxes with a high degree of saturation.

Figure 2 shows the ^{13}C NMR spectra for the five waxes in the aliphatic region. As can be seen, the signals of the straight hydrocarbons dominate, with a few signals of branched

Table 5. Characterization of the Aliphatic Portion of the Waxes by ^{13}C NMR

structure		ppm	Remal	Bouri	Sarir	Sedra	Faregh
α-CH_3	CH_3	14.14	5.073	4.134	5.329	4.474	5.861
$1B_1$		20.06	0.048	0.23	0.116	0.144	0.152
$1B_2$		11.46	0.07	0.36	0.123	0.142	0.076
$1B_{3-6}$		14.54	0.053	0.111	0.077	0.068	0.06
β-CH_2	CH_2	22.85	5.381	4.46	5.497	4.72	5.96
γ-CH_2		32.16	5.691	4.301	5.695	4.839	6.301
δ-CH_2		29.9	53.966	39.409	52.189	49.896	56.693
$\alpha\delta^+$-B_1		37.48	0.193	0.557	0.402	0.319	0.249
$\alpha\delta^+$-B_2		34	0	0.071	0	0	0
$\alpha\delta^+$-B_{3-6}		34.48	0.083	0.519	0.17	0.199	0.119
$\beta\delta^+$-B_1		27.26	0	0	0	0	0
$\beta\delta^+$-B_{2-6}		27.21	0.112	0.32	0.496	0.465	0.12
$\gamma\delta^+$-B_1		30.28	0.445	0.557	0.517	0.505	0.384
$\gamma\delta^+$-B_{2-6}		30.39	0	0.024	0	0	0
$2B_2$		27.59	0.148	0.296	0.185	0.255	0.16
CHB_1	CH	33.16	0.094	0.298	0.148	0.133	0.075
CHB_2		34.61	0.036	0.154	0.092	0.114	0.045
CHB_{3-6}		37.01	0.41	0.964	0.435	0.496	0.32
CN1	CN	26.84	0.093	0.145	0.094	0.102	0.113
CN2		33.85	0.271	0.286	0.285	0.261	0.212
percentage identified			72.167	57.196	71.851	67.131	76.901
percentage not identified			27.833	42.804	28.149	32.869	23.099
percentage of tertiary carbon			0.54	1.416	0.675	0.743	0.44

hydrocarbons. The aromatic carbon content was estimated according to the ASTM D5292-99[17] using the following equation:

$$\%\ \mathrm{C(ar)} = [A/(A+B)] \times 100 \qquad (3)$$

where A is the peak area of the aromatic portion of the spectra (100−170 ppm), while B is the peak area of the aliphatic portion of the spectrum (10−70 ppm). The results

(17) Petitjean, D.; Schmitt, J. F.; Laine, V.; Bouroukba, M.; Cunat, C.; Dirand, M. *Energy Fuels* **2008**, *22*, 697–701.

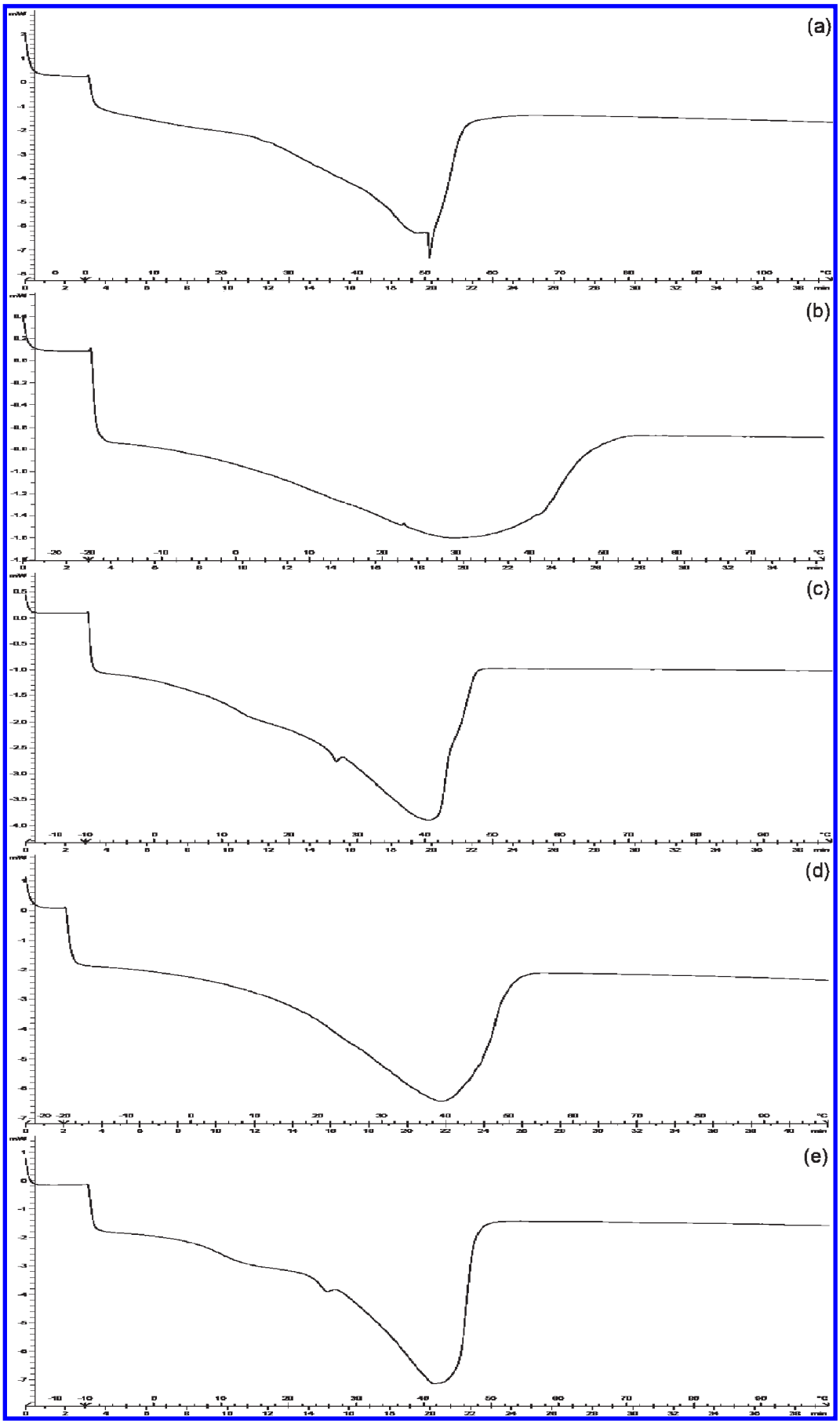

Figure 3. Thermograms for (a) Remal, (b) Bouri, (c) Sarir, (d) Sedra, and (e) Faregh.

are reported in Table 4, where it can be seen that Sedra has the highest content of aromatic carbon, with the other waxes presenting an aromatic carbon content equal or inferior to 1%. A good correlation was observed between the H/C ratio and the aromatic carbon content obtained from ^{13}C NMR spectra, allowing for an explanation for the lower H/C ratio observed for Sedra in the elemental analysis.

Using the peak identification mentioned above, an identification of the different carbon types was carried out and is reported in Table 5 using the nomenclature suggested by Sperber et al.[16]

The ^{13}C NMR spectra show that the waxes are formed essentially by alkyl chains with very limited amount of carbons in cyclic structures (CN < 0.5%) or tertiary carbons (CH), with the exception of Bouri, with a content of tertiary carbons close to 1.5%. The tertiary carbon content also seems to be related to the higher content of non-identified structures in Bouri wax. This indicates that the content of isoparaffins in Bouri must be higher than in the other waxes, as also suggested by the GC−FID analysis, and it must have some impact on the crystalline structure of the wax.

Melting Characteristics of the Waxes. DSC was used in this study to further characterize the structure of the waxes through the determination of their melting temperatures and heats of fusion. Panels a−e of Figure 3 show the thermograms for the various wax samples studied, while Table 6 presents the measured melting point temperatures, as well as the heats of fusion. These values show how the thermograms are affected by the wax composition. Remal, which presents the wax with a higher *n*-alkane content, displays a sharp peak with a narrow melting range and high heat of fusion. As the non-*n*-alkane content increases, the melting range becomes broader and the heats of fusion decrease. Bouri, with its relatively high content of branched paraffins, presents a very broad melting peak and the lowest heat of melting (83.0 J/g), indicating that this wax has a much lower crystallinity than the other waxes. A small secondary peak is observed for Faregh and Sarir at temperatures close to 25 °C, which may be due to a solid−solid phase transition of *n*-alkanes. The large heats of melting observed are typical of macrocrystalline waxes.

Table 6. Melting Point Temperatures and Heats of Melting for the Waxes Studied

	melting temperature (°C)	heat of melting (J g^{-1})
Remal	50.5	159.1
Bouri	30.2	83.0
Sarir	40.6	121.8
Sedra	39.2	119.7
Faregh	41.1	142.9

A good correlation between the measured melting points and heats of fusion is observed for these waxes, with higher melting points corresponding to the higher heats of fusion. A good correlation is also observed between the heats of fusion/melting temperatures and the content of tertiary carbon reported in Table 5. The lower the tertiary carbon content, the higher the crystallinity of the wax and, thus, its melting temperature and heat of fusion.

XRD of the Waxes. To obtain information on the crystalline structure of the waxes extracted from the oils under investigation, XRD was performed here on the purified wax samples. The diffractograms of the five waxes are presented in Figure 4. The crystallinity of the samples can be associated

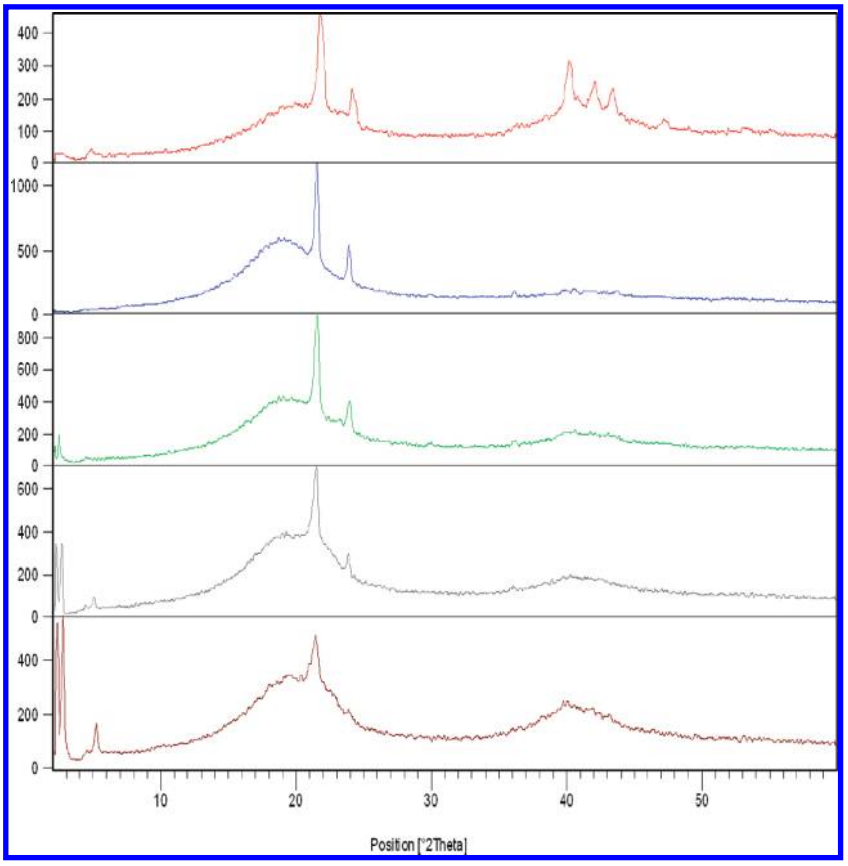

Figure 4. X-ray diffractograms of the studied waxes from top to bottom: (red) Remal, (blue) Bouri, (green) Sedra, (gray) Sarir, and (brown) Faregh, respectively.

with the $2\theta = 35-45$ region. Remal and Faregh are the most crystalline samples, while Bouri is the less crystalline sample. This is in good agreement with the observed heats of fusion. The low crystallinity of Bouri seems to be related with the large content in tertiary carbon of the Bouri waxes, as observed from the NMR spectra. Waxes with a higher isoparaffin content present poor crystalline structures, and their mechanical properties are also modified.[17] These waxes are favorable from a flow assurance point of view because they are softer and easier to melt and, thus, remove from the pipelines by pigging.

To evaluate if a thermal treatment would have any effect on the crystalline habit of the waxes, diffractograms were collected for the purified wax samples and samples undergoing different thermal treatments. No differences in the crystalline habit were observed with the thermal treatments.

Given the high *n*-alkane content of all of these waxes, it is not surprising that they all exhibit very similar XRD patterns. Their crystalline habit can be identified with an orthorhombic structure common in normal paraffins.[17,18]

Conclusions

Characterization of waxy crude oils and their waxes is necessary to be able to understand and predict their behavior to avoid various problems during production, transport, and processing, such as plugging and clogging of pipelines. It is thus very important to obtain reliable information concerning the nature of wax using a combination of various analytical techniques, because there is no single analytical method that can provide a complete picture on the chemical and physical nature of the wax. In this work, the characteristics of five Libyan waxy crudes, namely, Remal, Sarir, Sedra, Bouri, and Faregh, and their waxes were investigated.

Although the major characteristics of the oils seem to be in good agreement, displaying a good relationship between the average molecular weight, API gravity, viscosity, and wax content, it is shown here that the WAT is not just directly related with the wax content of the oil but also with its paraffin distribution. A correlation between the measured WAT and the pour points was also observed.

The results of ^{13}C NMR, elemental analysis, and GC−FID indicate, with a good agreement, that all of the studied Libyan crudes present macrocrystalline waxes, composed of essentially straight-chain saturated paraffinic hydrocarbons as *n*-alkanes. The aromatic content in the waxes was marginal, with the largest value of 2% being presented by Sedra. The waxes from Bouri have a higher quantity of isoparaffins than the other samples, with an important impact on their crystalline structure and, consequently, their melting characteristics.

The coherence between the results obtained from different analytical techniques helps to identify the most adequate, to provide the necessary information with lower effort and cost.

Acknowledgment. The authors are grateful to the various oil companies: Waha, Eni-Oil, and Arabian Gulf Oil, for providing the crude oil samples.

(18) Heyding, R.; Russell, K.; Varty, T.; St-Cyr, D. *Powder Diffr.* **1990**, *5*, 93–100.